

Groundwater delineation using vertical electrical sounding data in Sargodha, Pakistan.



BY

Aqib Bin Gulraiz

MPHIL (HYDROGEOLOGY)

SUPERVISED BY

Dr. Jamil Siddiq

بِسْمِ اللَّهِ الرَّحْمَنِ الرَّحِيمِ

**“In the Name of ALLAH, the Most Merciful
& Mighty”**

**“PAY THANKS TO ALLAH EVERY MOMENT
AND GO TOEXPLORE THE HIDDEN
TREASURES ITS ALL FOR YOUR BENEFIT”**

(AL-QURAN)

Table of contents

CERTIFICATE	viii
DEDICATION	ix
ACKNOWLEDGEMENT	x
ABSTRACT	xi
Chapter 01	1
Introduction	1
1.1 Introduction.....	1
1.2 Study area	3
1.3 Climate and Weather Conditions	4
1.4 Base Map	4
1.5 OBJECTIVES.....	6
Chapter 02	7
LITERATURE REVIEW	7
Chapter 03	12
Geology and Hydrogeology	12
3.1 Geology of the Area.....	12
3.2 Stratigraphy of the area.....	13
3.2.1 Salt Range Formation	15
3.2.2 Tobra Formation	15
3.2.3 Chinji Formation	15
3.3 Hydrogeology of the area.....	15
3.3.1 Aquifer System.....	16
3.3.2 Groundwater Availability.....	16
3.3.3 Recharge Sources.....	16

3.3.4 Water Quality	17
3.3.5 Over-Exploitation and Sustainability	17
3.3.6 Hydrological Studies.....	17
Chapter 04.....	18
Materials and Methods	18
4.1 Introduction.....	18
4.2 Vertical Electrical Sounding.....	19
4.3 Electrode Configuration.....	20
4.4 Importance of Schlumberger Configuration	22
4.5 Data Acquisition.....	23
4.5.1 Field Planning	23
4.5.2 Resistivity Data Collection.....	23
4.5.3 Resistivity Data Processing	23
4.6 Vertical Electrical Sounding Curves.....	23
4.6.1 Curve Matching Technique.....	24
4.6.2 Process of Iteration	24
4.6.3 RMS Error/Fixing	24
4.6.4 Adjusting Noisy Points	24
4.6.5 Vertical Lithological Columns.....	25
4.7 Rock Resistivities	25
4.8 Generation of Cross sections	27
4.9 Resistivity Configurations	27
4.10 The Parameters of Dar-Zarrouck (D-Z) and their Significance	27
Chapter 05.....	29
Geoelectrical Modelling	29

5.1 Interpretation of field curves	29
5.1.1 Curve matching method.....	29
5.2 Correlation between sounding curve and borehole lithology	29
5.3 Calibration	33
5.3.1 Modelling of VES-5	36
5.3.2 Modelling of VES-13	37
5.3.3 Modelling of VES-27	38
5.4 Ground water Quality Zonation.....	40
5.4.1 Iso-Resistivity Maps of the Study Area.....	40
5.4 PSEUDO-SECTIONS.....	47
5.4.1 Pseudo cross-section along profile A	49
5.4.2 Pseudo cross-section along profile B.....	49
5.4.3 Pseudo cross-section along profile C.....	50
5.4.4 Pseudo cross-section along profile D	51
5.4.5 Pseudo cross-section along profile E.....	52
5.4.6 Correlation between VES and Physio-chemical analysis.....	53
Chapter 06.....	57
Estimation of Dar-Zarrouck parameters of study area.....	57
6.1 Introduction.....	57
6.2 Longitudinal Conductance (Sc).....	61
6.3 Transverse Unit Resistance (Tr).....	62
6.4 Longitudinal Resistivity (Rs).....	64
Chapter 07.....	66
Conclusions	66
REFERENCES.....	68

APPENDIX 72

List of Figures

Figure 1.1 Location map of the study area.....	5
Figure 3.1 Stratigraphic map of Sargodha area (Powell, 1979; Kazmi and Rana) 14	
Figure 4.1 Showing Electrode Configuration (et al. Garofalo 2014).....	21
Figure 4.2 Theoretical procedure for determining the Dar zarrouck parameter	28
Figure 5.1 Correlation between sounding curves and borehole lithology 30	
Figure 5.2 Correlation between sounding curves and borehole lithology.....	31
Figure 5.3 Correlation between sounding curves and borehole lithology.....	32
Figure 5.4 Vertical Electrical Sounding VES-5.....	37
Figure 5.5 Vertical Electrical Sounding VES-13.....	38
Figure 5.6 Vertical Electrical Sounding VES-27.....	39
Figure 5.7 Iso-Resistivity Maps of Zone 1 at 20m	41
Figure 5.8 Iso-Resistivity Maps of Zone 1 at 50m	43
Figure 5.9 Iso-Resistivity Maps of Zone 3 at 100 m.....	44
Figure 5.10 Iso-Resistivity Maps of Zone 4 at 150 m.....	46
Figure 5.11 Showing VES profiles of the Study Area	48
Figure 5.12 Apparent resistivity pseudo cross section for profile A	49
Figure 5.13 Apparent resistivity pseudo cross section for profile B	50
Figure 5.14 Apparent resistivity pseudo cross section for profile C	51
Figure 5.15 Apparent resistivity pseudo cross section for profile D	52
Figure 5.16 Apparent resistivity pseudo cross section for profile E	52
Figure 6.1 3D Electrostratigraphic model showing total longitudinal conductance and total transverse resistance (modified from Reynolds, 1997). 58	
Figure 6.2 Contour map of the longitudinal conductance.....	62
Figure 6.3 Transverse Unit Resistance (Tr)	63
Figure 6.4 Contour map of the Longitudinal Resistivity	65

List of Tables

Table 4.1 Numerical values for various types of water.....	26
Table 4.2 Resistivities of some common rocks.	26
Table 5.1 Resistivity ranges for various sedimentary formations (Keller and Frischknecht 1966a, 1996b; Bhattacharya and Patra 1968a, 1968b).....	33
Table 5.2 Resistivity and Lithology Calibration in the Study	34
Table 5.3 Physio-chemical analysis data of Sargodha area.....	68
Table 5.4 VES data of the study area for comparing with Physio-chemical analysis data.....	69
Table 6.1 Values of Dar-Zarrouck parameters of all sounding locations with depth -----	60

CERTIFICATE

This dissertation submitted by **Aqib Bin Gulraiz S/O Mirza Gulraiz Akhtar** is accepted in its present form by the Department of Earth Sciences, Quaid-I-Azam University Islamabad as satisfying the requirement for the award of MPhil degree in Hydrogeology.

RECOMMENDED BY

Dr. Jamil Siddique _____
(Supervisor)

Dr. Mumtaz Shah _____
(Chairman Department of Earth Sciences)

EXTERNAL EXAMINER _____

DEDICATION

**“This dissertation is dedicated to ALLAH, the almighty”“His prophet
HAZRAT MUHAMMAD (P.B.U.H)”.**

&

**To My Parents, Family, and Respected
Teachers, as I could not have achieved this level
of achievement without their prayers, support,
and belief in me. I pray that Allah would always
keep your shadow over me and bless you.**

&

To My Department of Earth Sciences, (QAU)

ACKNOWLEDGEMENT

In the name of the Most Generous and Most Merciful Allah. All praise belongs to the All-Powerful Allah, the Universe's Creator, who gave me health and education. I attest that the Holy Prophet Muhammad (PBUH) is the final messenger whose life serves as an ideal example for the entirety of humanity up until the Day of Judgment. Allah has gifted me with earthly knowledge. Allah gives me the ability to finish my duties. Without Allah's blessings, I would not be able to do my task or be in this situation.

I express my gratitude to my respected supervisor, **Dr. Jamil Siddique**, for providing me with the motivation to do this work. The provision of inspired advice, dynamic supervision, and constructive criticism proved vital in enabling me to successfully accomplish this task within the designated timeframe. I express my gratitude to the entire faculty of my department for their valuable assistance and cooperation, which greatly contributed to my personal growth and academic journey.

I would like to express my sincere gratitude to my parents and my uncle, Mirza Tanveer Akhtar Jarral, for their unwavering support, boundless affection, and constant encouragement during my academic journey. Their sacrifices have played a crucial role in my educational pursuits.

Aqib Bin Gulraiz

**M.Phil
(Hydrogeology)
2021-2023**

ABSTRACT

In the realm of hydrogeology, conducting a thorough hydrogeologic evaluation is crucial for the efficient utilization of groundwater resources within an aquifer system. Throughout history, the process of obtaining hydraulic characteristics has heavily relied on costly and labor-intensive methods of collecting borehole data. As a consequence, the spatial coverage of these data has been limited, particularly in vast regions. However, the utilization of non-invasive geoelectric techniques offers a cost-effective and user-oriented alternative, hence reducing the need for several expensive boreholes in the exploration of groundwater reservoirs.

A research investigation was carried out in the Sargodha Area of Chaj Doab, employing a total of 28 Schlumberger rigs for Vertical Electrical Sounding (VES) purposes. The primary aim of this study was to assess the hydrogeological characteristics of the subsurface and provide estimations pertaining to the groundwater reserves. The objective of this study was to demonstrate relationships between subsurface resistivity, water quality, and lithology by the correlation of subsurface resistivity with lithological data.

The results of the study indicated clear patterns, such as the identification of silty clay with saline water displaying resistivity values below 20 Ω -m, the presence of sand with brackish water exhibiting resistivity values ranging from 25 to 100 Ω -m, and the occurrence of sand with gravel containing fresh water and resistivity values exceeding 100 Ω -m. The utilizations of electrical resistivity modelling in conjunction with borehole data has enabled the creation of cartographic depictions of subsurface lithological variations and aquifer thickness, while also facilitating an assessment of water quality. The existence of both lateral and vertical diversity in the underlying lithology has been identified, suggesting a significant likelihood for the infiltration of saline water into freshwater groundwater resources. The accurate identification and distinction of aquifer zones exhibiting fresh-saline features are of utmost importance for the purpose of accessing and utilizing potable freshwater supplies.

Traditionally, the procedure for attaining this segregation has entailed the gathering and examination of groundwater samples from boreholes utilizing various research approaches, which can be both costly and time-consuming.

The Dar-Zarrouck characteristics, which include transverse unit resistance, longitudinal resistivity, and longitudinal unit conductance, were employed to improve efficiency. Additionally, the Dar-Zarrouck characteristics, specifically the Longitudinal Unit Conductance (S) and Transverse Unit Resistance (Tr), provide additional evidence that corroborates the existence of fresh and saline water in regions characterized by high and low resistivity, respectively. The transverse unit resistance (Tr) has a notably higher magnitude in the high resistivity zone, exceeding $6600 \Omega \cdot m^2$, whereas it exhibits a comparatively lower value in the low resistivity zone, ranging between $0-3000 \Omega \cdot m^2$.

The longitudinal conductance (S) exhibits a modest magnitude. The high resistivity zone is commonly observed to fall within the range of 44 to 60 siemens, whereas the low resistivity zone demonstrates values spanning from 0 to 24 siemens. The enhancement of the conversion process from one-dimensional Vertical Electrical Sounding (VES) data to two-dimensional depictions of the adjacent subsurface has been greatly advanced through the use of modern display technologies. These models provide valuable insights that considerably improve our understanding of alluvium layers as distinct lithologic units within a two-dimensional spatial framework. In summary, the results of the study align closely with the prevailing hydrogeological knowledge pertaining to the particular area being exami

Chapter 01

Introduction

1.1 Introduction

Water is an essential element that accounts for approximately 70% of the Earth's surface and approximately 75% of the human body. It is a requirement for all organisms inhabiting the planet Earth. In addition to its consumption, it has numerous applications. With the rise in population and urbanization, coupled with the growth of industrial sectors, there has been a corresponding increase in water consumption.

The stress on subsurface groundwater resources has intensified due to an increase in various factors. Furthermore, the situation is made worse by the effects of climate change and global warming, resulting in a widespread and severe impact on worldwide. The water resource challenges in developing countries increase and pose unique difficulties. The primary challenges include the limited availability of potable water, occurrences of flooding, sediment accumulation in rivers, and the pollution of rivers and groundwater resulting from industrial activities. An estimated 1.1 billion individuals living in developing nations face insufficient access to clean water, while approximately 2.6 billion lack proper sanitation facilities. According to a report by the United Nations Development Program (UNDP) in 2016, approximately 1.8 million children succumb to the effects of diarrhea, while a significant number of women are compelled to dedicate their entire day to the task of water collection. The issue contributes to in South Asian nations characterized by expanding populations and industries. Among these countries, Pakistan stands out as the most affected, allocating a mere 0.2% of its GDP towards water and sanitation (ASP, 2011). Furthermore, compounding this problem is the absence of a regulatory authority tasked with monitoring issues caused by excessive water withdrawal for domestic and industrial purposes. The situation gets worse by the phenomenon of climate change and global warming, which leads to reduced rainfall, diminished glacial water resources, and increased instances of flooding. Additionally, the construction of dams by a neighboring country on the eastern rivers contributes

to further challenges. The aforementioned issues contribute to the growing significance of groundwater.

Groundwater, which is typically characterized by its high quality, occasionally exists at considerable depths. Therefore, it is strongly recommended to accurately determine the location, evaluate the quality, and quantify the quantity prior to embarking on the expensive drilling process. Non-destructive geophysical techniques have been extensively employed and have demonstrated their efficacy over time. The utility of proton magnetic resonance and electrical resistivity methods in water detection has been investigated and confirmed. The utilization of the Electrical resistivity method is an economically efficient and dependable approach for identifying subsurface formations containing water. The primary application of electrical resistivity techniques is the delineation of aquifer boundaries, determination of aquifer depth, and assessment of aquifer potential (Omosuyi et al., 2007; Bernstone et al., 2000; Oseji, 2005). Additionally, these methods are also relevant to the evaluation of geothermal and hydraulic conductivity within the aquifer (El-Qady, 2006). The utilization of electrical resistivity is the preferred method for water exploitation. To assess the vertical variations in resistivity associated with subsurface layers at a specific location, the vertical electrical sounding (VES) technique is employed. Moreover, this methodology has demonstrated greater efficacy in delineating sedimentary basin deposits (Kelly and Stainslav, 1993; Olorunfemi and Meshida, 1987). The electrical resistivity arrangement utilizes a configuration consisting of four electrodes. Two electrodes are used for injecting current into the subsurface, while the other two electrodes are employed for measuring the potential difference that arises as a result of the current flow. The potential difference is contingent upon the resistivity of the subsurface materials. According to Awani (2010), materials with high resistivity values exhibit greater resistance to electric current, while materials with lower resistivity values are more conductive. In the subsurface, the term "conductive layer" refers to a lithology that contains pores filled with water, allowing for the flow of electrical current. On the other hand, "resistive layers" are lithologies that lack water content between them, impeding the flow of electrical current. Multiple configurations are employed in electrical resistivity surveys. The most commonly utilized types of electrical resistivity measurement techniques include Wenner, Schlumberger, and dipole-dipole. Each configuration of electrodes possesses distinct advantages based on the topography, and the current is also influenced by subsurface resistivities in addition to ground conditions.

The estimation of apparent resistivity is achieved by multiplying the dimensions factor with the potential difference and subsequently dividing it by the current (Stanley and Deweist, 1996). The Schlumberger configuration is favored over other types due to its ability to achieve deeper penetration, making it the preferred choice for ground water detection (Adeot et al., 2012; Olowofela et al., 2005). This technique involves holding the potential electrodes at a consistent level while gradually increasing the current electrodes to obtain measurements of resistivity at greater depths. Forward and inverse modeling computer programs are utilized for the identification of resistivity variations with depth (Anomohanran, 2013). This approach offers advantages such as reduced boring and cost-effectiveness (Ako and Olorunfemi, 1989; Madan et al., 2008). The lithologs derived from surface Vertical Electrical Sounding (VES) data sets have demonstrated a high level of reliability and have effectively mitigated the need for costly borehole drilling. The vertical electrical sounding technique has been employed by numerous scientists in recent years to identify paleodepositional environments in quaternary deposits. This is because paleodepositional environments are closely associated with the presence of groundwater in the subsurface (Olowofela et al., 2005). Only a limited number of authors in India and Pakistan have conducted extensive research on quaternary paleo-depositional environments. In a study conducted by Kevin (1998), the occurrence of quaternary flood outbreaks in the Peshawar basin was identified. Baber et al. (2014) conducted a study on quaternary fluvial deposits within the Sindphana River in India. The vertical electrical sounding technique, although cost-effective, is not without its limitations. For instance, the current method is limited to providing subsurface coverage in only one dimension and lacks information pertaining to lateral variations.

1.2 Study area

The area of investigation Sargodha district situated in the province of Punjab, Pakistan. Sargodha city holds the 11th place in terms of size and has experienced rapid development in Pakistan. The city includes a total area of 5,854 square kilometers. The population of the area under consideration is 1,500,000 individuals, as reported in the 1998 census. The population density, calculated by dividing the total population by the area, is 3.49. The longitudinal extent of Sargodha district ranges from 72-05 degrees to 72-95 degrees, while its latitudinal extent spans from 31-5 degrees to 32-55 degrees. The city is effectively connected to the primary transportation hubs of the country.

The region under concern demonstrates a topography characterized by a predominantly level terrain, causing it suitable for agricultural activities, particularly the cultivation of citrus fruits. The physiography of Sargodha is characterized by a flat terrain, covering fertile agricultural land situated between the Jhelum River to the west and the Chenab River to the east of the city. Sargodha is characterized by its presence of small hills along the Faisalabad Road. The geographical features in question are referred to as the Kirana hills.

1.3 Climate and Weather Conditions

Sargodha is classified under the Koppen climate rating system as belonging to the Bsh category. The classification of climatic regions utilizes the letter "B" to represent arid conditions, the lowercase letter "s" to denote dry summers, and the lowercase letter "h" to signify hot temperatures. The city of Sargodha has exhibited indications of climate change in relation to its patterns of rainfall, temperature, and humidity. The region experiences severe weather patterns characterized by high temperatures reaching the 50 °C during the summer months, accompanied by high humidity levels from July to September. In contrast, winter temperatures plummet to 0 °C. Fog envelops a significant number of Punjab, including Chiniot and the surrounding areas. During the months of December to January, the region experiences persistent foggy conditions.

1.4 Base Map

A base map refers to a cartographic representation that serves as a foundational framework for displaying and arranging crucial data and interpretations. A base map commonly consists of the locations of VES (Vertical Electrical Sounding) within a study region, together with their accompanying geographic references, such as latitude and longitude coordinates. The base map in Figure 1.1 displays the electrical resistivity data of 28 sites for research purposes. The locations of these points, together with their corresponding names, have been incorporated into the base map using ArcGIS software.

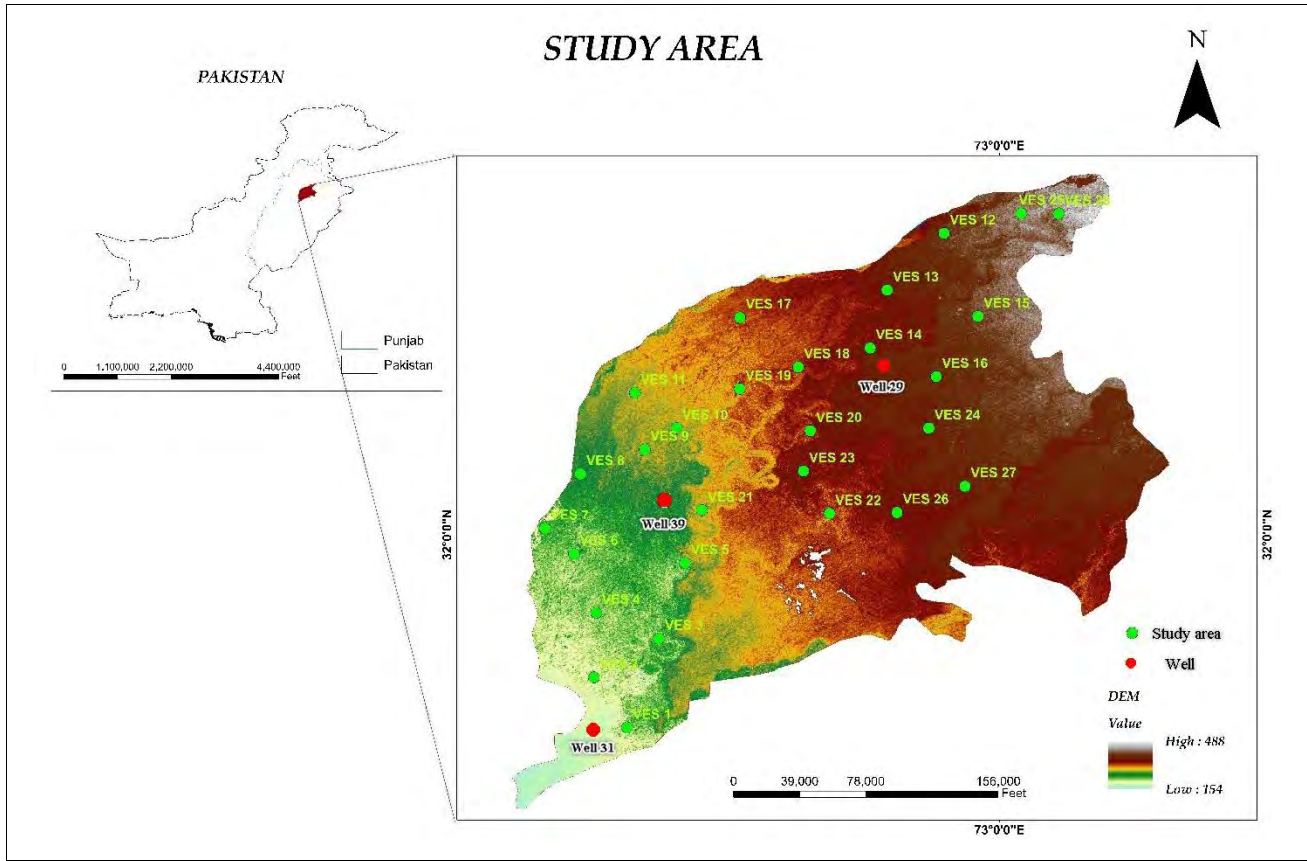


Figure 1.1 Location map of the study area

1.5 OBJECTIVES

- The identification of possible aquifers requires investigating geological, hydrological, and geophysical data to determine subsurface formations capable of storing and transferring groundwater.
- Determine aquifer characteristics using vertical electrical sounding for precise well-site selection and sustainable groundwater management
- Analyze VES data to indirectly assess groundwater quality and identify potential contaminants or salinity levels.
- Utilize VES techniques to enhance the probability of profitable well excavation in regions with favorable aquifer features.
- Assess VES-derived data to optimize long-term water supply through sustainable extraction and replenishment strategies.
- Identify and apply VES-informed methodologies for selecting sites conducive to successful water well installation and management.

Chapter 02

LITERATURE REVIEW

In their study conducted in 1985, Arafin and Lee employed the electrical resistivity method to identify appropriate locations for boreholes and determine the depth of bedrock in the Perlis region of Malaysia. The region is predominantly composed of limestone, which possesses secondary porosity that has the potential to act as a source for groundwater occurrence.

Reynolds (1987) employed the electromagnetic approach to investigate the relationship between electrical resistivity and several factors in the Nigerian state of Kano. The groundwater zones with lower groundwater potential were accurately recognized. This study has demonstrated significant utility for the aforementioned region, as it has effectively addressed the issue of drilling wild cat wells without the implementation of geophysical techniques. The study has resulted in a notable reduction of the failure rate by 32%.

Yadav (1995) conducted a vertical electrical sounding study at nine pumping sites in India. In this study, Yadav established a correlation between hydraulic parameters obtained from well testing and geo-electrical parameters generated from geo-electrical data. Furthermore, he contended that by utilizing acoustic data, one may determine the transmissivity of an aquifer if the hydraulic transmissivity of a certain reference point is already known.

Steinich et al. (1999) conducted a study in Chipas, Mexico, wherein they examined a survey consisting of twenty-four vertical electrical soundings. The purpose of this survey was to analyze the aquifer geometry and the presence of a fresh water carrying body. The findings encompassed the assessment of basement topography, which consists of profound valleys and hills, as well as the estimation of the water reserve, amounting to 75 Km². This estimation was derived by analyzing the volume of dissolved water samples using chemical analysis and considering the dimensions of the aquifer.

Zouhri (2001) employed the electrical resistivity approach to delineate the impermeable basement structure of the Mamora basin in Morocco. The findings of the investigation revealed the flow direction of groundwater and the characteristics of the saturated aquifer.

The number 15 is the subject of discussion. In a study conducted by Thomas (2002), an extensive investigation was undertaken to analyze the groundwater structures in the north lake of Noivasha, Kenya. This endeavor involved the collecting of transient electromagnetic (TEM) and electrical resistivity tomography data. A total of 137 Transient Electromagnetic Soundings (TEM) and 13 Electrical Resistivity Profiles (ERPs) were conducted, each with varying lengths. The characteristics that were attained in this endeavor encompassed lithology, formation resistivity, and water quality. Subsequently, these parameters were employed for the purpose of aquifer modelling.

Lashkaripour (2003) utilized 596 Vertical Electrical Soundings (VES) to delineate distinct subsurface regions within the Sistan and Baluchistan province of Iran, which exhibited significant water reserves of commercial value. The study encompassed a comprehensive assessment of the hydrogeological conditions. Based on the findings of this investigation, a number more tube wells were subsequently erected. A study conducted by Lashkaripour et al. (2005) involved the implementation of a similar methodology, this time in the Chah Hashan plain located in Iran. The research utilized a total of 400 vertical electrical sounding stations, encompassing seven distinct profiles. The researcher successfully found an alluvial aquifer characterized by the predominant presence of lithologies such as sand, clay, gravel, and silt. The investigation additionally unveiled other locations suitable for the development of tube wells.

The utilization of electrical resistivity technique has been observed in previous studies conducted by various researchers (Jeong et al., 2005; Mohammad et al., 2008; Ozebo et al., 2008; Rao et al., 2008) to delineate bedrock boundaries, assess aquifer characteristics, determine aquifer extent, and evaluate aquifer thickness in relation to the hydrogeological conditions of the investigated region.

One increasingly prevalent use that has gained global recognition among scientists is the utilization of electrical resistivity technologies for the purpose of mapping quaternary basin architecture. In their study conducted in Kuala Selangor, Malaysia, Hamzah et al. (2002) employed the schlumberger configuration to determine the thickness of alluvium.

In their study, Kshetrimayum and Bajpai (2011) employed a geo-electrical survey technique to demarcate Quaternary paleochannels that were submerged between two rivers, namely the Markanda River and the Vedic Sarawasti River, located in the state of Haryana, India. The predominant lithological compositions observed encompassed various types of sand and boulders.

In their study, Yadav et al. (2010) employed the electrical resistivity approach to discern the stratigraphy of the shallow subsurface in the expansive alluvial region of India. A total of forty-six (46) vertical sounding locations were employed, along with seven (7) cores obtained from drilled bores. The research findings indicate the existence of notable variations in subsurface composition, revealing the occurrence of saline aquifers in multiple areas. The continuity of the aquifer was interrupted by the presence of muddy deposits at various locations, which served as a significant element within the interfluvial system.

In their study, Leopold et al. (2013) employed a technique known as two-dimensional electrical resistivity tomography to discern the subsurface structure of the Boulder Creek Critical Zone Observatory in Australia. The researchers employed the Wenner configuration, utilizing a 1-meter electrode spacing. In addition, they compared the obtained data with seismic data. Notably, the resistivity data revealed the presence of a layer, approximately 0.5 to 1.5 meters thick, situated above the bedrock. This discovery provided a novel perspective for interpreting the depositional processes, surpassing the capabilities of the seismic method.

Kenneth and Edirin (2012) conducted a study in Yegona city, located in south Nigeria, to investigate the correlation between quaternary sediments and the presence of fresh groundwater with lower concentrations of conducting minerals. The study also examined the infiltration zones that facilitate the transport of contaminants from the surface to the subsurface aquifer system. The researchers employed an electrode distance of 300-400m for their investigation.

Amaya et al. (2016) conducted measurements of electrical resistivity profiles in Panata, Bolivia, amounting to a total of 30 profiles. The data acquisition process utilized a multi-gradient array. The upper portion of the subsurface material is composed of boulders embedded inside a matrix of smaller particles. The resistivity of the aforementioned deposits exhibits a range between 200 and 1000 Ω m, whereas the values of chargeability were found to be less than 0.05 ms/v. The resistivity and chargeability values of the lower lithologies were seen to fall within the range of 10

to 100 Ωm and 0.07 ms/v, respectively. The study not only examined the correlation between electrical resistivity and induced potential change, but also provided insights into the aquifer system of the studied area.

In their study, Aning et al. (2014) employed continuous electrical resistivity profiles within the KNUST campus located in Ghana. The main aim of this study was to determine the bearing capacity of the bedrock in order to support the construction of large structures in the designated region. To do this, a total of eight (08) 2D electrical resistivity profiles were obtained using the Wenner array method. The findings indicated a clear demarcation between arid and humid granitic compositions.

In a study conducted by Weerasiri et al. (2013), the authors examined the paths through which arsenic was being transported from a gold mine, resulting in the contamination of subterranean water reservoirs in Wangsa Phung, a location located in the north-eastern part of Thailand. During the process of acquisition, a dipole array was employed, consisting of electrodes spaced at intervals of 1.5m, 3m, and 10m. This arrangement facilitated the measurement of different depths. Additionally, surface fluxes were approximated using a Geographic Information System (GIS) approach. The findings indicate that the transportation of arsenic occurs through the movement of water from areas of higher elevation to lower elevation, particularly during periods of increased rainfall.

In their study, Akaninyen et al. (2011) employed electrical resistivity survey as a means of identifying and assessing groundwater contamination in Uyo, Nigeria. A comprehensive set of vertical electrical readings was conducted both on and around a dumpsite, accompanied by the collection of electrical resistivity data and fine geochemical samples. This was done in order to provide empirical evidence that supports the obtained resistivity values. The findings revealed the presence of contamination, primarily in the form of hydrocarbon residues that were observed to be floating on the water table in close proximity to the dumpsite.

In their study, Benson et al. (1997) employed a total of thirty-two (32) electrical resistivity points, in conjunction with very low frequency profiles, to delineate regions that encompass solutes. The dipole arrangement was employed for the measurement of electrical resistivity. The findings indicated elevated resistivity values within saturated regions, suggesting the existence of solutes

that exhibit resistance to electrical current. However, in the region above the water table, the zone exhibited lower resistivity values, suggesting a lower level of contamination.

Bayode et al. (2011) employed a two-dimensional resistivity survey utilizing Schlumberger and dipole configurations to delineate a structurally controlled plume in Akure, located in the southwestern region of Nigeria. Three distinct zones were found, including the topsoil, worn layer, and bedrock layer. The investigation additionally disclosed that fissures existing in the bedrock are transporting toxins to the underlying subterranean aquifer.

In the study conducted by Al-Bassam (2005), a total of 145 vertical sounding sites were utilized, which were obtained using the schlumberger and wenner configurations. These sounding points were specifically employed in the tertiary sequence located in Jeddah, Kingdom of Saudi Arabia. The findings demonstrated the presence of freshwater regions, as well as a demarcation line distinguishing freshwater from connate water.

In their study, Song et al. (2007) employed a total of thirty (30) electrical resistivity points. Sea water infiltration was found in the coastal area of Byunsan, Korea by identifying a high conductive layer located between resistive layers.

In their study on sea water invasion in Korba, Tunisia, Kaizana et al. (2009) employed a set of thirty-eight (38) vertically aligned sounding stations that were calibrated for data collection purposes. The results were calibrated using borehole data. The findings indicate that the displacement of fresh water zones by sea water has occurred as a consequence of heightened extraction of fresh water.

The objective of the current study was to perform vertical electrical sounding and electrical resistivity tomography surveys in Hattar and its surrounding regions (Haripur Basin). The aim was to determine the Paleo-depositional environments and assess the influence of Hattar industrial effluents on the local villages and groundwater. In order to accomplish that objective, A total of sixty vertical sounding points were utilized to cover the Hattar region and its surrounding areas, including Haripur, Kangra Deedan, Dingi, Mota, Havelian, and Khalabut township.

Chapter 03

Geology and Hydrogeology

3.1 Geology of the Area

The geological characteristics of the Sargodha region in Pakistan are influenced by the convergence of the Indian Plate and the Eurasian Plate, leading to the tectonic uplift of the Himalayas and the subsequent accumulation of sedimentary rock formations. One of the noteworthy geological features is the Salt Range Formation, which comprises sandstones, shales, and limestones that were produced in a shallow marine setting during the Mesozoic era. The Tobra Formation is comprised of sedimentary deposits consisting of clays, sands, and gravels, which are indicative of their likely formation in fluvial settings. The region has a significant abundance of gypsum, limestone, and several other industrial minerals. The process of river erosion has given rise to several discernible geographical features, such as river valleys and floodplains. The Chenab River has had a significant role in the formation and cultivation of fertile alluvial plains that are very conducive to agricultural activities.

The Kirana Hills are geological formations that originated from significant volcanic activity that took place during the Precambrian era inside the Kirana-Malani Basin of the northeastern region of the Gondwana supercontinent. These hills are currently found as solitary outcrops spread across the Punjab Plain, stretching from Chiniot to Sargodha. This information is supported by studies conducted by Chaudhary et al. in 1999 and Shah in 1977. The Kirana Hills Volcanics predominantly consist of mafic and felsic rocks. However, the mineralogy division of the Atomic Energy Minerals Centre Lahore has also verified the existence of intermediate rocks within this geological complex. The rocks under consideration are classified as part of the tholeiitic basalt-rhyolite magma association, which also contains intercalated meta-sediments.

Geologically, the region is situated on the prominent protrusion of the Indian plate, resulting from the convergence of the Indian and Eurasian plates. The Kirana hill is considered to be the western extension of the Precambrian shield of India, as stated by Kazmi and Jan (1997). The Sargodha-Shahkot ridge, oriented in a northwest-southeast direction, exhibits similarities to prominent geological formations in the central Himalayas (Powell, 1979). It can be considered as an extension

of the Aravalli Mountain belt located in the Rajasthan region. In this area, the ridge demonstrates a distinct northeast-southwest trend, which is prominently visible from Champanar in Gujarat, situated at the upper end of the Gulf of Cambay, extending towards Delhi, traversing across the Rajasthan region. Located in the vicinity of Delhi, at the northern extremity of the Aravalli range, a distinct section of the geological formation undergoes a significant change in direction, veering sharply towards the northwest and NNW. This altered segment persists as a subterranean ridge, demarcating the border of the Punjab plains, and extends further to encompass the Kirana and Sangla Hills, which are situated in close proximity to the eastern terminus of the Salt Range.

The ridge under consideration is postulated to be the flexure bulge originating from the Indian plate, exhibiting significant seismic activity. This region corresponds to a contiguous seismic zone (as observed by the Tarbella network), which runs parallel to the Himalayas but is situated 200 km to the south of the primary boundary thrust (Seeber and Armbruster, 1977). The area under discussion pertains to the buried ridge known as the Sargodha – Shahkot, which is exposed on the surface. The region generally encounters seismic activity of low magnitude, which is attributed to the periodic release of accumulated tension on the flexure bulge of the Indian plate. However, it is important to note that the pace of tectonic strain release in this area is relatively minimal (Kazmi and Jan, 1997).

The age of the igneous suite was determined using the Rb-Sr dating method and is reported as 870 ± 40 Ma, as documented by Davis and Crawford in 1971. The alluvial plains of the Punjab region contain Precambrian basement rocks, which exhibit a range in size from 100 square metres to 20 square kilometers. This geological characteristic has been documented in the southeastern area of Sargodha by Kazmi and Jan in 1997.

3.2 Stratigraphy of the area

The Sargodha region in Pakistan has a stratigraphic arrangement including a succession of sedimentary rock formations that have undergone deposition over an extensive geological timeframe that shows in (figure 3.1). Several noteworthy formations may be found in the region, including:

Age				Group	Formation	Lithology	Systematic evolution of Sargodha High				
Eon	Era	Period	Epoch								
P h a n e r o z o i c	Cenozoic	Neogene	Miocene	Kirthar	Siwaliks		Miocene to younger sequences of Siwaliks onlap on the Oligocene erosional unconformity.				
					Drazinda Mem.		Paleocene-Eocene sequence deposited in association of sea level rise, then again Sargodha High uplifted during Oligocene owing of the plate collision in the north.				
		Pirkoh Mem.									
		Domanda Mem.									
		Habib Rahi Lst.									
		Baska Sh.									
		Paleogene	Eocene		Ghazij Fm.						
					Dunghan Fm.						
					Ranikot Fm.						
		Mesozoic	Cretaceous			Baroch		Lumshiwai Fm.		The Mesozoic sequence deposited with depo-center in the west and the sequence may have been eroded over the Sargodha high area, due to uplifting, during the Cretaceous-Tertiary unconformity.	
	Chichali Fm.										
	Jurassic		Samanasuk Fm.								
			Shinawari Fm.								
			Data Fm.								
	Triassic			Musa Khel			Kingriali Fm.				
							Tredian Fm.				
							Mianwali Fm.				
	Paleozoic		Permian				Zaluch	Chhidru Fm.			Paleozoic sequence deposited with depo-center in the east; the sequence is thin out in the west and thicker in the east. There is evidence that the area has been uplifted from the east during the Permo-Triassic unconformity.
								Wargal Lst.			
		Amb Fm.									
Nilawahan		Sardhai Fm.									
		Warchha Fm.									
		Dandot Fm.									
Cambrian			Jhelum	Tobra Fm.							
				Khisor Fm.							
				Jutana Fm.							
				Kussak Fm.							
Pre-Cambrian					Salt Range Formation						
					Khewra S.St.						

Figure 3.1 Stratigraphic map of Sargodha area (Powell, 1979; Kazmi and Rana)

3.2.1 Salt Range Formation

This geological formation holds great importance within the region. The geological formation comprises a sequence of sedimentary rocks, encompassing sandstones, shales, and limestones. The rocks under consideration were deposited within the temporal confines of the Mesozoic era, which included a time period of approximately from 245 to 66 million years in the past. The Salt Range Formation offers valuable insights into the prehistoric marine habitats that were present in the region during that particular period.

3.2.2 Tobra Formation

The Tobra Formation has a somewhat more recent stratigraphic succession in relation to the Salt Range Formation. The composition comprises several constituents such as clays, sands, and gravels. The age and depositional environment of the Tobra Formation exhibit variability, although it is commonly inferred to have originated in riverine and fluvial contexts.

3.2.3 Chinji Formation

This formation consists of sandstones, siltstones, and conglomerates. It is a piece of the Siwalik Group, a series of sedimentary rocks that were formed during the Miocene period (about 23 to 5.3 million years ago) in terrestrial conditions. The Chinji Formation provides light on the prehistoric ecosystems and landscapes that formerly covered this area.

3.3 Hydrogeology of the area

The major rivers in Punjab, Pakistan are the Indus River, Chenab River, Jhelum River, Sutlej River, and Ravi River. The geographical region situated between two rivers is commonly referred to as a Doab. The region of Punjab is comprised of four distinct Doabs, namely Rachna, Ravi, Bari, and Chaj. The management of water resources in the Rachna Doab region primarily relies on the conjunctive consumption of both groundwater and surface water sources.

Groundwater is mostly utilised to augment canal water supply in situations where the available water is inadequate, especially during the summer season when river discharges are at their lowest levels.

The depletion of groundwater resources has been exacerbated by the rapid proliferation of privately-owned tube wells utilised for irrigation purposes. The extraction of groundwater from these wells is resulting in a gradual decline in the water table level. In regions with low discharge

rates in the middle Doab of Rachna, the transportation system and excessive irrigation in grasslands often lead to water resource crises in canals. These crises primarily occur during the summer season when the river's discharge rate is significantly reduced. In addition, Similar to other aquifers located in the Punjab region. Rachna possesses unconfined aquifers. Encountering a constrained scenario may be observed when significant clay horizons are present, particularly if these horizons are located in close proximity to the surface. The uppermost layer of the alluvium, measuring 183m in depth, primarily comprises fine to medium sand and silt particles. Alluvium was encountered in the entirety of the test borehole, which reached a maximum depth of approximately 1,500 feet. Therefore, there is a lack of evidence on the comprehensive measurement of the width of alluvium and the depth to the cellar complex in the Rachna Doab districts (Kidwai, 1962; WASID, 1964). The volume of total dissolved solids in groundwater exhibits great variation, with salinity perhaps being the primary issue associated with groundwater in the majority of places within Rachna Doab (Gupta et al., 1996; Bakhsh and Awan, 2002).

3.3.1 Aquifer System

The primary hydrogeological formation in the Sargodha region consists of unconsolidated alluvial sediments, serving as a significant reservoir of subsurface water resources. The previously discussed deposits possess considerable thickness and typically exhibit porosity and permeability, facilitating the transport and retention of groundwater.

3.3.2 Groundwater Availability

Groundwater serves as a significant water resource inside the Sargodha region, catering to several essential needs such as household, agricultural, and industrial applications. The availability of groundwater is contingent upon various factors, including the recharge rate, which is determined by precipitation, interactions with surface water, and irrigation techniques.

3.3.3 Recharge Sources

The major mechanism by which the groundwater system is replenished is through precipitation in the form of rainfall. Moreover, the implementation of irrigation techniques has the potential to facilitate the replenishment of groundwater by the infiltration of surplus water from canals or fields into the underlying aquifer.

3.3.4 Water Quality

The variability of groundwater quality in the Sargodha region is evident. The phenomenon is subject to various influences, including the geological characteristics of the region, land utilization methods, and anthropogenic actions. harmful problems may arise over salinity, nitrate contamination resulting from agricultural runoff, and other harmful contaminants.

3.3.5 Over-Exploitation and Sustainability

Similar to several regions that heavily depend on groundwater, the Sargodha area is susceptible to potential issues associated with the excessive utilization of its groundwater reserves. The act of pumping water excessively can result in various negative consequences, including the depletion of water tables, the sinking of land, and the degradation of water quality. The implementation of sustainable groundwater management strategies is of paramount importance in order to guarantee the long-term availability of this vital resource.

3.3.6 Hydrological Studies

The Sargodha area benefits significantly from the implementation of local hydrological studies, groundwater monitoring networks, and research endeavors, as these are vital in comprehending and effectively managing the hydrogeological conditions in the region.

To obtain the most up-to-date and comprehensive understanding of the hydrogeology in the Sargodha region, it is advisable to refer to recent geological surveys, scholarly articles, or studies published by local water management authorities in Pakistan.

Chapter 04

Materials and Methods

4.1 Introduction

The earth's ability to react to electric currents facilitates the utilization of various geophysical techniques. During the early 19th century, the technique of utilizing natural electrical current measurement was employed for the purpose of detecting subterranean ore deposits. Despite being utilized in the year 1800, it took a whole century for this technology to attain practicality. The geo-electrical approaches primarily aim to identify and measure the resistivity values of the subsurface. Subsequently, these values are employed for the estimation of several subsurface parameters, including lithology, fractures, faults, pore content, cavities, and pollution. The resolution, depth, and aerial extent of these research are contingent upon the subsurface variation. Electrical measurement can be broadly categorized into two primary areas. For instance, there are two types of variables in experimental research: controlled variables and uncontrolled variables. The uncontrolled methods encompass natural sources, such as electrical currents and electromagnetic variations produced by underlying ore bodies. This category of methods is capable of detecting deeper variations and is particularly suitable for huge bodies. Additionally, aircraft techniques can also be employed to conduct this type of survey. The controlled approaches encompass the process of introducing artificial current into the subsurface through the use of electrodes, followed by the measurement of the resulting current movement in the subsurface using additional electrodes. This methodology is primarily employed to get superficial information. Vertical electrical sounding (VES) and electrical resistivity tomography (ERT) are two prominent techniques that have gained recognition in the field of subsurface geophysical studies, among other controlled procedures. The Vertical Electrical Sounding (VES) method is extensively utilized for groundwater detection. Additionally, the interpretation of paleo-depositional environments in quaternary deposits is another significant application of electrical sounding. This technique not only aids in identifying water-bearing zones but also serves as a valuable tool for understanding recent basin deposition.

4.2 Vertical Electrical Sounding

The vertical electrical sounding technique was first identified and documented in 1920 by Gish and Rooney (1925). Since its inception, this method has gained significant traction in the field of groundwater study. Its widespread usage may be attributed to several factors, one of which is the affordability, portability, and user-friendly nature of the equipment employed in this technique. The desired outcomes manifest as apparent resistivities of the underlying layers. The electrical resistivity of various sediments and rocks on Earth varies due to their heterogeneity, which is influenced by factors such as material density, porosity, pore size, form, and the physical characteristics of water. Resistivity measurements are influenced by topography and local variations in surface conductivity, mostly attributed to factors such as moisture content and weathering.

The fundamental idea entails the introduction of an electric current through the utilization of two electrodes that are coupled to a battery. The electrode that is linked to the negative terminal is commonly referred to as the sink, whereas the electrode that is connected to the positive terminal is commonly referred to as the source. The presence of a potential difference results in the establishment of a current that is driven to traverse pathways that extend from the source to the sink. The determination of three-dimensional current flow patterns can be achieved by the combination of source and sink effects (Bryan & Cox, 1968). The electrical resistance of the surface layers can be assessed by employing Ohm's law. According to Consoliver and Mitchel (1920), the Ohm's law postulates that the magnitude of electric current passing through a conductor connecting two places is directly proportional to the voltage across the conductor, while being inversely proportional to the resistance offered by the conductor.

Mathematically;

$$V \propto I \quad (4.1)$$

$$I = V/R \quad (4.2)$$

$$V = IR \quad (4.3)$$

Where

R= Resistivity in Ohms.

I= Current in Amperes.

V= Potential Difference in Volts.

The interpretation of resistivity data relies on the fundamental assumption that the subsurface geological layers are characterized by a sequence of finite thickness, homogenous, isotropic, and horizontally oriented strata (Koefoed, 1979). The interpretation of actual resistivity values of subsurface strata in relation to hydrogeology and geology is challenging because to the broad range of resistivity values exhibited by different rock types and the presence of suppression and equivalence principles in resistivity techniques. However, via the utilization of well data and geological knowledge pertaining to the region, it becomes possible to identify distinct zones of resistivity that correspond to various hydrogeological and geological divisions. The combined utilization of electrical resistivity survey and well inventory survey has been shown to yield favorable outcomes in the identification and demarcation of aquifer zones, as well as the determination of the depth and thickness of various subsurface formations. Furthermore, this approach enables the mapping of both vertical and horizontal extensions of these formations (Telford, 1990). The field resistivity values obtained by measurement may not accurately represent the characteristics of the earth's strata due to the inherent anisotropy and heterogeneity of the earth. Furthermore, the aforementioned numbers are the combined outcomes of the resistivity exhibited by subsurface layers, with the measured resistivity being referred to as the apparent resistivity.

It is important to note that the apparent resistivity is determined by calculating the ratio of the measured voltage to the applied current. The variation in the location and spacing of the four electrodes will result in alterations to the apparent resistivity. The resistivity variation is heavily influenced by the distribution and resistivity of underlying material (Walton, 1970).

4.3 Electrode Configuration

The term "configuration" refers to the specific arrangement of electrodes employed in the process of measuring. The configuration of electrodes can vary significantly based on factors such as the

nature of the problem being studied, the feasibility of conducting measurements in the field, the depth of the research, and potential limitations in measurement and interpretation. The Wenner setup, Schlumberger configuration, and Dipole configuration (as shown in Figure 3.1) are frequently employed in practice.

The Wenner arrangement is characterized by the presence of electrodes that are uniformly separated, and this spacing remains constant throughout the survey. The aforementioned technique demonstrates effective lateral coverage. However, it is important to note that following each reading, all four electrodes are subsequently relocated to adjacent positions. It is worth mentioning that the depth of infiltration is inversely proportional to the distance between electrodes within the same ground. By altering the spacing between electrodes, valuable insights regarding the stratification of the ground can be obtained (Dahin, 2001).

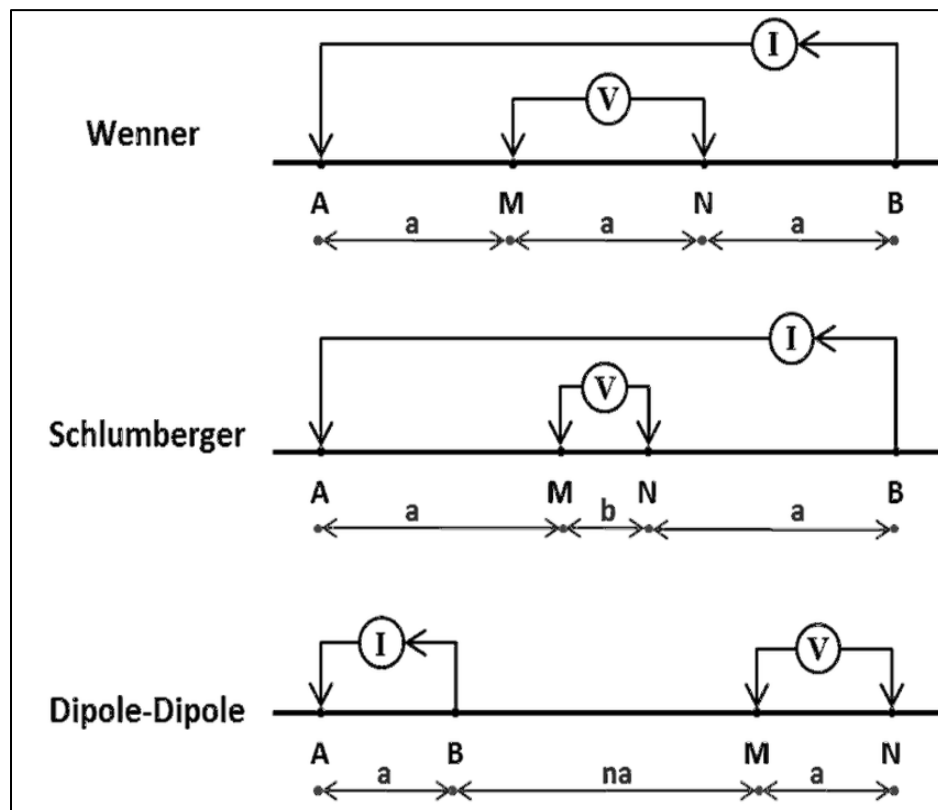


Figure 4.1 Showing Electrode Configuration (et al. Garofalo 2014)

The Schlumberger array is comprised of four electrodes. However, in this particular arrangement, the electrodes responsible for potential measurement remain stationary, but the electrodes responsible for current measurement are adjusted after each reading. The potential electrode and liner arrays are commonly positioned in close proximity, generally at a distance that is less than one-fifth of the spacing between the current electrodes (see Figure 3.1). According to Fetter (1994), it is commonly observed that the length of AB is five times more than the length of MN. The resistivity is determined by the following equation:

$$\rho_a = kdvI$$

Where,

ρ_a = apparent resistivity

k = geometric factor

dv = potential difference

I = current

The dipole configuration exhibits distinct differences when compared to both the Wenner and Schlumberger arrangements. The system is comprised of four electrodes. The sole distinction is in the spatial separation between the potential electrodes and the current electrodes. That is to say, the placement of potential electrodes within current electrodes is not a need. This approach provides comprehensive data in both horizontal and vertical dimensions, with the sole constraint being the necessity for a more powerful battery.

4.4 Importance of Schlumberger Configuration

The Schlumberger configuration has been proposed as an analytical framework to account for both subsurface anomalies and surface irregularities (Bhattacharya, 1968). The Wenner arrangement allows for a greater depth of penetration, specifically $AB/2$, compared to a depth of $AB/3$ in other configurations. The vertical electrical sounding is not influenced by surface inhomogeneities. The utilization of the partial matching technique can also be extended to the

analysis of multilayer curves. However, it is important to note that this approach can only yield accurate results when applied to the Schlumberger setup, as depicted in (Figure 3.1).

It is vital to acknowledge that the configuration of electrodes necessitates less exertion, time, and labor, since it solely requires the relocation of current electrodes at each stage. In addition, the electrodes MN are affixed in a set manner to ensure a consistent amount of readings.

4.5 Data Acquisition

The following are the steps involved in planning and collecting resistivity data at the study area.

4.5.1 Field Planning

It all comes down to picking the right spots to measure the local resistivity. When choosing a location, factors such as topographical variety, vegetation, and accessibility are crucial. There are 28 VES points in the current study region. The vertical electrical sounding technique was used to collect all of the data points.

4.5.2 Resistivity Data Collection

Using a Schlumberger electrode setup, data was acquired. $AB/2$ values and apparent resistivity make up the acquired data. Apparent resistivity is displayed on the screen after the geometric factor "K" is determined automatically by the device.

4.5.3 Resistivity Data Processing

Data processing for resistivity is completed after acquisition. Data processing provides an estimate of the true resistivity values and depth of subsurface layers. Subsurface units have been interpreted lithological based on their conventional resistivity values. In order to process the field data as needed, the software IPI2WIN is employed. This software, on the other hand, was simple and quick to use. The following are some of the more common data processing tasks involved in electrical resistivity prospecting.

4.6 Vertical Electrical Sounding Curves

Sounding curves show the effective relationship between apparent resistivity (ρ) and electrode spacing ($AB/2$). The current electrode separation was shown on the horizontal abscissa and the equivalent apparent resistivity readings along the ordinate in the bi-logarithmic sheet field data

for each sounding. The acquired curve is referred to as the VES field curve. Different types of VES curves are generated based on subsurface lithological strata.

4.6.1 Curve Matching Technique

The approach for partial curve matching, as defined by Mooney et al. (1966), was employed for interpretation subsequent to the identification of curve types. The worldwide methodology employs a combination of two-layer master curves and auxiliary point diagrams. The thickness and actual resistivity of each layer were obtained for each sounding station curve. The traditional curve matching method was employed to determine the thickness and true resistivities of subsurface layers including various ground models.

4.6.2 Process of Iteration

In cases when the field curve and resistivity curves do not align completely, the process of iteration is employed to refine the determination of the true resistivity value and thickness. The disparity between the observed and calculated curves serves as a determinant for the condition of the estimated parameters. The modified factors are once again employed in the calculation of the sounding curves in order to account for the relative nature of the outcome. The iterative technique is employed to the sounding curve until it aligns with the Master curve.

4.6.3 RMS Error/Fixing

Root Mean Square is referred to as RMS. The application sets a default value of 2.5%, however it can be changed as desired. A percentage is used to compute the new goal RMS error. RMS error is also computed using the curve window. At the top of the curve, it appears to be a bar menu. The iteration technique gradually lowers the RMS error. The RMS error progressively reduces until the sounding curve and master curve have been perfectly matched. For optimal results, the RMS error should be less than 1%.

4.6.4 Adjusting Noisy Points

The points that exist outside the curve are referred to as outliers. The potential causes of the observed noisy data points in the field may include current leakage and improper placement of electrodes to the ground, among other factors. By using an iterative process, the root mean square (RMS) error will decrease. However, if the RMS error does not decrease, it indicates that the data points need to be explicitly defined and afterwards adjusted to account for the presence of

noisy data points. The IPI2WIN software offers many options for modifying noisy points, including single point adjustment, moving of the entire segment, and eccentricity alteration.

4.6.5 Vertical Lithological Columns

The thickness and real resistivity values of several earth layers were determined using resistivity analysis, and subsequently represented in the form of lithological columns. The aforementioned columns provide information regarding the subsurface lithologies observed at the VES sites. Various lithologies have been recognized by the utilization of standardized resistivity data.

4.7 Rock Resistivities

Minerals and rocks exhibit a diverse spectrum of resistivity. The existing movement in the Earth's crust is governed by the fluids that exist within the pore spaces. Several factors influence the passage of current, including the characteristics of the rock matrix, porosity, water quality, and its contents. Metallic ores and clay minerals possess the ability to conduct electric current. According to Zohdy et al. (1974), the resistivity of dry and unsaturated rocks is greater than that of saturated rocks, and the resistivity is further reduced by the presence of fluids with lower salinity.

According to Todd and Mays (2005), sedimentary rocks often exhibit low resistivity as a result of fluid present, whereas igneous rocks tend to display high resistivity. Metamorphic rocks, on the other hand, have resistivity values that fall within an intermediate range.

Table4.1 Numerical values for various types of water.

Type of Water	Resistivity(ohm-m)	Conductivity (micros/cm)	Salinity (mg/l)
Very fresh	200	50	35
Fresh	20	500	150
Salted	10	1000	700
Sea Water	0.3	30000	35000

Table 4.2 Resistivities of some common rocks.

Material	Nominal resistivity ($\Omega \cdot m$)
Quartz	$3 \times 10^2 - 10^6$
Granite	$3 \times 10^2 - 10^6$
Granite (weathered)	30 – 500
Consolidated shale	$20 - 2 \times 10^3$
Sandstones	200 – 5000
Sandstone(weathered)	50-200
Clays	1 – 10^2
Boulder clay	15 – 35
Clay (very dry)	50 – 150
Gravel (dry)	1400
Gravel (saturated)	100
Lateritic soil	120 – 750
Dry sandy soil	80 – 1050
Sandy clay/clayey sand	30 – 215
Sand and gravel(saturated)	30 – 225
Mudstone	20-120
Siltstone	20-150

4.8 Generation of Cross sections

The lithologs derived from the Vertical Electrical Sounding (VES) data were linked in order to construct cross sections. Through this procedure, a total of seven cross sections, namely A-A/, B-B/, C-C/, D-D/, E-E/, F-F/, and G-G/, were produced. These cross sections provide a description of the distribution of paleo-depositional channels within the research area.

4.9 Resistivity Configurations

All three configurations, namely Wenner, Schlumberger, and Dipole-Dipole, were employed in order to measure apparent resistivity values, which allows the mapping of even the most modest subsurface features.

4.10 The Parameters of Dar-Zarrouck (D-Z) and their Significance

The geological section exhibits a compilation of stratified rock strata, accompanied by diverse surface features that delineate specific geological limits. Furthermore, the geoelectrical modelling portion encompasses distinct zones characterized by varying lithological borders, which exhibit different thicknesses and specific resistivities. The geological part and geoelectrical segment do not exhibit any overlapping boundaries. According to Zohdy (1974), it is possible to build a geoelectrical section unit by combining many strata that possess consistent electric properties. The identification of many geoelectrical stratums within a single lithological layer, characterized by varying salinity values of groundwater at different depths, can be elucidated through the use of examples. On the contrary, it is plausible that rocks of varying ages and lithology, or their amalgamation, may have comparable resistivity values, thereby forming a unified geoelectrical layer. The geoelectrical properties of a unit in a layered section are commonly described using five fundamental parameters known as Dar-Zarrouck parameters (Maillet, 1947). The parameters discussed in this study are determined through the use of the thickness (h_i) and resistivity (ρ_i) values associated with a geoelectrical layer. The most noteworthy of these characteristics are visually presented in Figure 3.2

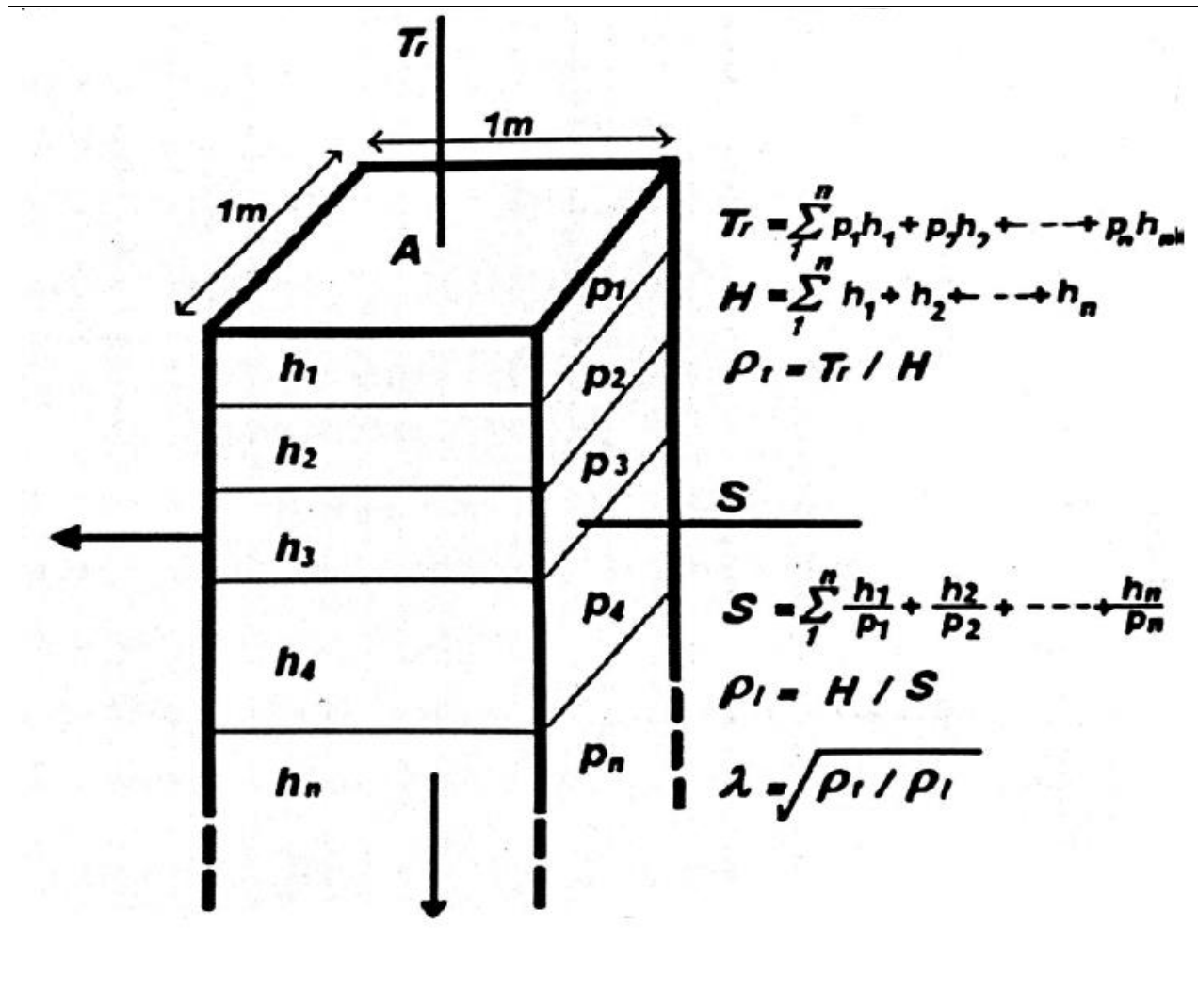


Figure 4.2 Theoretical procedure for determining the Dar zarrouk parameter

The necessary parameters for a model are derived by integrating several combinations of resistivity and thickness values for each stratum (Orellano, 1963; Singh, 2005). The parameters discussed herein have shown to be highly valuable in the field of geoelectrical methodology. Notably, Maillet employed the terminology of Dar-Zarrouk parameters (D-Z) to refer to these specific parameters. The aforementioned characteristics are employed in the computation of a distribution of surface potentials. This distribution pertains to a unit consisting of 'N' layers, each characterized by distinct resistivity values ($P_1, P_2, P_3, \dots, P_m$) and variable thicknesses ($h_1, h_2, h_3, \dots, h_n$). These layers collectively form a square unit area with a total thickness denoted as H, which is the sum of the individual thicknesses ($\sum_{i=1}^n h_i$).

Chapter 05

Geoelectrical Modelling

5.1 Interpretation of field curves

The challenge of accurately interpreting resistivity sounding data in relation to the thickness and resistivity of the underlying beds poses a significant difficulty. In order to accurately interpret geoelectrical sounding curves, it is important to possess a comprehensive understanding of the geological characteristics specific to the area under investigation, as well as substantial practical expertise. The interpretation of geoelectrical sounding curves is conducted in a qualitative manner with respect to the geological characteristics of the surveyed region. The present study used the curve matching technique as one of the methods for interpreting VES data.

5.1.1 Curve matching method

The determination of layer parameters from the VES curves is achieved by the utilization of a curve matching technique.

The field curves are aligned with standard curves in order to determine the layer parameters. The layer parameters in this investigation were acquired through the utilization of the 'IPI2WIN' program.

5.2 Correlation between sounding curve and borehole lithology

The lithological data acquired from the borehole and the geological features of the study region have been utilized to rigorously analyze and calibrate the Vertical Electrical Sounding (VES) data. This calibration was performed by closely comparing the VES data with the adjacent well data. The examination of the relationship between resistivity and grain size offers significant insights into the interpretation of resistivity data in respect to sedimentary formations. In the field of geology, it is commonly recognized that gravel exhibits greater resistivity values in comparison to sand. In a similar manner, it is noteworthy to mention that the resistivity of sand exceeds that of clay, as emphasized by Akhter and Hasan (2016). To build a coherent link between the different lithologies present in the sub-surface integrated layers and the resistivity values derived from the models, it is most desirable to employ the inverse electrical models. These models provide the

most exact matching. The geological sections in close vicinity to the boreholes have been determined by employing the calibrated Vertical Electrical Sounding (VES) data. The calibration of these sections has been conducted using the lithologies acquired from three boreholes located within our designated research region, as seen in Figure 5.1, 5.2 and 5.3. There is an evident association that can be discerned between the inferred vertical electrical sounding (VES) geologic sections and the lithological composition of the boreholes.

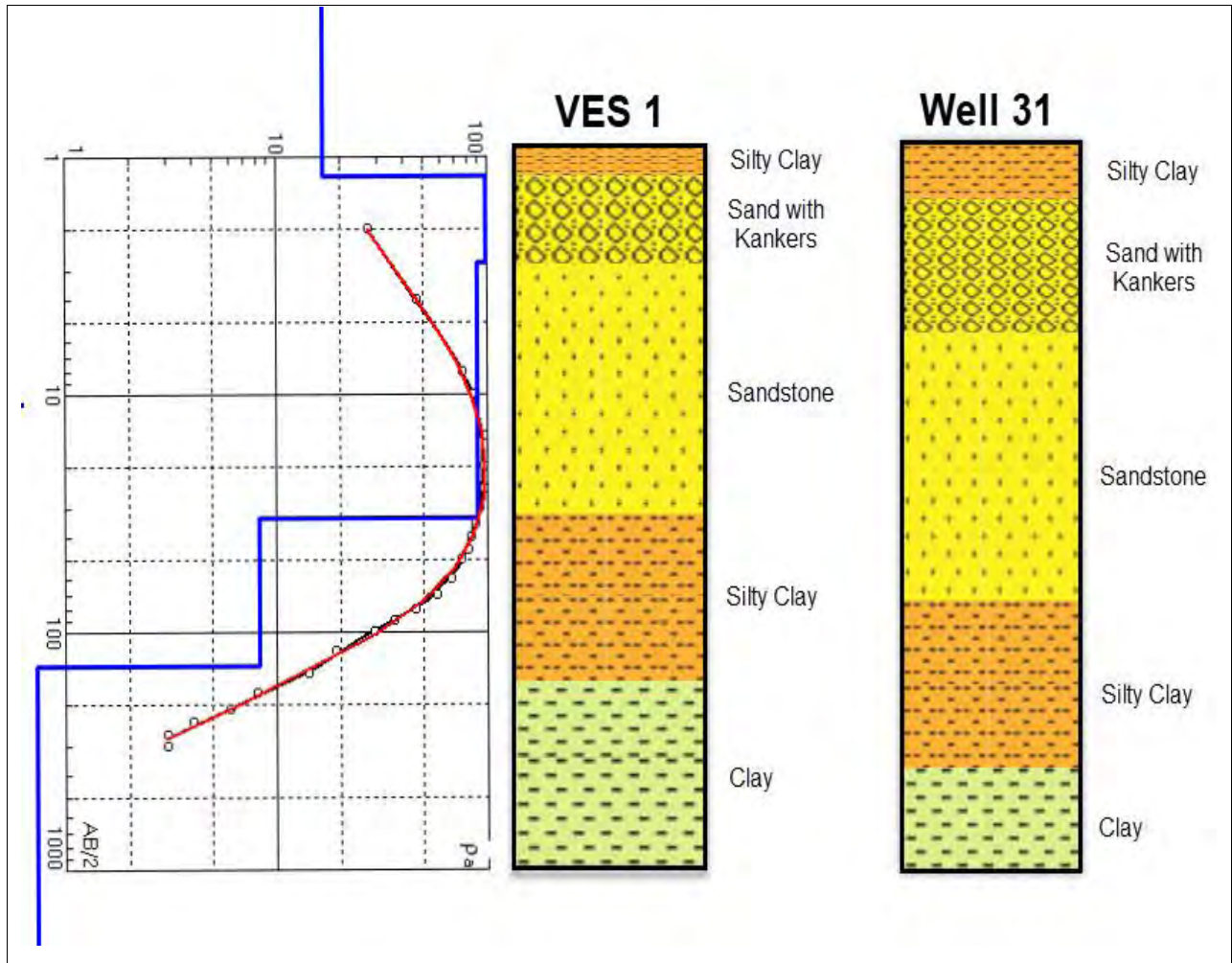


Figure 5.1 Correlation between sounding curves and borehole lithology

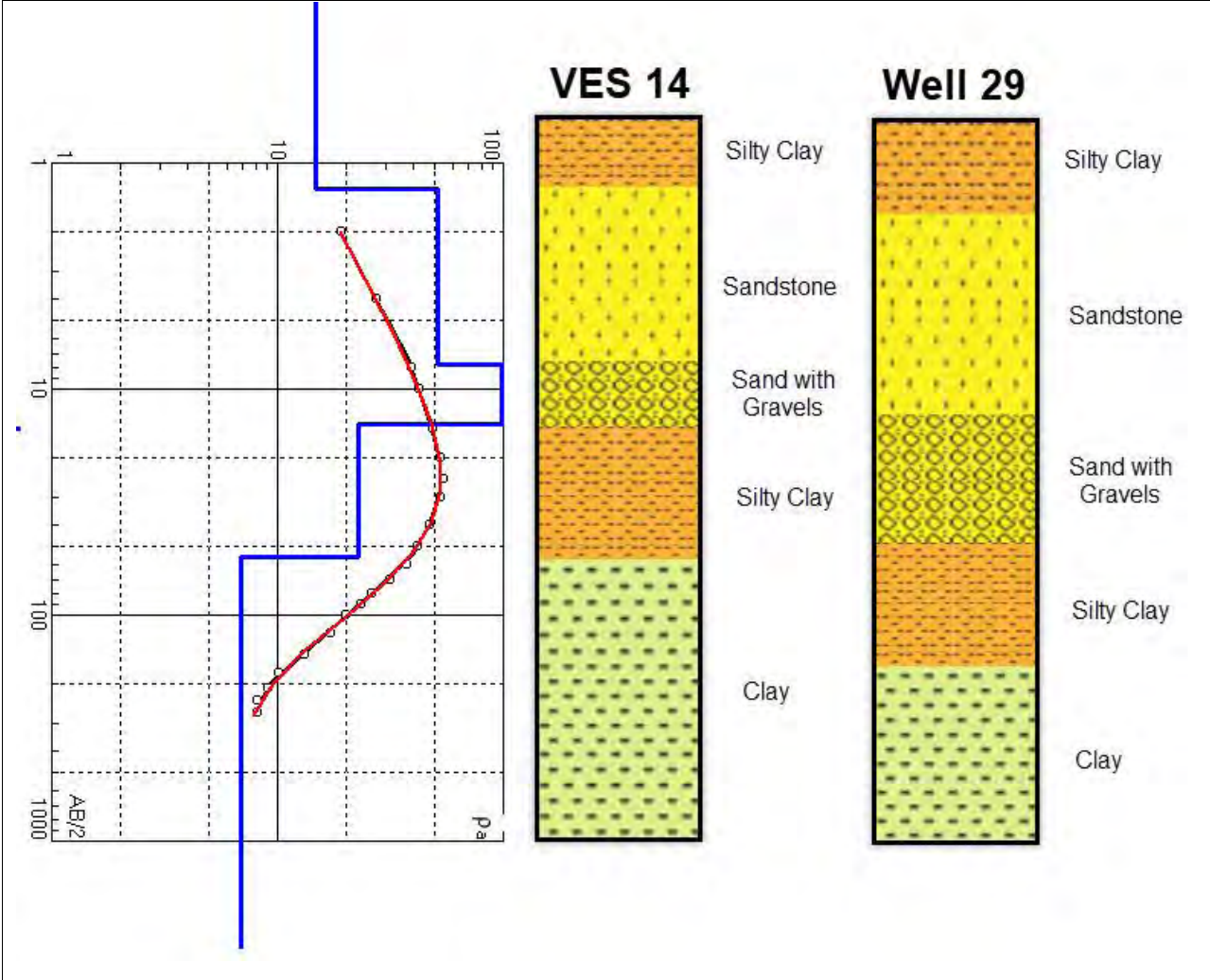


Figure 5.2 Correlation between sounding curves and borehole lithology

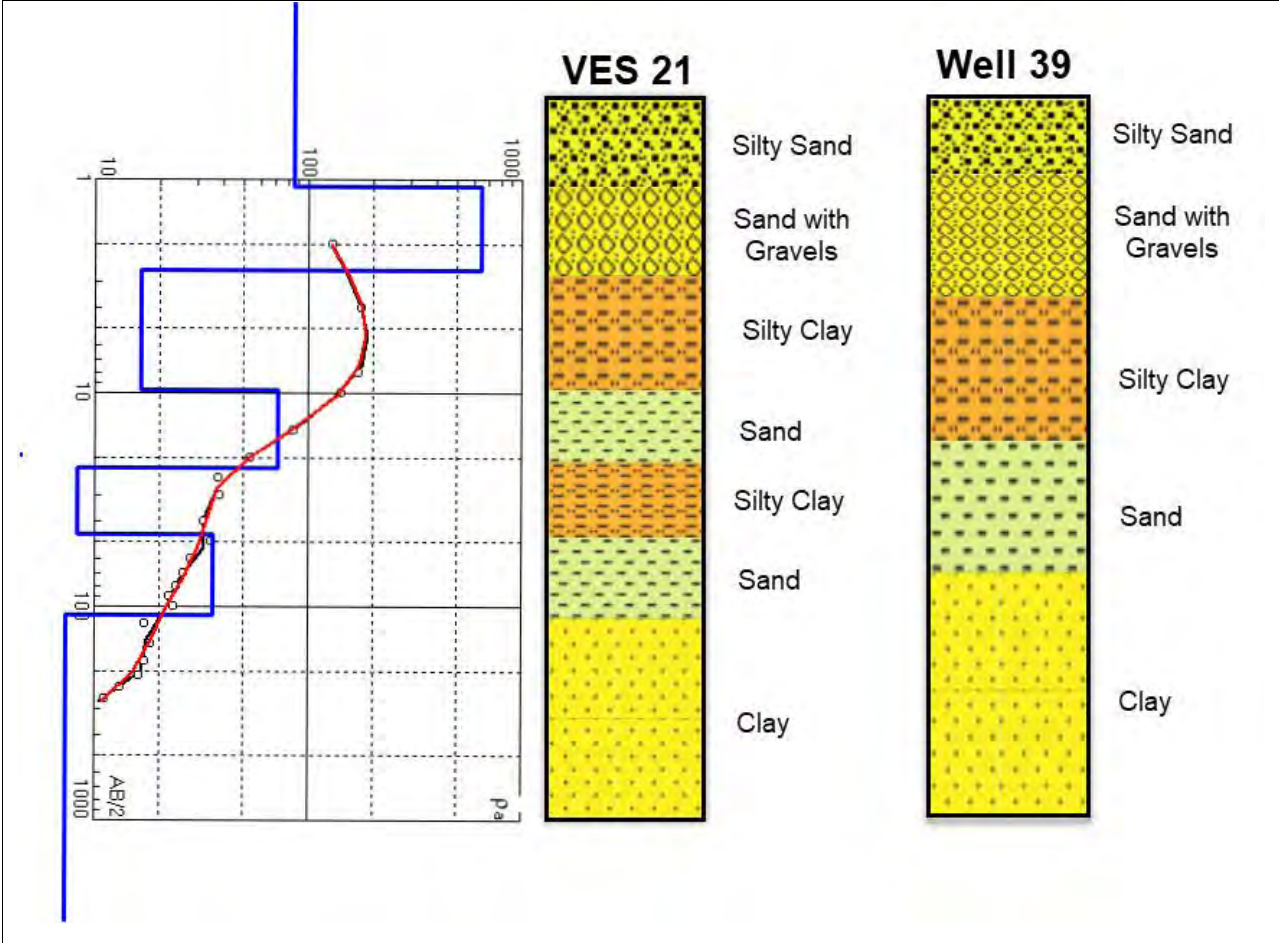


Figure 5.3 Correlation between sounding curves and borehole lithology

5.3 Calibration

The interpretation of resistivity data poses significant challenges, with the level of difficulty varying depending on the interpreter's expertise, particularly among those who possess advanced knowledge in the field. In order to facilitate accurate interpretation, it is imperative to possess comprehensive geological data pertaining to the specific region. The quality of interpretation is greatly enhanced when one possesses a solid understanding of geology, as certain interpretations may require less geological data but benefit greatly from a geological perspective. The collaborative effort between geologists and geophysicists is commonly regarded as the most dynamic approach to the interpretation of geological data (Zohdy et al., 1990).

Table 5.1 Resistivity ranges for various sedimentary formations (Keller and Frischknecht 1966a, 1996b; Bhattacharya and Patra 1968a, 1968b)

Formation	Resistivity ($\Omega\text{-m}$)
Sandstones with fresh water	30–150
Clay with fresh water	7–15
Sandstones with clay	20–40
Clay with sand lenses	8–25
Clay with saline water	3–6
Sand	100

Table 5.2 Resistivity and Lithology Calibration in the Study

Formation	Resistivity ($\Omega\text{-m}$)
Clay and Silty clay	< 25
Sandstone	25-100
Sand with Gravel	100-120
Dry Strata	> 120

The geoelectrical resistivity is a dynamic physical property that is mostly found in complex sedimentary formations characterized by a high proportion of alluvial fans. The resistivity of sand and clay demonstrates fluctuations in response to minor modifications in its composition. The existence of these complexities within the data may give rise to confusion and doubt throughout the process of interpretation, as emphasized by Zhdanov and Keller in their influential publication in 1994. Therefore, it is crucial to align the VES data collected in the field with the matching borehole data, as highlighted by Batayneh (2011). Therefore, it is imperative to assign geoelectrical observations to their corresponding lithologic equivalents in order to guarantee a reliable interpretation of the underlying aquifer. To achieve the stated purpose, a research was undertaken on three boreholes located within the defined study region to determine the correlation of the Vertical Electrical Sounding (VES) results. In order to determine the electrical characteristics of the rock formations at different depths, a comparison was made between the vertical electrical sounding (VES) results obtained from sounding number 1 and the lithology seen in borehole number 31, as illustrated in Figure 5.1.

Based on the observed link between VES 1 and borehole 31, a geological interpretation can be proposed as follows: (i) A resistive layer with a resistivity of 448 $\Omega\text{-m}$ is present, exhibiting variations in thickness and made of a combination of sand and gravel. (ii) A layer of sand with a notable thickness is seen, exhibiting resistivity values of 89.5 $\Omega\text{-m}$. (iii) there is a layer of dry strata above the water table.

The existing body of literature presents a thorough collection of resistivity ranges for various forms, as reported by (Keller and Frischknecht 1966a, 1966b; Bhattacharya and Patra 1968a, 1968b). The previous results have been efficiently condensed and shown in Table 5.1.

The resistivity values presented in Table 5.1 demonstrate a fairly close and overlapping range, indicating a remarkable similarity.

The data reported in Table 5.1 illustrates the presence of a geological formation characterized by the occurrence of clay that is fully saturated with fresh water. The clay layer under consideration demonstrates a resistivity range that extends from 7 to 15 m. Nevertheless, it has been noted that the above clay layer is subject to the impact of an adjacent geological stratum consisting of a mixture of clay and sand. The resistivity values of the clay-sand layer range from 8 to 25 m.

As a result, the existence of these two separate layers presents a difficulty in appropriately understanding the resistivity data. Additionally, it is important to highlight that sandstones that include freshwater have resistivity values that span from 30 to 150 m, a range that roughly corresponds to the resistivity range observed in sandstones containing clay, which typically falls between 20 and 40 m.

The resistivity values of clay when exposed to fresh water normally exhibit a range of 7 to 15 m, however in the presence of saltwater, the range typically falls between 3 and 6 m. The presence of small fluctuations in resistivity ranges poses a significant challenge in accurately delineating underlying geological formations. This phenomenon is particularly applicable to substances like clay, where there may be parallels in resistivity levels seen in both freshwater and saltwater circumstances. Table 5.2 has been constructed to present the resistivity ranges demonstrated by different formations. This achievement has been attained by conducting an examination of layer parameters and afterwards comparing them with the lithological logs that are peculiar to the designated research location.

The research region demonstrates a variety of resistivity in sand when coupled with fresh water, with values ranging from 25 to 100 Ω -m. It is worth mentioning that this particular range exhibits a disparity when compared to the range of 30 to 150 Ω -m that has been seen in the context of sand coupled with fresh water, as shown in Table 5.1.

Similar to geological data, it is worth noting that the resistivity range of clay, namely silty clay, within the research region displays a discernible fluctuation when exposed to the influence of salty water. The measured resistivity value of less than 25 Ω -m is found to be beyond the resistivity range typically associated with clay, as indicated in Table 5.1. It is important to note that the assumption of constant resistivity ranges should not be made, as geological formations can display fluctuations in composition.

5.3.1 Modelling of VES-5

The VES data of apparent resistivity of VES-5 was imported in IPI2Win software. The true resistivity and thickness of subsurface layers was calculated by best fitting the mod with measured filed data.

Figure 5.4 shows that there are 6 geoelectrical layers at VES-5 point. The first layer has true resistivity of 18.3 Ω -m and thickness of 3.01 m. This show that first layers is silty clay. The second layer has 41.9 Ω -m resistivity and 1.15 m thickness. The true resistivity value shows that the second layer is sand together with fresh water. The third stratum has 16.2 Ω -m resistivity and 21.1 m thickness. The third layer true resistivity shows that it consists of silty clay with sand along with brackish water. The 4' stratum has resistivity 7.14 Ω -m indicates silty clay with having salty water. The fifth layer displays a remarkably low resistivity of 0.6 Ω -m, suggesting clay composition and the presence of salty water. In contrast, the sixth layer stands out with a high resistivity of 91 Ω -m, indicating sand and freshwater content.

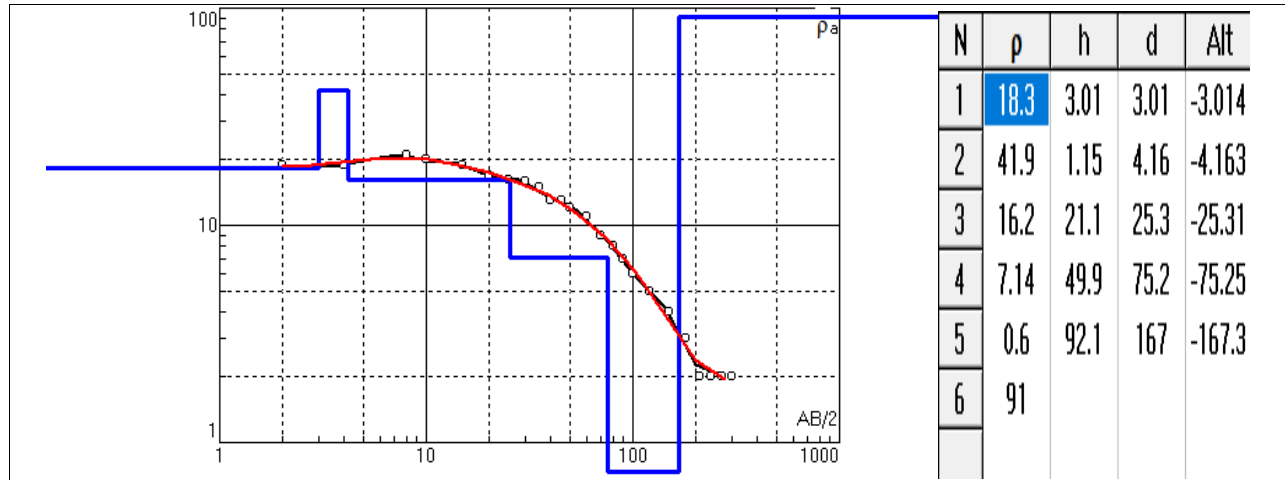


Figure 5.4 Vertical Electrical Sounding VES-5

5.3.2 Modelling of VES-13

The apparent resistivity data of VES-13 was loaded into the IPI2Win software. The determination of the authentic resistivity and thickness of subsurface layers was achieved through the process of optimizing the fit between the model and the measured field data.

According to Figure 5.5, it can be observed that VES-13 point exhibits the presence of four distinct geoelectrical layers. The initial stratum possesses a genuine resistivity value of 14 Ω -m and a thickness measuring 2.39 m. This observation indicates that the uppermost strata consist of silty clay. The resistivity of the second layer is measured to be 27.3 Ω -m, with a thickness of 25.8 m. Based on the obtained resistivity value, it may be inferred that the second layer consists of sand with a brackish water composition. The resistivity of the third stratum is measured to be 81.1 Ω -m, with a thickness of 115 m. The analysis of the third layer's real resistivity indicates the presence of sand and fresh water. The presence of a 4th layer with a resistivity of 1 Ω -m suggests the existence of clay containing saline water.

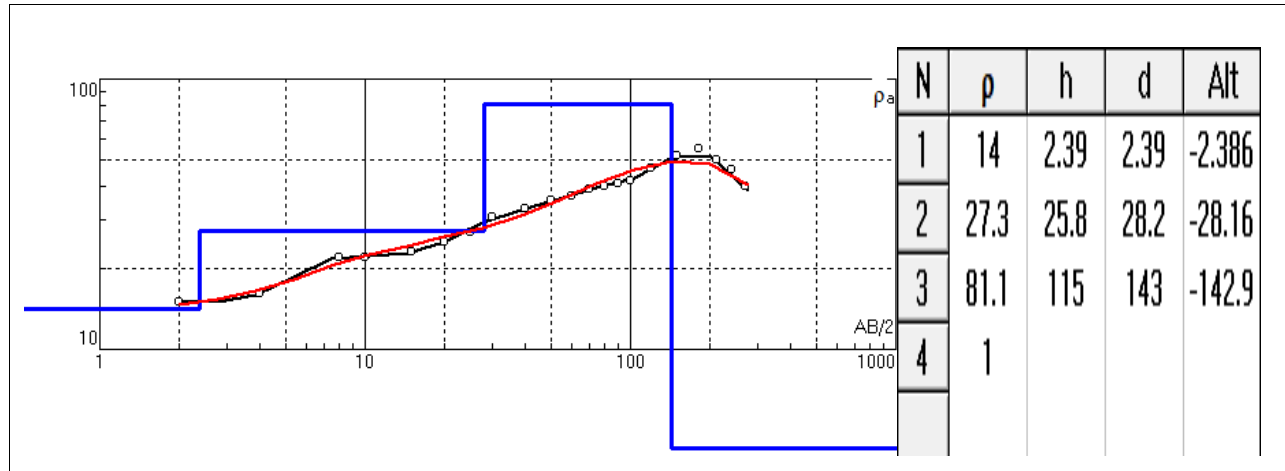


Figure 5.5 Vertical Electrical Sounding VES-13

5.3.3 Modelling of VES-27

The apparent resistivity data obtained from VES-27 was inputted into the IPI2Win software. The method of optimizing the fit between the model and the measured field data was employed to determine the authentic resistivity and thickness of subterranean layers.

Based on the data presented in Figure 5.6, it is evident that the VES-27 point displays the existence of four observable geoelectrical layers. The initial layer exhibits a resistivity value of 13.59 Ω -m and has a thickness of 0.89 m. This observation suggests that the highest layers are composed primarily of clay. The resistivity of the second layer was determined to be 16.4 Ω -m, and it has a thickness of 8.63 m. Based on the acquired resistivity measurement, it can be deduced that the second layer is composed of silty clay with a brackish water composition. The resistivity of the third layer is determined to be 268 Ω -m, and it has a thickness of 3.26 m. The examination of the actual resistivity of the third layer suggests the existence of sand. The identification of a fourth layer exhibiting a resistivity of 35.5 Ω -m implies the potential occurrence of sand and the presence of freshwater.

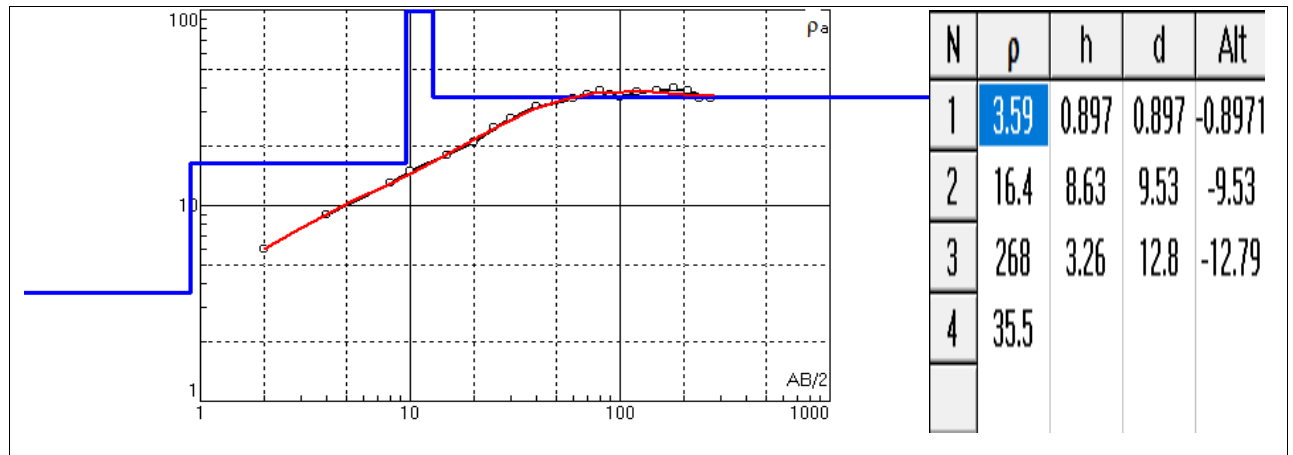


Figure 5.6 Vertical Electrical Sounding VES-27

5.4 Ground water Quality Zonation

The groundwater quality in the research area is depicted using iso-resistivity maps. High resistivity levels indicate the existence of sand particles ranging from slightly mild to fine, hence providing insight into the potential occurrence of freshwater. Medium resistivity values indicate the presence of silt and sand, suggesting the existence of somewhat saline water. Conversely, very low resistivity values indicate the presence of silty and clayey beds, which contain saline water.

5.4.1 Iso-Resistivity Maps of the Study Area

In order to enhance comprehension of the subsurface lithologies, a contour map depicting differences in resistivity of the uppermost layer has been generated, as illustrated in Figure 5.7.

5.4.1(A) Iso-Resistivity Maps of Zone 1 (20)m

Vertical electrical sounding (VES) is used to reveal subsurface properties within a particular zone on the provided map. This method allocates color to the electrical resistivity values measured at various depths beneath the Earth's surface. Low resistivity zones are highlighted, with the colour spectrum signifying their resistivity levels. The red areas indicate the maximum resistivity values, indicating the presence of materials that are highly resistant to electrical current, typically associated with sand and other low-conductivity materials. Due to its low moisture content and large, non-conductive granules, sand typically demonstrates a high resistivity. In contrast, the blue regions indicate the lowest resistivity values, signifying more conductive materials that facilitate the flow of electrical current. These regions correspond to clay, sediment, or other materials with a higher percentage of moisture. Due to their ability to retain water, clay and sediment typically exhibit greater conductivity.

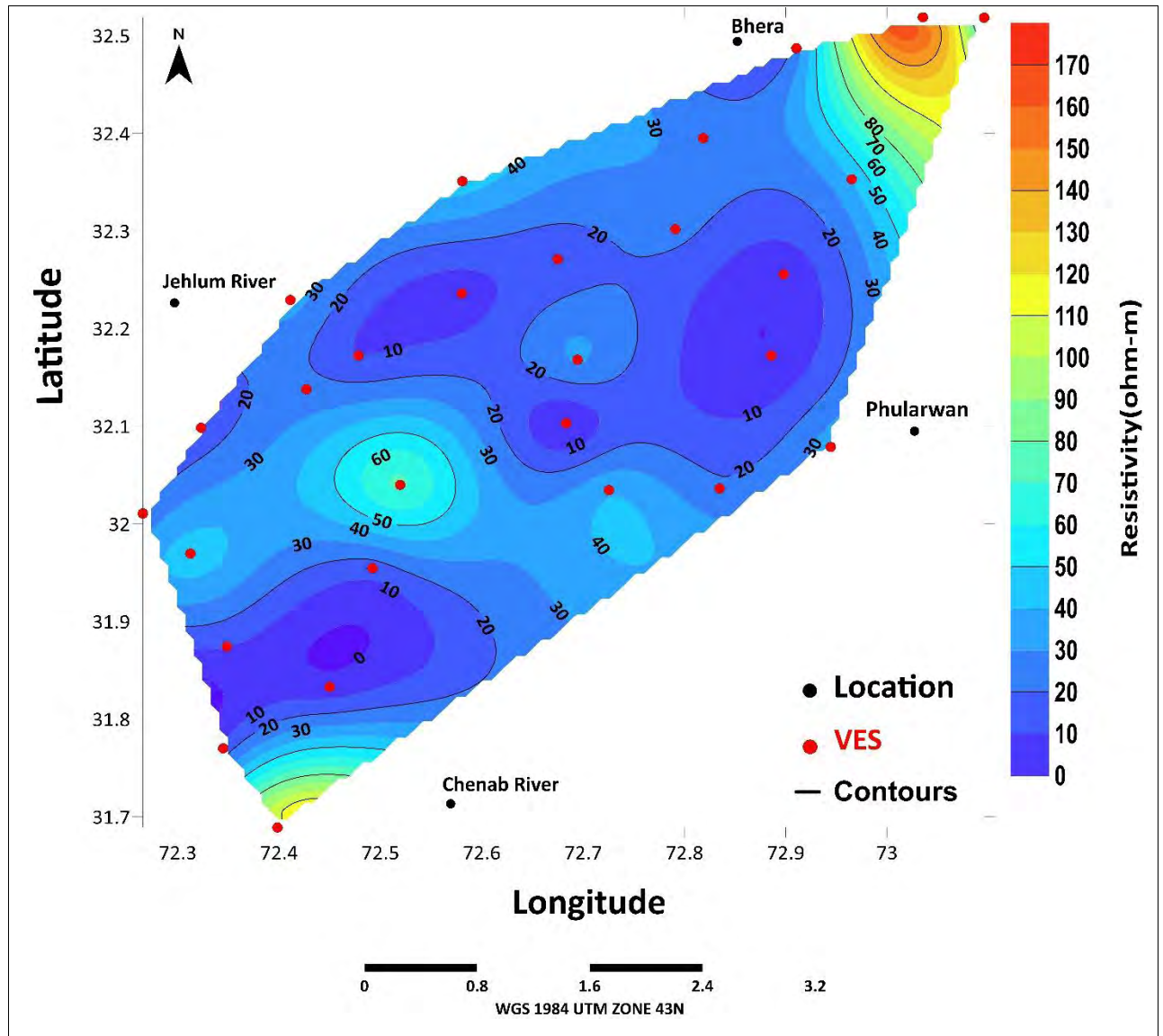


Figure 5.7 Iso-Resistivity Maps of Zone 1 at 20m

5.3.1(B) Iso-Resistivity Maps of Zone 2 (50)m

The Iso-resistivity map of Zone 2 provides a complete depiction of subsurface attributes through the utilizations of color-coded regions, which correspond to distinct electrical resistivity values. The region characterized by a red coloration, exhibiting resistivity values within the range of 220 to 260 Ω -m, indicates the presence of sand and gravel materials.

These substances, consisting of comparatively large and non-conductive particles, demonstrate elevated resistivity and are frequently linked to aquifer formations, underscoring their significance in groundwater systems. Within the region characterized by a green hue, exhibiting resistivity values ranging from 100 to 140 Ω -m, the prevailing geological composition primarily consists of sand.

Although sand has a relatively low resistivity as a result of its smaller particle size in comparison to gravel, it nevertheless plays a substantial role in the movement and storage of groundwater. The blue zone, characterized by resistivity values below 90 Ω -m, signifies the occurrence of silty clay and sand. The presence of silty clay, which possesses high moisture retention capabilities, combined with the conductivity properties of sand, implies a higher capacity for water retention and decreased drainage in comparison to the other zones.

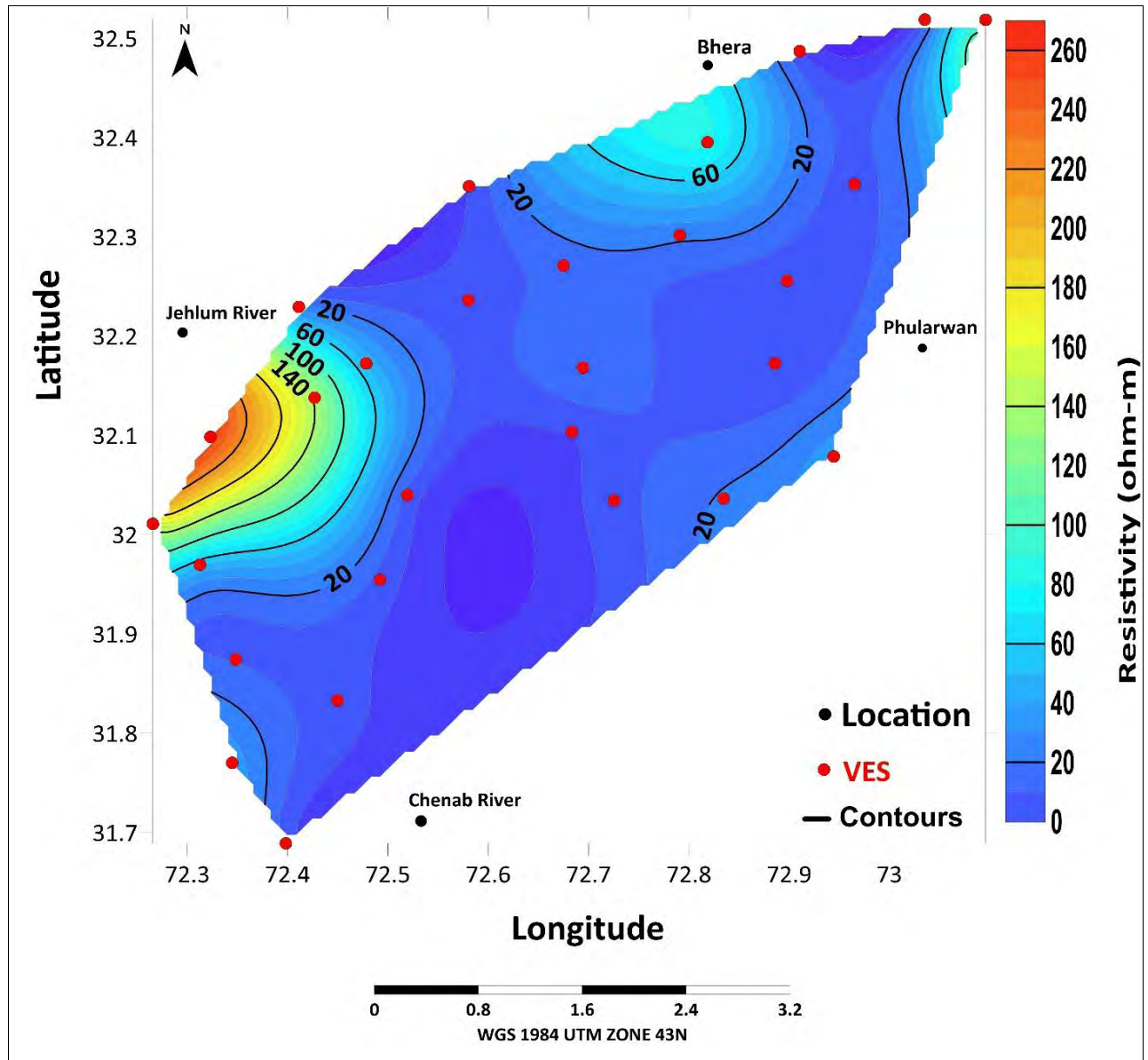


Figure 5.8 Iso-Resistivity Maps of Zone 1 at 50m

5.3.1(C) Iso-Resistivity Maps of Zone 3 (100) m

The Iso-resistivity map of zone 3 depicts the region where greater resistivity values, ranging from 80-100 Ω -m, are represented by the red colour. This particular area exhibits lithology characteristics associated with fresh water. The region characterized by the green colour exhibits a resistivity range of 35-60 Ω -m, whilst the region denoted by the blue colour demonstrates a resistivity below 25 Ω -m.

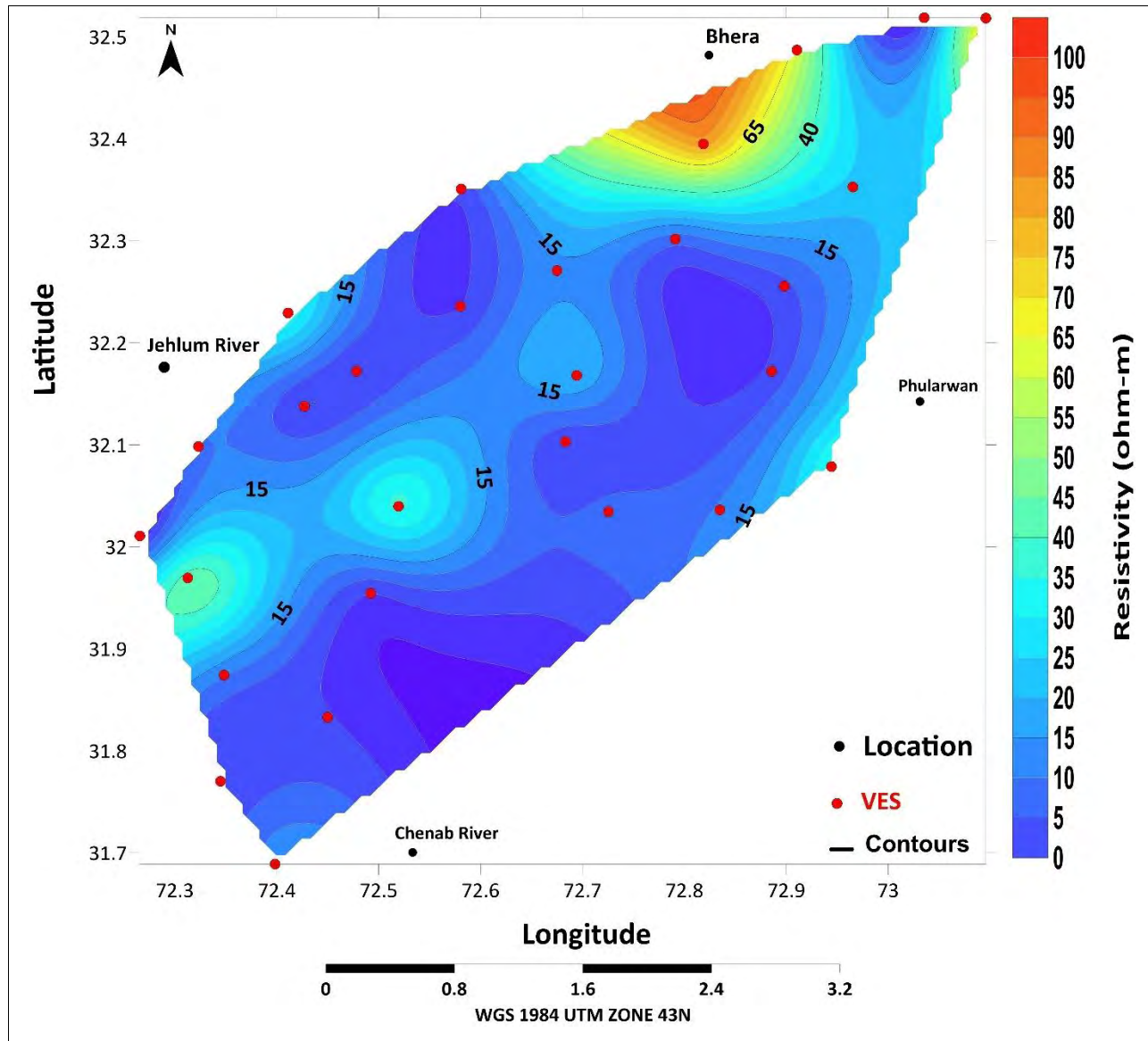


Figure 5.9 Iso-Resistivity Maps of Zone 3 at 100 m

5.3.1(D) Iso-Resistivity Maps of Zone 4 (150) m

In Iso-resistivity map of zone 4 the area under red color shows the higher values of resistivities ranging from 70-100 Ω -m and the lithology and this area have fresh water. Area under green and yellow color has the resistivity range of 35-65 Ω -m. The Iso-resistivity map of Zone 4 holds significant value within the area of hydrogeology as it provides vital insights into the subsurface hydrological conditions.

The map displays regions that exhibit elevated resistivity values ranging from 70 to 100 Ω -m, which indicate the existence of aquifers containing fresh water. The aforementioned zones are commonly characterized by the presence of clean sands and gravels with relatively low conductivity, rendering them highly desirable for the purpose of groundwater exploration and extraction. On the other hand, it can be observed that the green and yellow areas, characterized by resistivity values ranging from 35 to 65 Ω -m, are most likely composed of sandy soils and sediments. These geological features are known to facilitate the storage and movement of groundwater, but with a slightly lower conductivity when compared to the red parts.

The blue regions, characterized by resistivity values below 25 Ω -m, indicate the potential existence of materials with high conductivity, such as fine-grained sediments, clays, or saturated soils. The presence of low-resistivity zones is frequently observed in situations characterized by waterlogging or where groundwater is easily accessible.

Within the realm of hydrogeology, this particular map serves the purpose of facilitating the identification of possible freshwater resources, demarcating the limits of aquifers, and comprehending the geological conditions present under the Earth's surface. These aspects have significant importance in the realm of sustainable groundwater management and resource planning. 5 Ω -m while area under blue color has <25 Ω -m.

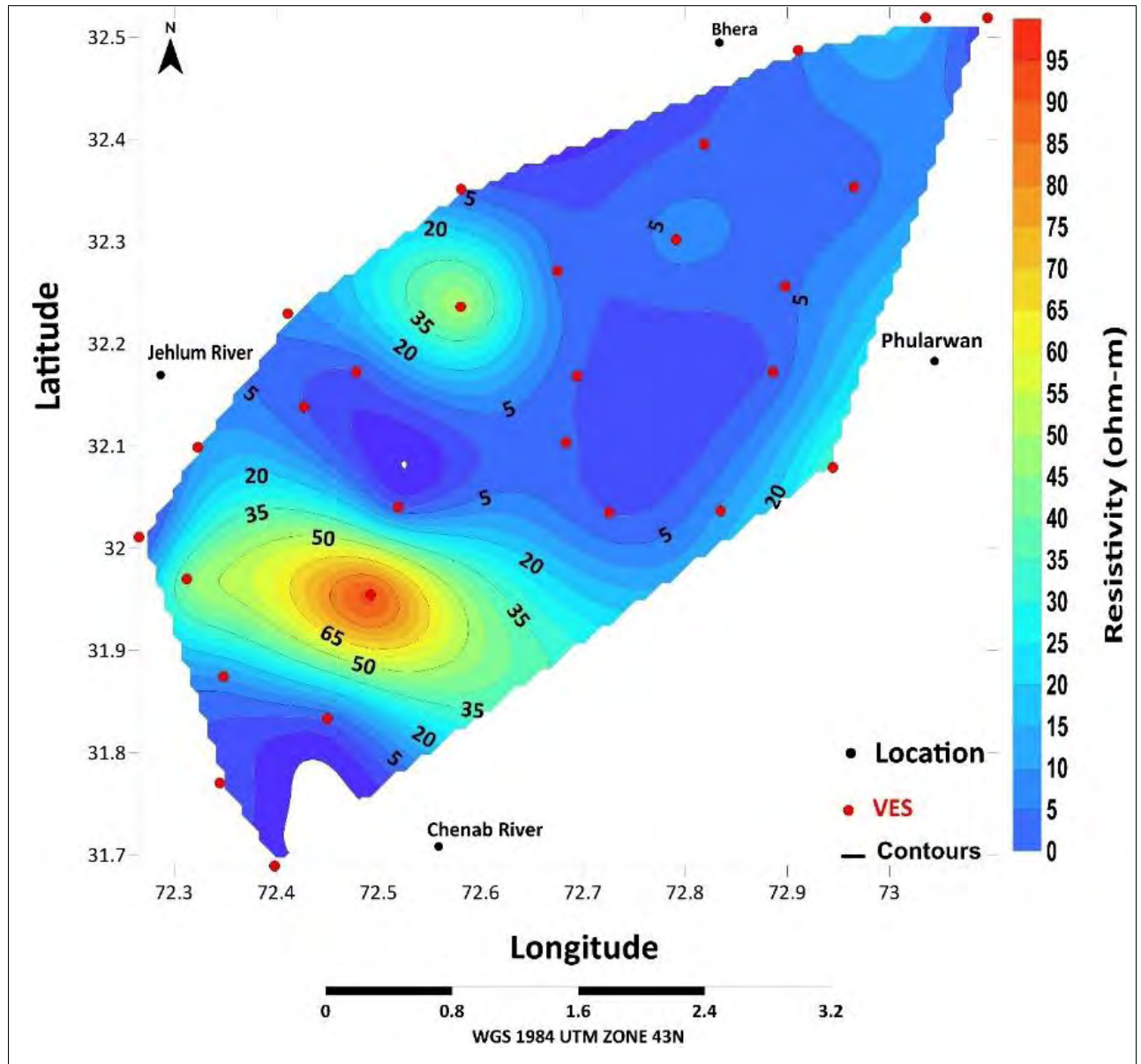


Figure 5.10 Iso-Resistivity Maps of Zone 4 at 150 m

5.4 PSEUDO-SECTIONS

Pseudo-sections play a crucial role in the fields of geophysics, hydrogeology, and environmental sciences by providing essential visual aids for converting intricate subsurface data into easily understandable, two-dimensional depictions. Graphical representations are highly useful in presenting data gathered through linear or profiled data gathering techniques, such as geophysical surveys, groundwater evaluations, and environmental studies.

Pseudo-sections provide valuable insights into subsurface properties, geological structures, groundwater flow patterns, and environmental phenomena by utilizing a graphical representation. This representation involves plotting data points along one axis to indicate distance or depth, while the other axis represents a variable of interest, such as resistivity, groundwater levels, or contaminant concentrations.

A pseudo-section profile is essential to groundwater exploration and characterization in hydrogeology. Electrical resistivity, lithological changes, and water quality readings are plotted versus depth or distance along a survey line to create pseudo-section profiles. Hydrogeologists use these profiles to understand geological formations, aquifer borders, and groundwater potential. Pseudo-section profiles help locate groundwater sources, interpret flow patterns, and assess groundwater quality and quantity by showing the distribution of elements with different electrical or water properties.

Pseudo-section profiles are essential hydrogeological tools for groundwater exploration, sustainable management, and protection. The utilization of five Pseudo-section profiles, namely A, B, C, D, and E, is illustrated in Figure 5.10.

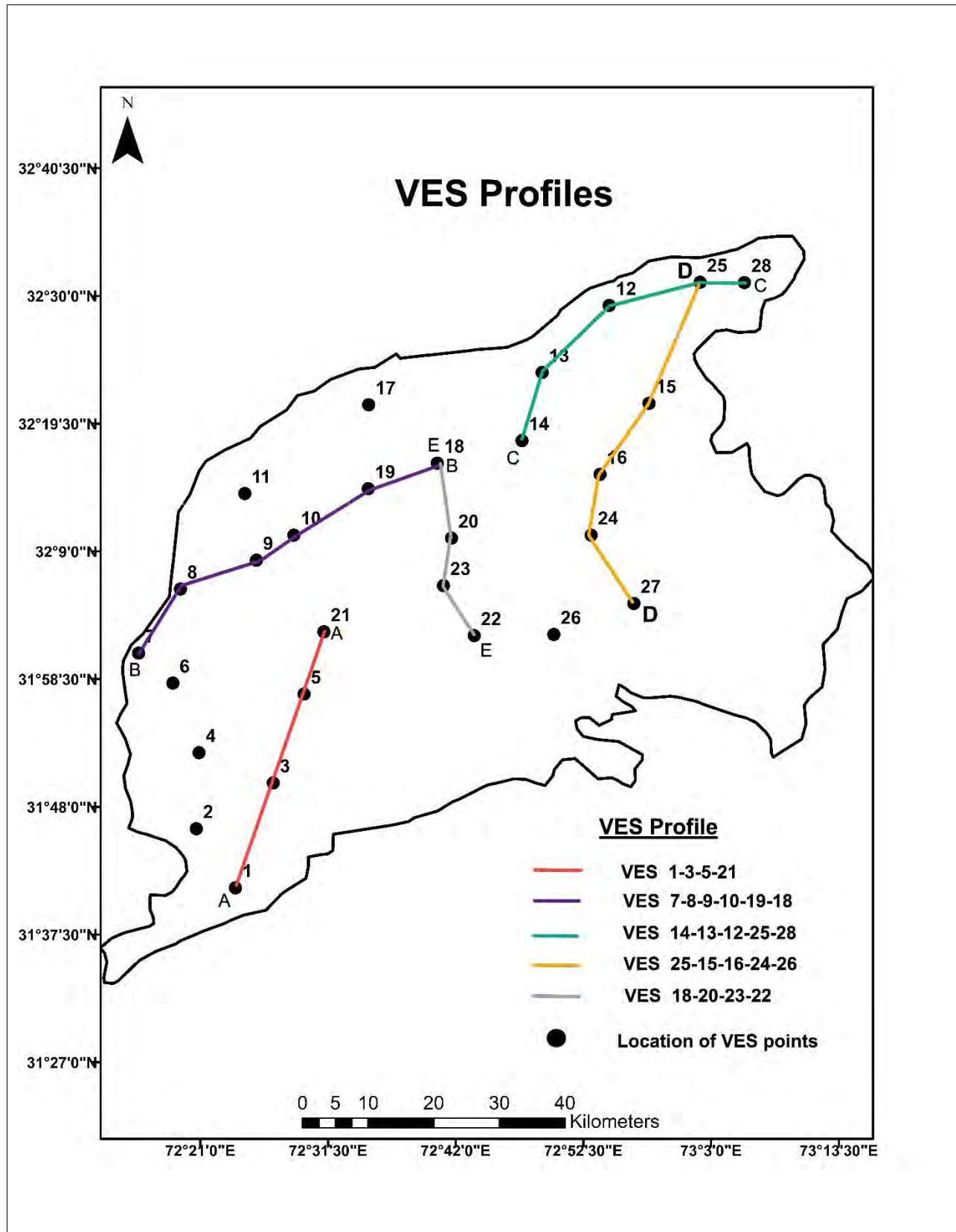


Figure 5.11 Showing VES profiles of the Study Area

5.4.1 Pseudo cross-section along profile A

In the profile A VES 1, 3, 5, and 21 provide hydrogeological insights into the research areas subsurface. A low resistivity zone at the base of VES 1 and VES 3 suggests saturated sediments or an aquifer, suggesting groundwater supplies.

Middle-layer high resistivity may indicate worn or partially cemented minerals that affect groundwater movements. High resistivity in VES 5 midsection suggests a confining layer that affects groundwater flow and recharging. VES 21 low resistivity at the top shows more conductive materials, which could indicate saline or brackish water near the surface, which affects groundwater quality.

These observations suggest an alluvial deposit with groundwater storage potential.

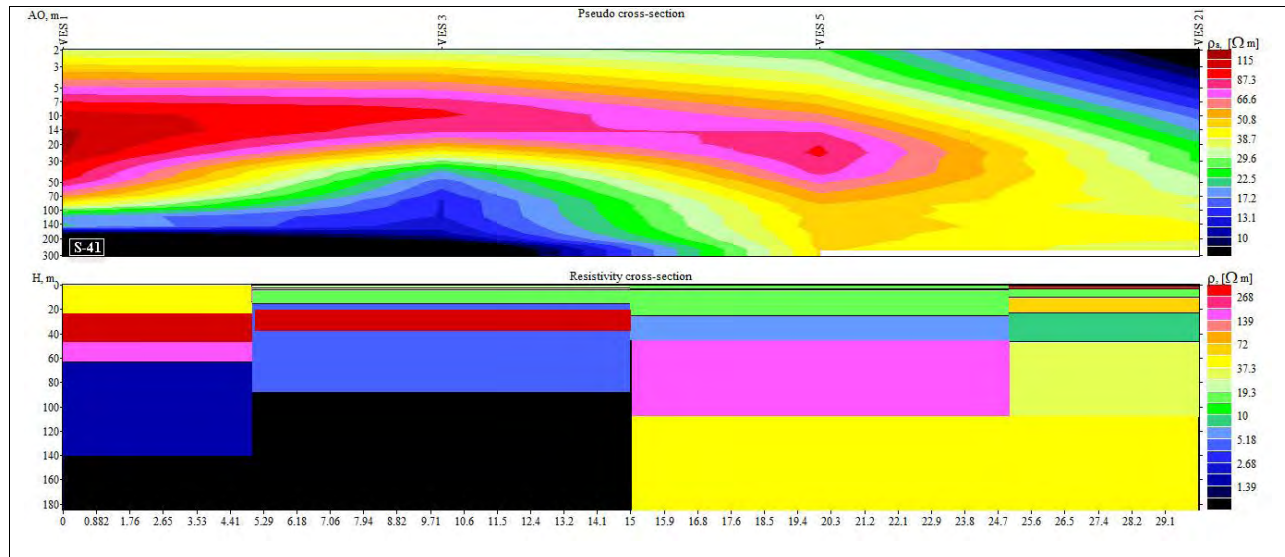


Figure 5.12 Apparent resistivity pseudo cross section for profile A

5.4.2 Pseudo cross-section along profile B

The hydrogeological examination of profile B in (Figure 5.12) shows numerous noteworthy findings. First, at VES-7 and VES-8, resistivity increases with depth, suggesting less porous or denser geological formations. VES-9 and VES-10 have lower top layer resistivity, indicating salty or highly conductive water. The intermediate strata have considerable resistivity, indicating lithological diversity. A prominent "sandwich" pattern of low resistivity at the bottom strata suggests a large groundwater zone, potentially fresh or low-salinity. The penultimate (VES-19,18) has intermediate resistivity with a low-resistivity zone at the bottom, suggesting access to

groundwater with different properties. These data help analyze hydrogeological conditions and groundwater supplies in the examined area.

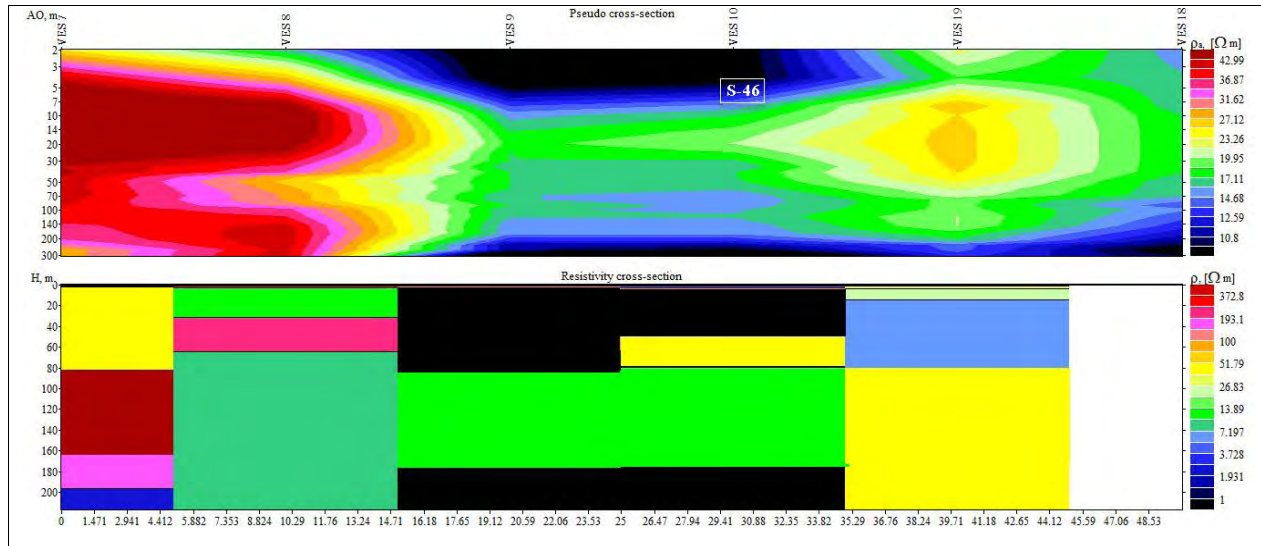


Figure 5.13 Apparent resistivity pseudo cross section for profile B

5.4.3 Pseudo cross-section along profile C

In the profile C, as seen in Figure 5.13, investigated a total of five Vertical Electrical Sounding (VES) locations, namely VES 14, VES 13, VES 12, VES 25, and VES 28. The resistivity measurements of VES 13, VES 12, and VES 25 exhibited a steady and moderate pattern, suggesting a uniformity in the underlying characteristics.

The VES 14 survey revealed a notable decrease in resistivity values towards the lower depths, which implies the presence of a plausible groundwater reservoir. The VES 28 survey exhibited higher resistivity values in the top and intermediate strata, whereas the base had reduced resistivity, suggesting the presence of lithological variation and the likely existence of an aquifer. These results provide valuable information that may be utilized in the evaluation of groundwater potential and the characterization of subsurface variability.

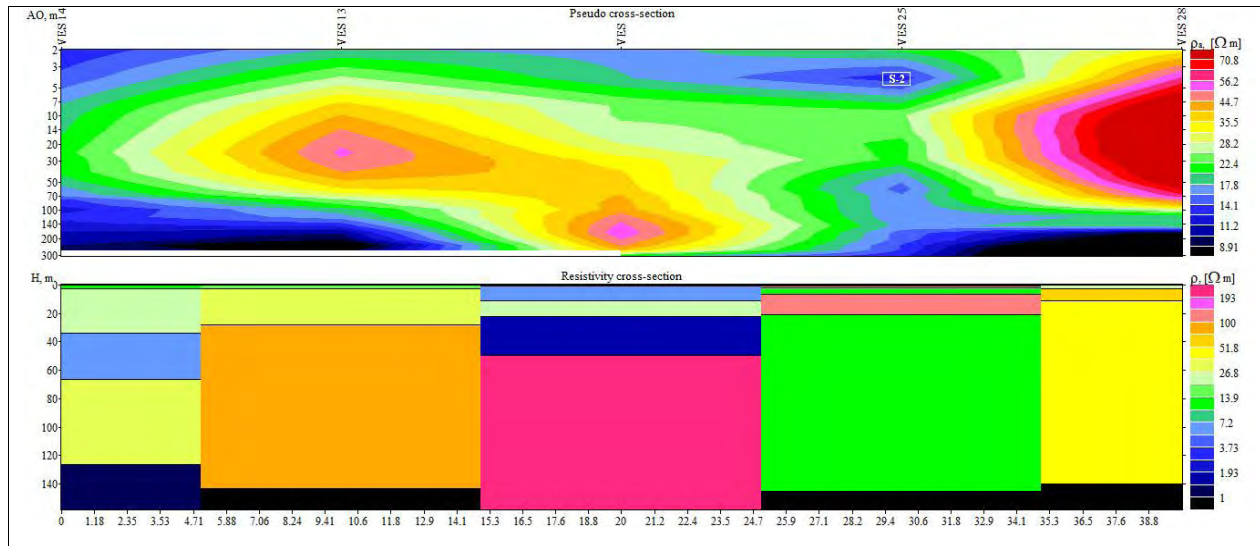


Figure 5.14 Apparent resistivity pseudo cross section for profile C

5.4.4 Pseudo cross-section along profile D

The investigation found hydrogeological trends in Profile D, which comprises VES sites 25, 15, 16, 24, and 26 (Figure 5.14).

In the VES 16 survey, hydrogeological study showed a steady decrease in resistivity towards shallower strata. This pattern suggests a hydrogeological transition toward thicker subsurface strata, with higher layers made of consolidated rock and lower layers of loosely packed materials. The hydrogeological evaluation helps understand subsurface lithological variations and porosity changes, revealing groundwater circulation and aquifer features.

However, the other VES sites in this profile show moderate resistivity, indicating a consistent subsurface. VES 26 features a low-resistance layer in the highest section, suggesting an aquifer.

Profile D shows subsurface lithology changes, probable aquifer zones, and rock density variations, providing hydrogeological information. The above findings help us understand groundwater potential and geological aspects in the researched region.

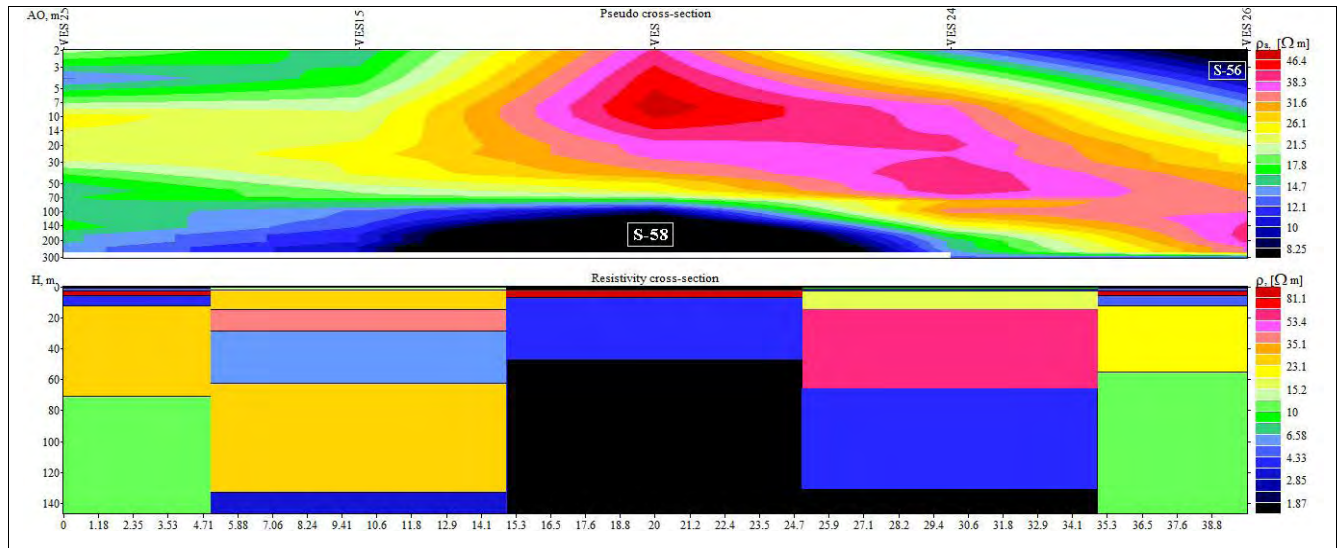


Figure 5.15 Apparent resistivity pseudo cross section for profile D

5.4.5 Pseudo cross-section along profile E

In the profile E that shows in (Figure 5.15) emphasizes four VES locations (VES 18, 20, 23, and 22), revealing important hydrogeological features. The VES 20 survey shows a greater resistivity zone in the top strata, indicating non-water-containing geological elements.

However, VES 22 shows lower resistivity inside the underlying geological strata, indicating a high chance of a hydrogeological unit such a water-bearing layer or aquifer. The above findings are significant for assessing groundwater resources and underlying geology in the region. They help identify probable aquifers and non-aquifers deposits.

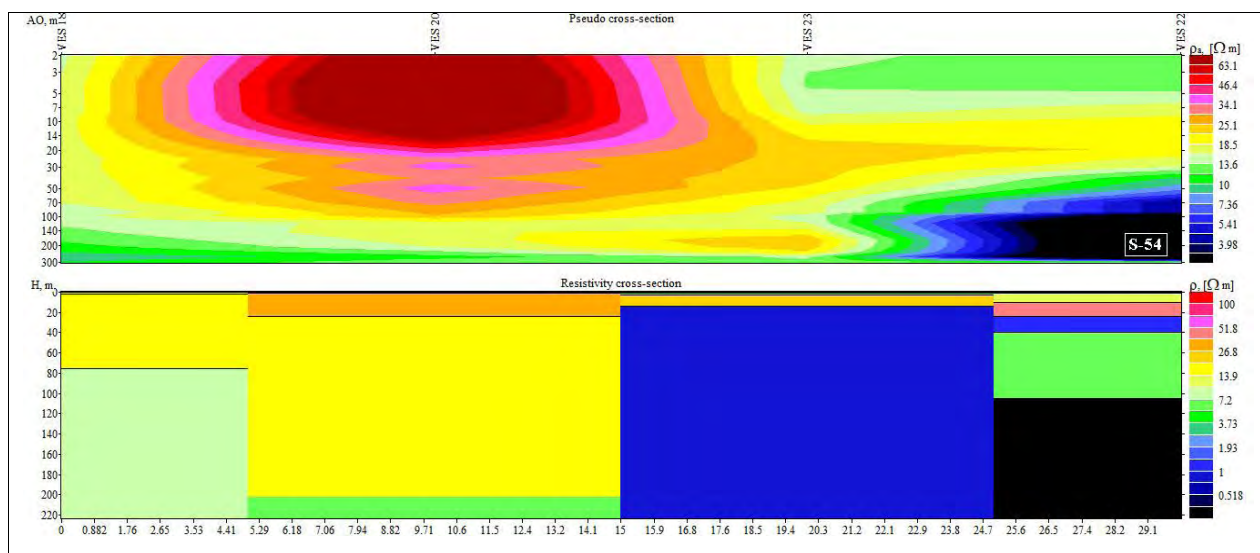


Figure 5.16 Apparent resistivity pseudo cross section for profile E

5.4.6 Correlation between VES and Physio-chemical analysis

The correlation between Vertical Electrical Sounding (VES) data and physio-chemical analysis serves to validate and substantiate the salinity interpretations derived from VES results by establishing a direct link between geophysical measurements and the actual chemical composition of groundwater. This correlation aims to provide empirical evidence supporting the reliability of VES in accurately predicting or reflecting salinity levels within the subsurface aquifers.

Absolutely, a figure illustrating the close proximity and correlation between the Vertical Electrical Sounding (VES) points and their corresponding physio-chemical analysis points, marked as Figure 5.17, would effectively demonstrate the spatial relationship between these data sets.



Figure 5.17 Correlation between VES and physio-chemical analysis

In order to provide a comprehensive understanding of subsurface characteristics in our groundwater analysis, a comparison between VES (Vertical Electrical Sounding) data (Table 5.4) and physiochemical analysis (Table 5.3) has been incorporated. The aim is to correlate and depict a clear picture of the subsurface features and the presence of high salinity levels.

Table 5.3 and 5.4 delineate the key parameters obtained from VES and physiochemical analyses, respectively. Our focus lies in establishing a correlation between the two datasets to emphasize the existence of high salinity zones. Notably, in the pseudo cross-sections, the VES data indicates regions with elevated salinity at specific depths. This corresponds closely with findings from the physiochemical analysis, which indicates heightened levels of dissolved minerals like chloride, sodium, magnesium, and calcium in the same depth intervals.

This confluence of data from VES and physiochemical analyses acts as strong evidence affirming the presence of high salinity in the subsurface aquifers. It's imperative to note that the elevated salinity levels, attributed to the abundance of dissolved minerals, particularly chloride, sodium, magnesium, and calcium, contribute significantly to the groundwater's overall characteristics. This information is pivotal for a comprehensive assessment of groundwater quality, its suitability for various uses, and subsequent measures for its management and remediation.

The synchronized insights from VES and physiochemical analyses offer a robust foundation for understanding subsurface conditions, particularly in identifying high salinity areas caused by mineral dissolution. This comprehension is vital for groundwater resource management, facilitating informed decision-making for sustainable utilization and preservation of this crucial natural asset.

Table 5.3 Physio-chemical analysis data of Sargodha area

Physio-chemical analysis

	Longitude	Latitude	Sample Name	Alkalinity (m.mol/l)	PH	EC	TDS (mg/l)	TH (mg/l)	Na (mg/l)	Ca (mg/l)	Mg (mg/l)	K (mg/l)	Cl (mg/l)	HCO3(mg)
1	72.323056	31.641667	S-41	9.2	7.59	923	591	305	90	70	31.5	13.2	21	460
2	72.488056	32.144167	S-46	7.9	7.25	1901	1141	420	255	88	48.6	8	258	395
3	73.037222	32.532778	S-2	7.8	7.42	956	612	425	66	124	28	6	104	390
4	72.856111	32.236111	S-58	7.5	7.76	1215	729	278	140	32	48	4.6	45	375
5	72.835	32.006944	S-56	5	7.72	662	424	250	50	42	35	2.9	75	250
6	72.730278	32.088611	S-54	6.9	7.93	1678	1074	505	190	80	73	4.6	86	345
				Alkalinity (m.mol/l)	PH	EC	TDS (mg/l)	TH (mg/l)	Na (mg/l)	Ca (mg/l)	Mg (mg/l)	K (mg/l)	Cl (mg/l)	HCO3(mg)
			Mean	7.383333	7.611667	1222.5	761.8333	363.8333	131.8333	72.666667	44.016667	6.55	98.16667	369.1667
			Medain	7.65	7.655	1085.5	670.5	362.5	115	75	41.5	5.3	80.5	382.5
			S.D	1.390563	0.246205	478.0756	285.6777	100.609	79.2475	33.242543	16.561451	3.67573122	83.72196	69.52817

Table 5.4 VES data of the study area for comparing with Physio-chemical analysis data.

VES Data														
	Longitude	Latitude	Sample Name	ρ 1	ρ 2	ρ 3	ρ 4	ρ 5	ρ 6	h1	h2	h3	h4	h5
1	72.39833	31.68889	VES 1	16.6	448	89.5	8.32	0.07		1.2	1.6	30.5	105	
2	72.47833	32.17222	VES 10	13.6	4.34	114	10.2	47.9	0.23	0.83	1.48	2.19	32.8	41
3	73.03528	32.51861	VES 25	4.43	109	10.8	126	11.3		0.87	1.3	4.36	14.5	
4	72.89806	32.25556	VES 16	6.06	1.12	113	3.64			0.74	1.24	4.43		
5	72.83472	32.03611	VES 26	45.8	5.32	122	4.61	22.9	11.4	0.87	1.31	2.98	6.75	43.2
6	72.72556	32.03444	VES 22	29.3	13.3	38.9	1.07	6.67	0.01	0.57	9.42	14.1	15.5	65.4

Chapter 06

Estimation of Dar-Zarrouck parameters of study area

6.1 Introduction

Hydrogeologists apply Dar Zarrouck attributes to characterize subsurface formations and determine groundwater potential. These measurements, which were named after Tunisian geophysicist Tahar Zarrouck, are crucial to understanding hydrogeological qualities, especially in arid and semi-arid regions where freshwater resources are scarce.

The Dar Zarrouck metrics include the apparent resistivity (ρ_a) and subsurface layer thickness (h). Electrical resistivity methods inject electrical currents into the ground and measure voltage differentials to estimate geological material resistivity. However, geological and geophysical research define subsurface layer thickness.

The interpretation of resistivity data in resolving saline, brackish, and fresh water bodies may lack uniqueness. Assigning a number to the resistivity of fresh water, saline water, and brackish water aquifers is challenging due to several factors that influence the resistivity value. The uncertainty constant in the interpretation of resistivity data can be minimized by employing geophysical parameters that have been specifically designed and identified for this purpose. In the present context, it can be asserted that the utilization of D-Z parameters has the potential to effectively facilitate the interpretation of resistivity data and mitigate the inherent uncertainties associated with such analyses.

The diverse ranges of the D-Z parameters observed in salty, brackish, and fresh water bodies have shown to be valuable in the interpretation of resistivity data. The study conducted by Batayneh et al. (2013) reveals significant variations in the ranges of parameters observed in contour maps and graphical analyses of fresh, brackish, and saline water aquifers.

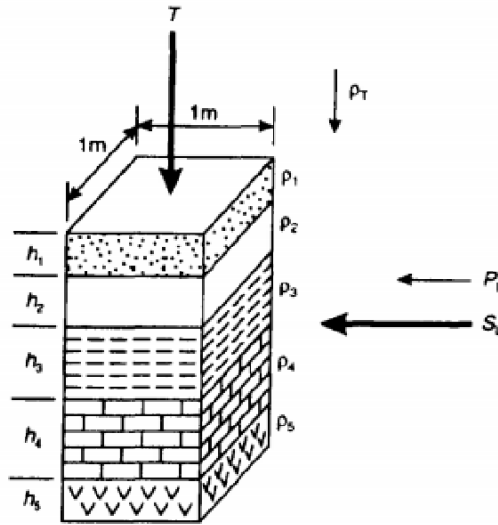


Figure 6.1 3D Electrostratigraphic model showing total longitudinal conductance and total transverse resistance (modified from Reynolds, 1997).

The Dar Zarrouck (D-Z) parameters were introduced by Maillet in 1947. The resistance normal to the face, denoted as T , and the conductance parallel to the face, denoted as S , are key factors in resistivity soundings. These parameters are defined for a single cross-sectional area and have significant implications in this field of study. The utilization of D-Z characteristics is adequate for the calculation of the surface potential distribution, thus enabling the construction of an electrical resistivity graph (Honriet, 1976).

Suppose that a section consists of N fine layers with thickness h_1, h_2, \dots, h_n and resistivity $\rho_1, \rho_2, \rho_3, \dots, \rho_n$ for a block of unit square area and thickness $H = \sum_{i=1}^N h_i$.

So that, Longitudinal unit conductance,

$$S = \frac{h_1}{\rho_1} + \frac{h_2}{\rho_2} + \frac{h_3}{\rho_3} + \dots + \frac{h_n}{\rho_n} = \sum_{i=1}^N \frac{h_i}{\rho_i} \quad (1)$$

Transverse unit Resistance,

$$T = \rho_1 h_1 + \rho_2 h_2 + \rho_3 h_3 + \dots + \rho_n h_n = \sum_{i=1}^N \rho_i h_i \quad (2)$$

Longitudinal Resistivity,

$$R_s = \frac{H}{S} \quad (3)$$

Transverse Resistivity,

$$R_T = \frac{T}{H} \quad (4)$$

The sum of the entire longitudinal conductance and of the transverse resistance for a layer ground is called Dar-Zarrouck parameters (Maillet, 1947).

Table 6.1 Values of Dar-Zarrouck parameters of all sounding locations with depth

VES	Longitude	Latitude	Sc (Siemens)	Tr (Ωm^2)	H (m)	Rs ($\Omega\text{-m}$)	Curve type
VES 1	72.39	31.68	13.03684	4340.14	138.3	10.6084	K
VES 2	72.34	31.77	4.536033	2401.828	73.49	16.2013	K
VES 3	72.45	31.83	17.20597	665.192	87.87	5.1069	K
VES 4	72.34	31.87	2.349122	642.279	4.63	1.9709	A
VES 5	72.49	31.95	3.55	947.634	167.26	1.0325	Q
VES 6	72.31	31.96	0.129393	1591.252	7.54	58.2720	K
VES 7	72.26	32.01	1.603888	5672.8332	63.62	39.6661	A
VES 8	72.32	32.09	2.353192	9803.974	64.71	27.4988	KH
VES 9	72.42	32.13	1.608233	5675.5272	63.72	39.6211	A
VES 10	72.47	32.17	4.49289	2566.0612	78.3	17.4275	K
VES 11	72.41	32.22	4.249846	5449.6321	142.48	33.5259	K
VES 12	72.91	32.48	18.25785	2010.7142	49.38	2.7045	A
VES 13	72.81	32.39	2.533772	10065.3	143.19	56.5125	A
VES 14	72.79	32.30	2.060827	2116.3026	55.29	26.8290	K
VES 15	72.96	32.35	10.13643	2743.1924	132.83	13.1042	K
VES 16	72.89	32.25	1.268459	510.1032	6.41	5.0533	K
VES 17	72.58	32.35	69.20117	2116.2196	207.11	2.9928	Q
VES 18	72.67	32.27	10.47643	2204.314	151.43	14.4543	Q
VES 19	72.58	32.23	10.5755	1059.905	163.33	1.0042	Q
VES 20	72.69	32.16	10.08889	4197.0174	202.51	20.0725	K
VES 21	72.51	32.03	5.176779	4612.673	108.93	21.0420	K
VES 22	72.72	32.03	25.38127	1143.29	104.99	4.1365	HK
VES 23	72.68	32.10	1.033188	232.6448	13.5	13.0663	K
VES 24	72.88	32.17	1.120299	231.1755	14.39	12.8447	K
VES 25	73.03	32.51	0.727098	2030.9421	21.03	28.9232	K
VES 26	72.83	32.03	3.640334	1442.1727	55.11	15.1387	HK
VES 27	72.94	32.07	0.786295	1053.9071	12.78	16.2534	A
VES 28	73.09	32.51	2.738047	7257.558	139.85	51.0765	K

6.2 Longitudinal Conductance (Sc)

A contour map of Sc values of the study area prepared by using the resistivity data of 28 soundings prepared with a contour interval of 4 Siemens is shown in (Figure 6.2).

Certainly! Longitudinal Conductance (Sc) in Vertical Electrical Sounding (VES) essentially measures how easily electrical current moves vertically through underground materials. It's a parameter derived from VES data analysis, indicating the conductivity of layers beneath the surface. Higher Sc values suggest more conductive materials, often associated with increased water content or salinity, aiding in identifying potential groundwater zones or aquifers during surveys.

Based on value ranges of 'Sc', three zone of aquifer differentiating fresh, saline and brackish water. In the (figure 6.2) Sc values increases 44 to 60 siemens saline water Aquifers with red colour. Sc values increases as of 24 to 40 siemens with parrot Green and yellow colour demarcate the brackish water while the fresh water is identified with the 'Sc' value values increases as of 0 to 24 siemens with blue colour.

The use of a contour map to visually depict Sc values within a hydrogeological framework provides significant insights into the characteristics of groundwater within the specified study area. The graphical representation utilizes a system of colour coding to demarcate three distinct aquifer zones. The zones depicted in red on the map are indicative of areas exhibiting Sc levels ranging from 44 to 60 Siemens.

The previously mentioned places exhibit characteristics consistent with freshwater aquifers that have a diminished presence of minerals, rendering them suitable for both potable water use and farming. Regions exhibiting Sc values between 24 and 40 Siemens can be visually discerned by the notable occurrence of hues in parrot green and yellow. These colors function as markers of brackish water characterized by a moderate salinity level, making it suitable for particular agricultural and industrial applications.

In summary, the inclusion of the blue hue on the map implies Sc values ranging from 0 to 24 Siemens, denoting the existence of saline water with increased mineral concentration. This particular kind of water is typically unsuitable for human consumption and possesses little utility

in practical applications. This data aids hydrogeologists in assessing the suitability of groundwater for various uses and in effectively managing groundwater resources.

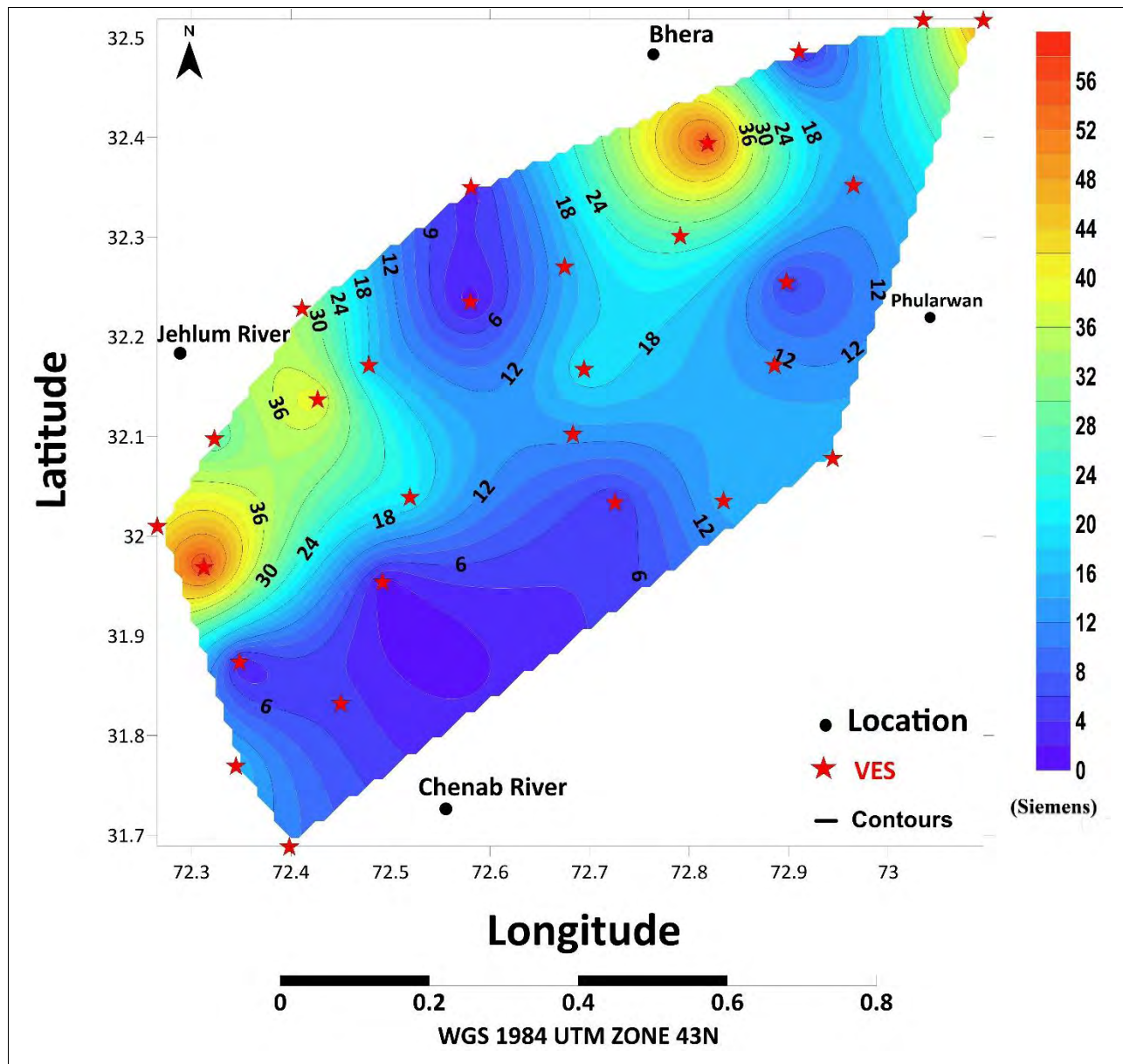


Figure 6.2 Contour map of the longitudinal conductance

6.3 Transverse Unit Resistance (T_r)

Transverse Unit Resistance (T_r) in Vertical Electrical Sounding (VES) measures how resistant underground materials are to electrical flow sideways. This parameter, derived from VES surveys, indicates the lateral variations in resistivity within subsurface layers. Lower T_r values often suggest more conductive materials horizontally, potentially signaling areas with higher water

content or potential aquifers during geophysical investigations. Understanding T_r helps delineate horizontal variations in subsurface conductivity during surveys.

Using 28 sounding sites, values of transverse unit resistance (T_r) are acquired and are incorporated to prepare a map of contours for study area having $600 \Omega\text{-m}^2$. Interval as displayed in Figure 6.3. The contour map illustrates the categorization of aquifers within the examined region into three distinct groups: fresh, brackish, and saline water.

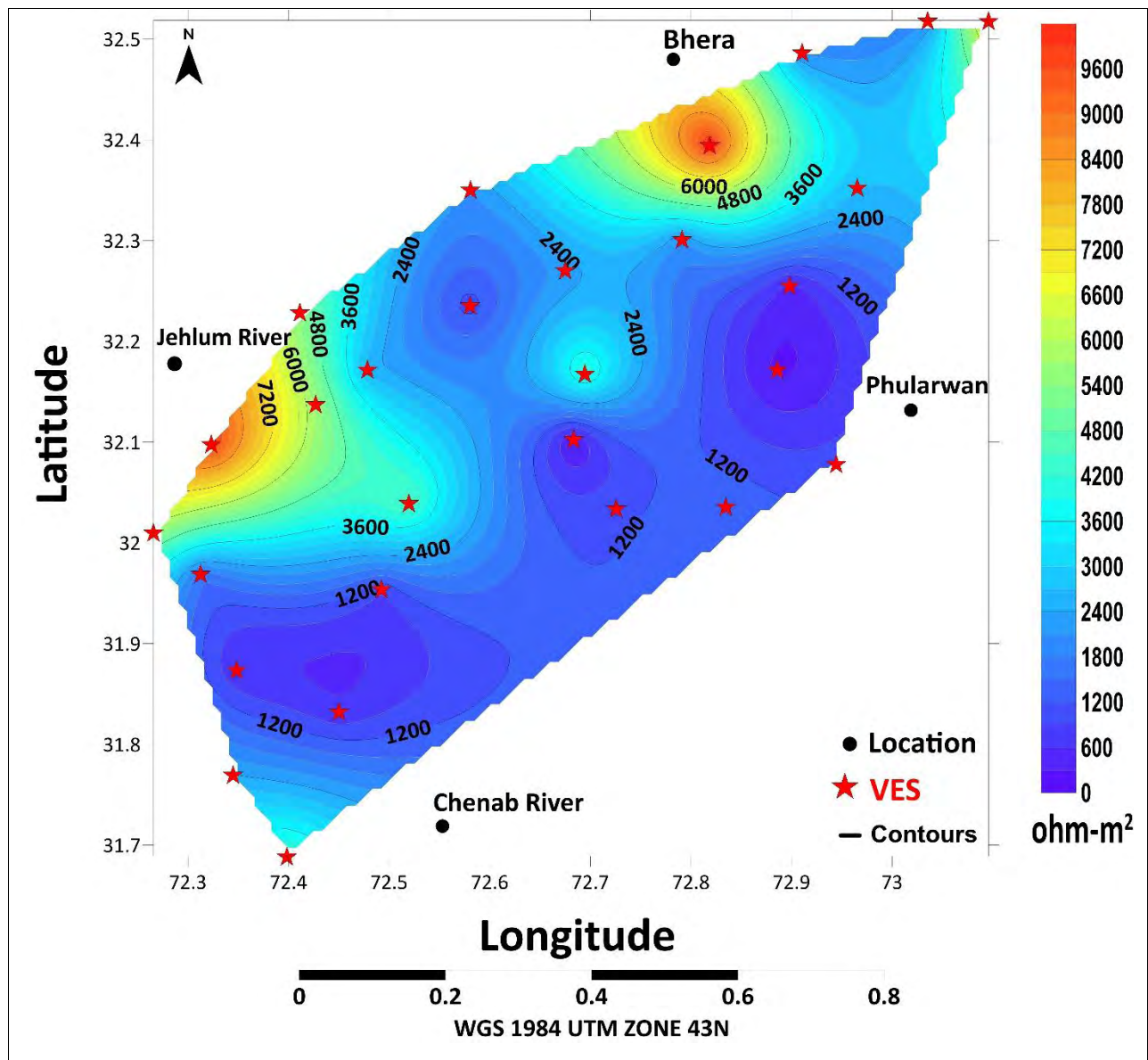


Figure 6.3 Transverse Unit Resistance (T_r)

The observed rise in transverse unit resistance (T_r) values, ranging from 0 to $3000 \Omega \cdot m^2$, suggests the existence of saline aquifers. Within the field of brackish water aquifers, scientific proof has been gathered to establish that the T_r value consistently resides within the numerical spectrum of 3600 to $6600 \Omega \cdot m^2$.

The resistivity measurement exceeding $3600 \Omega \cdot m^2$. T_r suggests the existence of freshwater aquifers. Figure 6.3 effectively demonstrates the precise demarcation between discrete zones of fresh water, brackish water, and saltwater water, without any observable overlap between these zones.

6.4 Longitudinal Resistivity (R_s)

A contour map prepared using longitudinal resistivity values of the 28 geoelectrical soundings carried out in the study area, shown in (Figure 6.4) demarcates the saline water aquifer region, brackish water, and freshwater aquifer region into three different entities based on their attained magnitudes. The contour interval in the maps is $2 \Omega \cdot m$. The saline water aquifers possess the range of $0-8 \Omega \cdot m$.

The brackish water is in intermediate shows in green and yellow color range in between $28-40 \Omega \cdot m$ and those of fresh water aquifers possess a range of $40-60 \Omega \cdot m$. They reflect very clear, conspicuous and widely varying ranges for saline water and fresh water aquifers. The contour map shown in (Figure 6.4) clearly demarcates the saline water and the fresh water aquifers. The contour interval in the maps is $2 \Omega \cdot m$. The saline water aquifers possess the range of $0-8 \Omega \cdot m$. The brackish water is in intermediate shows in green and yellow color range in between $28-40 \Omega \cdot m$ and those of fresh water aquifers possess a range of $40-60 \Omega \cdot m$.

They reflect very clear, conspicuous and widely varying ranges for saline water and fresh water aquifers. The contour map shown in (Figure 6.4) clearly demarcates the saline water and the fresh water aquifers.

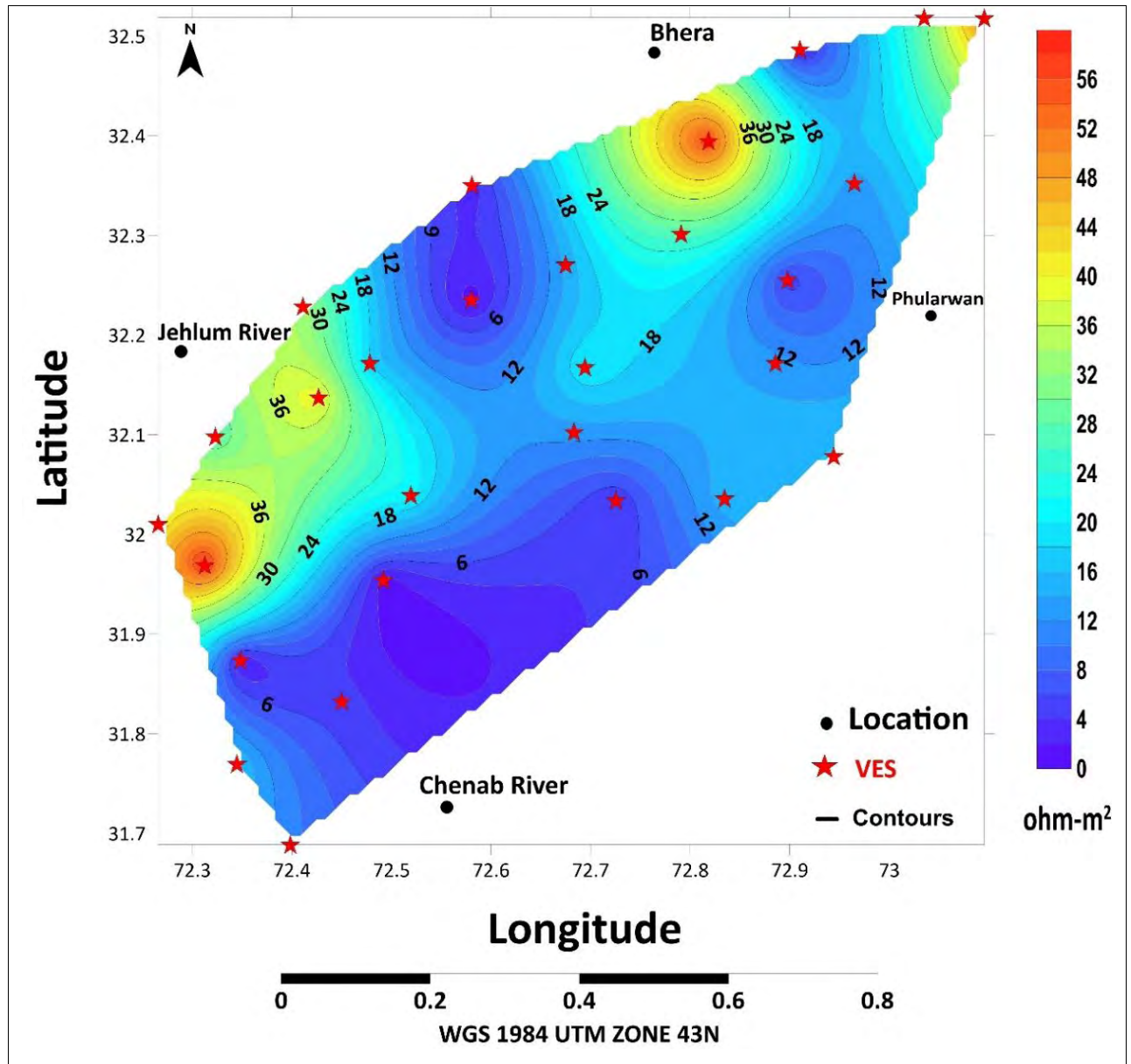


Figure 6.4 Contour map of the Longitudinal Resistivity

Chapter 07

Conclusions

In summary, the results of our study highlight the efficacy of Vertical Electrical Sounding (VES) surveys as a sophisticated method for categorizing the most favorable aquifer layers in underground environments and for delineating the degrees of groundwater salinity. The results of our study suggest that the use of Vertical Electrical Sounding (VES) is a cost-effective alternative for assessing crucial aquifer properties, including as transmissivity and hydraulic conductivity. The application of this geophysical technology offers a viable alternative to labor-intensive and expensive pumping testing.

The Vertical Electrical Sounding (VES) method has been recognized as a practical tool in the domain of groundwater characterization and exploration, showcasing its capability to evaluate groundwater parameters.

The application of field data collecting has played a crucial role in the advancement of resistivity modelling, hence facilitating a comprehensive analysis of subsurface lithologies at varying depths. The utilization of the Vertical Electrical Sounding (VES) methodology for estimating Dar-Zarrouck parameters provides valuable insights for identifying potential aquifer zones. The validation of the reliability of this technology in identifying zones with potential for aquifer development is achieved through the congruence between formation characteristics derived from electrical resistivity and pumping trials.

Furthermore, our study effectively shows a significant association between resistivity measures and the lithology of aquifers, as well as the water quality present, facilitating the distinction between saline and fresh groundwater and their corresponding geological strata. It is important to acknowledge that elevated levels of resistivity are suggestive of diminished electrical conductivity, which serves as a substantial indicator of water quality.

Moreover, the Dar-Zarrouck characteristics, namely the Longitudinal Unit Conductance (S) and Transverse Unit Resistance (Tr), offer supplementary evidence that supports the presence of fresh

and saline water in areas distinguished by high and low resistivity, respectively. The transverse unit resistance (T_r) exhibits a significantly elevated magnitude within the high resistivity zone, Greater than $6600 \Omega\text{-}m^2$), whereas it demonstrates a somewhat diminished value within the low resistivity zone, falling within the range of $0\text{-}3000 \Omega\text{-}m^2$). In the case of longitudinal conductance (S), it has a low value. The high resistivity zone is typically found within the range of 44 to 60 siemens, whereas the low resistivity zone exhibits values ranging from 0 to 24 siemens.

The length of summers is increasing as a result of global warming. In the study location, the temperature during the summer season is significantly elevated, occasionally surpassing or reaching temperatures of 50°C . The impact of elevated temperatures is resulting in alterations to precipitation patterns.

The comparison between VES and physiochemical analyses revealed a strong correlation, confirming the existence of high salinity zones within the subsurface aquifers. Elevated levels of chloride, sodium, magnesium, and calcium observed in both datasets underscore the significant contribution of dissolved minerals to groundwater salinity. This comprehensive understanding is crucial for effective groundwater management strategies, ensuring informed decisions to preserve and sustainably utilize this essential natural resource.

In conclusion, it is imperative to recognize that the geographical area being examined is confronted with the challenges presented by rising temperatures associated with the phenomenon of global warming. As a result, this has resulted in the occurrence of exceptionally high summer temperatures, typified by temperatures exceeding 50°C . The confluence of high temperatures and erratic precipitation patterns underscores the considerable importance of employing accurate and efficient groundwater assessment techniques, such as Vertical Electrical Sounding (VES), to ensure the sustainable agricultural productivity and water resource management in the Sargodha region.

Our study underscores the significance of Vertical Electrical Sounding (VES) surveys in the domain of groundwater investigation, offering crucial insights on aquifer characteristics and water composition, particularly in regions grappling with the complexities arising from changing climatic conditions.

REFERENCES

- ❖ Adepelumi, A. A., & Olorunfemi, M. O. (2000). Engineering geological and geophysical investigation of the reclaimed Lekki Peninsula, Lagos, South West Nigeria. *Bulletin of Engineering Geology and the Environment*, 58, 125-132.
- ❖ Anomohanran, O. (2013). Geophysical investigation of groundwater potential in Ukelegbe, Nigeria. *Journal of Applied Sciences*, 13(1), 119-125.
- ❖ Ako, B. D., & Olorunfemi, M. O. (1989). Geoelectric survey for groundwater in the Newer Basalts of Vom, Plateau State. *Journal of Mining and Geology*, 25(1), 247-250.
- ❖ Arafin, M. S., & Lee, C. Y. (1985, July). A resistivity survey for groundwater in Perlis using offset Wenner technique. In *Karst Water Resources (Proceedings of the Ankara-Antalya Symposium, July 1985)*.
- ❖ Akhter, G., & Hasan, M. J. O. G. (2016). Determination of aquifer parameters using geoelectrical sounding and pumping test data in Khanewal District, Pakistan. *Open Geosciences*, 8(1), 630-638.
- ❖ Bayode, O. J. A., & Adewunmi, E. A. (2011). Environmental implications of oil exploration and exploitation in the coastal region of Ondo State, Nigeria: A regional planning appraisal. *Journal of Geography and Regional planning*, 4(3), 110.
- ❖ Batayneh, A. T. (2013). The estimation and significance of Dar-Zarrouk parameters in the exploration of quality affecting the Gulf of Aqaba coastal aquifer systems. *Journal of Coastal Conservation*, 17, 623-635.
- ❖ El-Qady, G. (2006). Exploration of a geothermal reservoir using geoelectrical resistivity inversion: case study at Hammam Mousa, Sinai, Egypt. *Journal of Geophysics and Engineering*, 3(2), 114.

- ❖ Hasan, M., Shang, Y., Akhter, G., & Khan, M. (2017). Geophysical investigation of fresh-saline water interface: A case study from South Punjab, Pakistan. *Groundwater*, 55(6), 841-856.
- ❖ Koefoed, O., & Dirks, F. J. H. (1979). Determination of resistivity sounding filters by the Wiener-Hopf Least-Squares Method. *Geophysical Prospecting*, 27(1), 245-250.
- ❖ Kelly, W. E., & Mareš, S. (Eds.). (1993). *Applied geophysics in hydrogeological and engineering practice*. Elsevier.
- ❖ Khuan, L. Y., Hamzah, N., & Jailani, R. (2002, July). Prediction of water quality index (WQI) based on artificial neural network (ANN). In *Student Conference on Research and Development* (pp. 157-161). IEEE.
- ❖ Kshetrimayum, K. S., & Bajpai, V. N. (2011). Establishment of missing stream link between the Markanda river and the Vedic Saraswati river in Haryana, India—geolectrical resistivity approach. *Current science*, 1719-1724.
- ❖ Kenneth, S. O., & Edirin, A. (2012). Determination of aquifer properties and groundwater vulnerability mapping using geoelectric method in Yenagoa City and its environs in Bayelsa State, South Nigeria. *Journal of Water Resource and Protection*, 2012.
- ❖ Lashkaripour, G. R. (2003). An investigation of groundwater condition by geoelectrical resistivity method: A case study in Korin aquifer, southeast Iran. *Journal of Spatial Hydrology*, 3(2).
- ❖ Lashkaripour, G. R., & Zivdar, M. (2005). Desalination of brackish groundwater in Zahedan city in Iran. *Desalination*, 177(1-3), 1-5.
- ❖ Mooney, H. M., Orellana, E., Pickett, H., & Tornheim, L. (1966). A resistivity computation method for layered earth models. *Geophysics*, 31(1), 192-203.

- ❖ Maillet, R. (1947). The fundamental equations of electrical prospecting. *Geophysics*, 12(4), 529-556.
- ❖ Omosuyi, G. O., Adeyemo, A., & Adegoke, A. O. (2007). Investigation of groundwater prospect using electromagnetic and geoelectric sounding at afunbiowo, near Akure, Southwestern Nigeria. *The pacific journal of science and technology*, 8(2), 172-182.
- ❖ Oseji, J. O., Atakpo, E. A., & Okolie, E. C. (2005). Geoelectric investigation of the aquifer characteristics and groundwater potential in Kwale, Delta state, Nigeria.
- ❖ Olowofela, J. A., Jolaosho, V. O., & Badmus, B. S. (2005). Measuring the electrical resistivity of the earth using a fabricated resistivity meter. *European Journal of Physics*, 26(3), 501.
- ❖ Pairojn, P. (2019). The Application of CRU-Resistivity Meters for Groundwater Investigation in Chantaburi, Thailand. *Journal of Environmental and Engineering Geophysics*, 24(1), 145-149.
- ❖ Seeber, L., & Armbruster, J. G. (1981). Great detachment earthquakes along the Himalayan arc and long-term forecasting. *Earthquake prediction: an international review*, 4, 259-277.
- ❖ Sikandar, P., & Christen, E. W. (2012). Geoelectrical sounding for the estimation of hydraulic conductivity of alluvial aquifers. *Water resources management*, 26(5), 1201-1215.
- ❖ Sikandar, P., Bakhsh, A., Arshad, M., & Rana, T. (2010). The use of vertical electrical sounding resistivity method for the location of low salinity groundwater for irrigation in Chaj and Rachna Doabs. *Environmental Earth Sciences*, 60, 1113-1129.

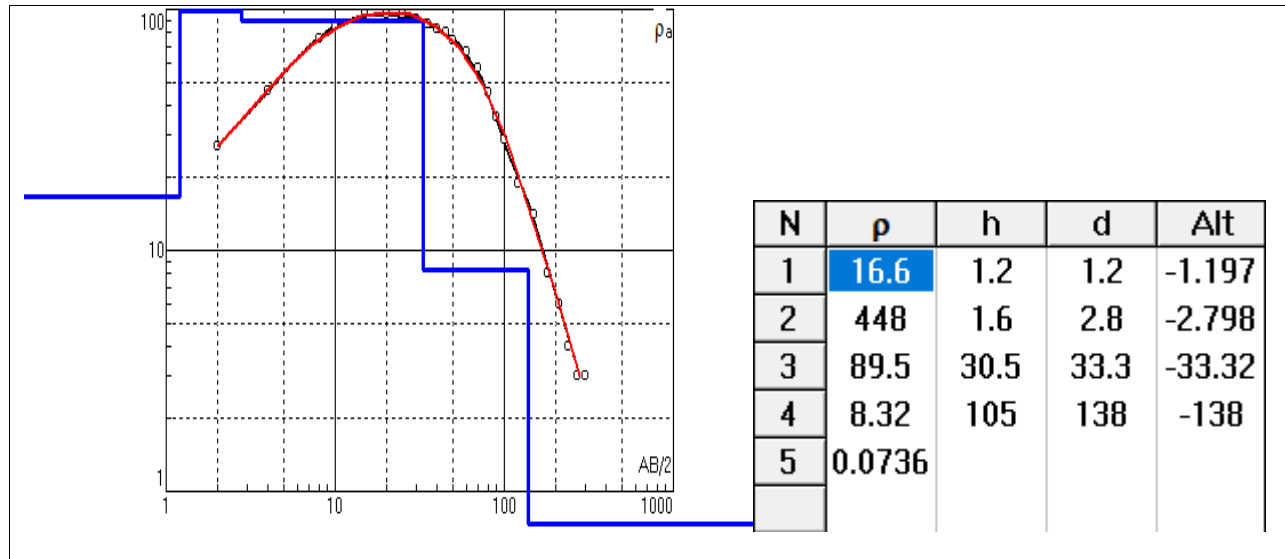
- ❖ Spicer, H. C. (1957). The application, technique, and theory of Gish-Rooney instruments, methods, and interpretation in electrical resistivity measurements (No. 58-99). US Geological Survey.
- ❖ Steinich, B., Bocanegra, G., & Sánchez, E. (1999). Basement topography and fresh-water resources of the coastal aquifer at Acapetahua, Chiapas, Mexico. *Geofísica Internacional*, 38(2), 107-115.
- ❖ Telford, W. M., Geldart, L. P., & Sheriff, R. E. (1990). *Applied geophysics*. Cambridge university press.
- ❖ Zouhri, L., Lamouroux, C., & Buret, C. (2001). La Mamora, charnière entre la Meseta et le Rif: son importance dans l'évolution géodynamique postpaléozoïque du Maroc/The Mamora Plain, a hinge between the Meseta and the Rif. Its importance in the post-Paleozoic geodynamic evolution of Morocco. *Geodinamica Acta*, 14(6), 361-372.
- ❖ Zohdy, A. A., Eaton, G. P., & Mabey, D. R. (1974). Application of surface geophysics to ground-water investigations (No. 02-D1). US Dept. of the Interior, Geological Survey: US Govt. Print. Off.
- ❖ Zohdy, A. A., & Bisdorf, R. J. (1990). Schlumberger sounding near Medicine Lake, California. *Geophysics*, 55(8), 956-964.
- ❖ Zhdanov, M. S., & Keller, G. V. (1994). The geoelectrical methods in geophysical exploration. *Methods in geochemistry and geophysics*, 31, I-IX.

APPENDIX

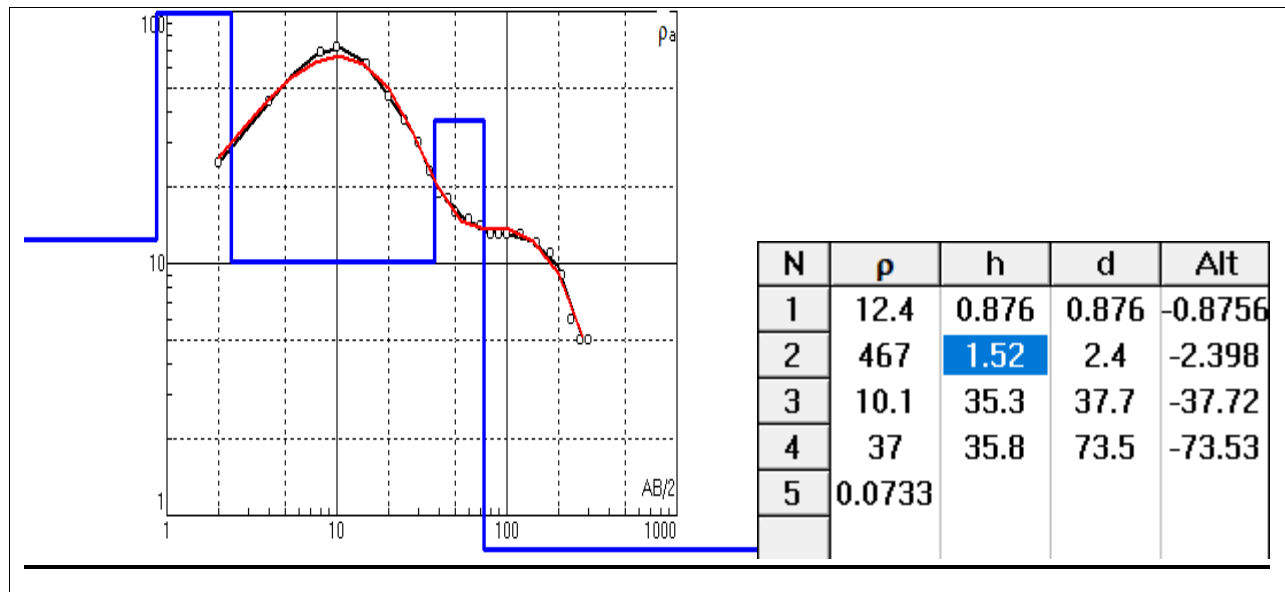
(Vertical Electrical Soundings)

Modeled Resistivity Curves

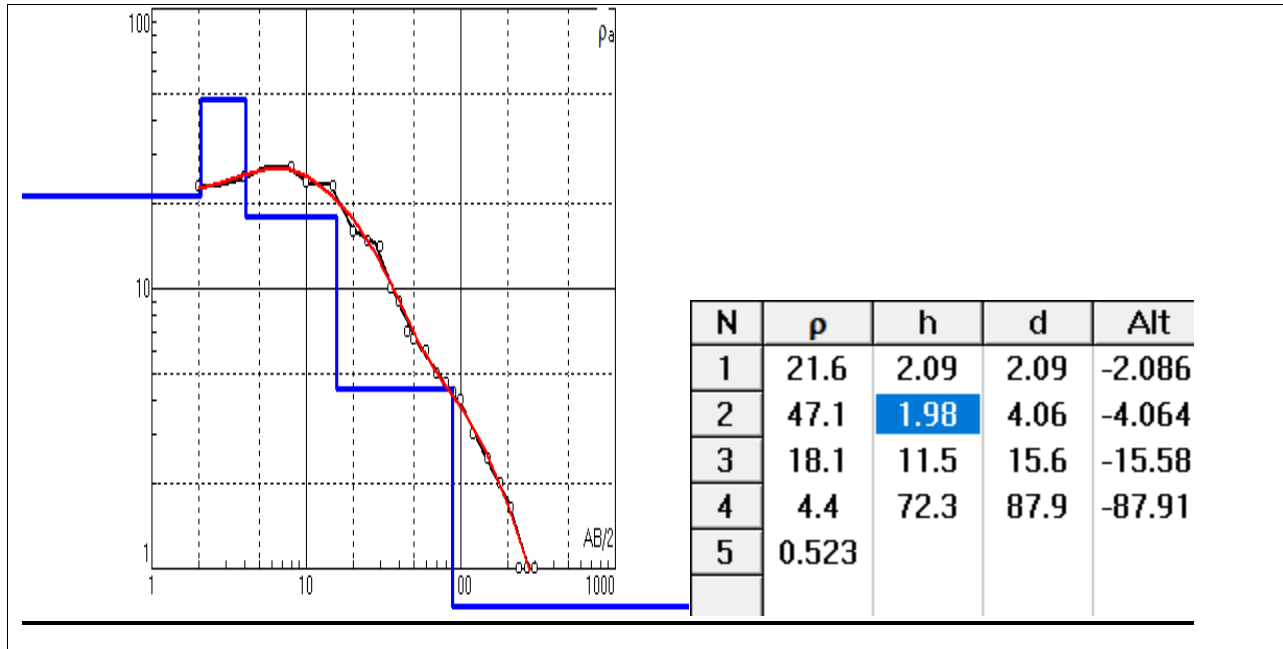
VES-1



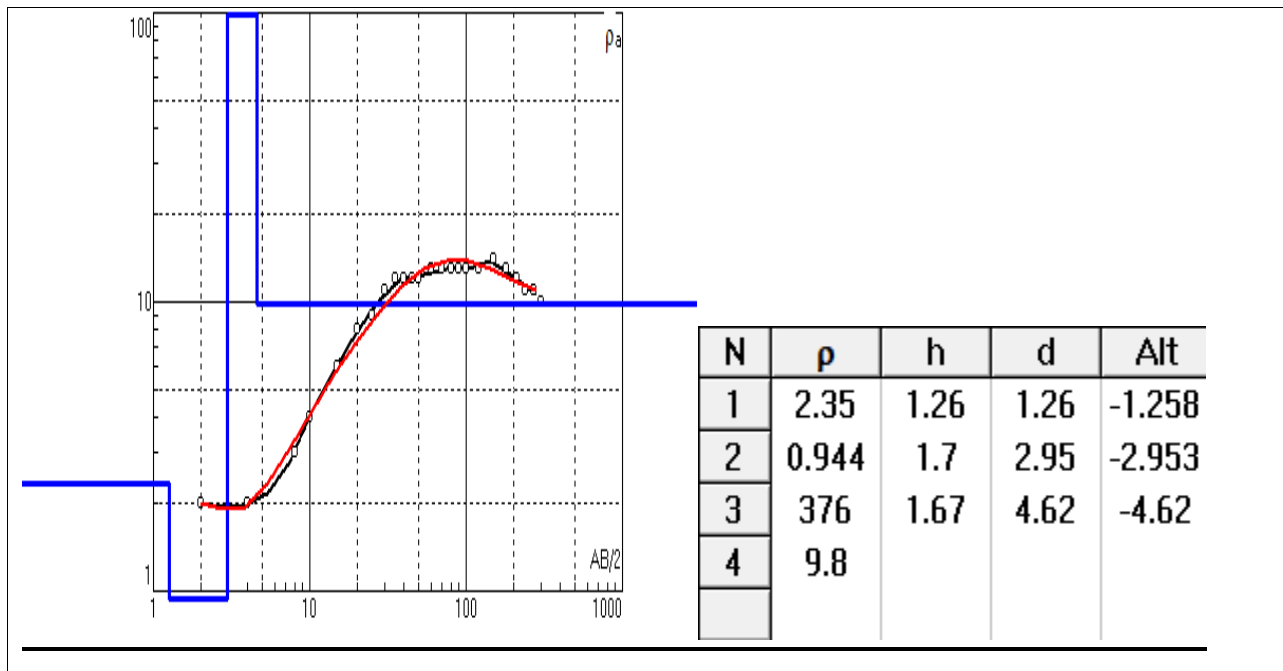
VES-2



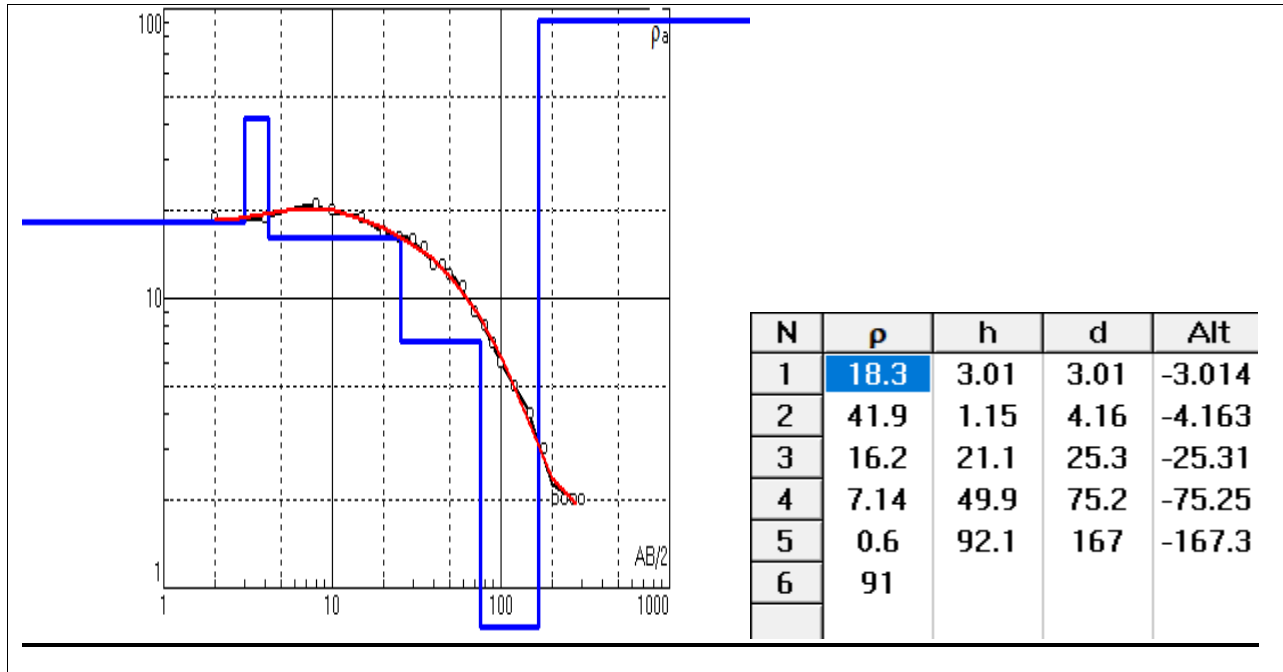
VES-3



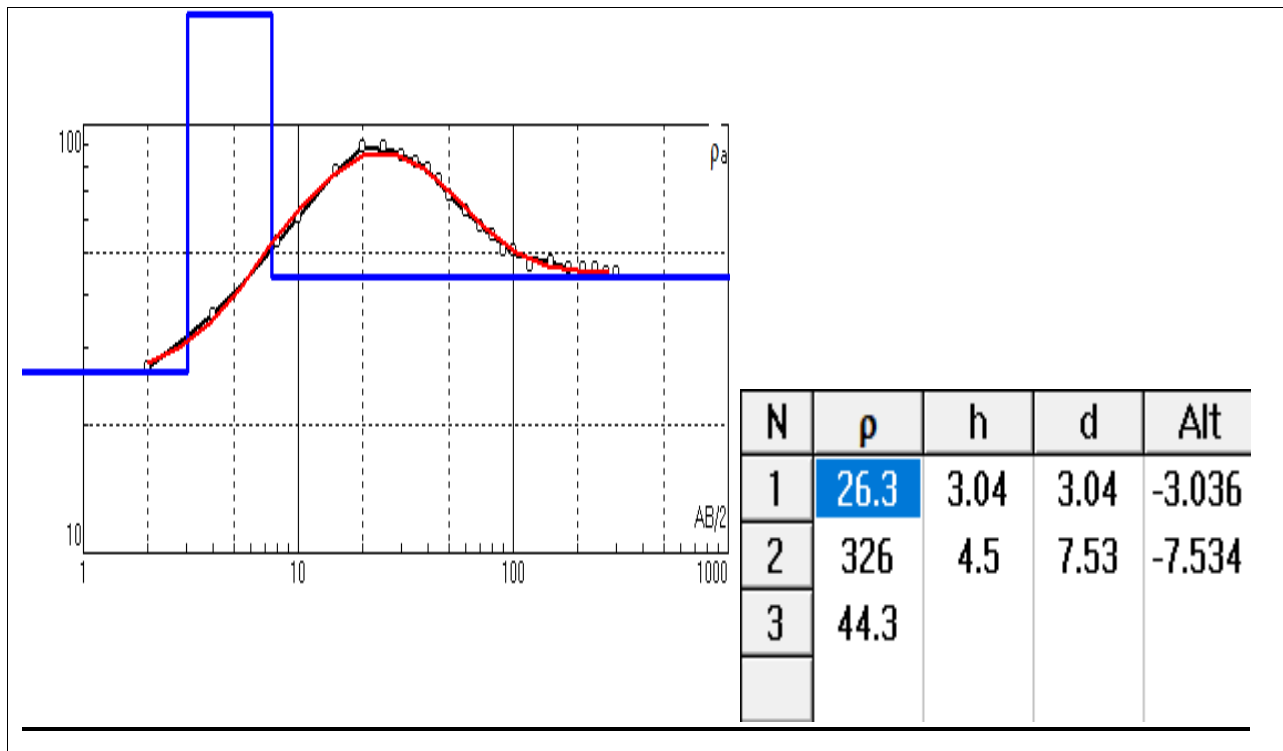
VES-4



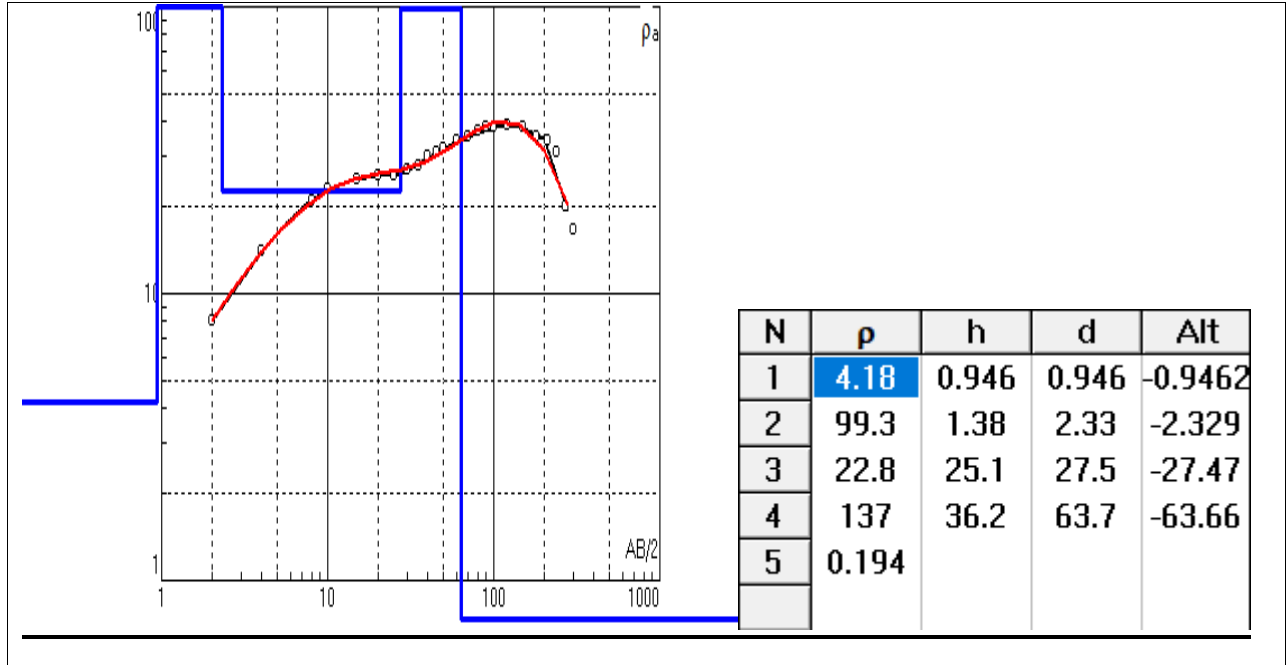
VES-5



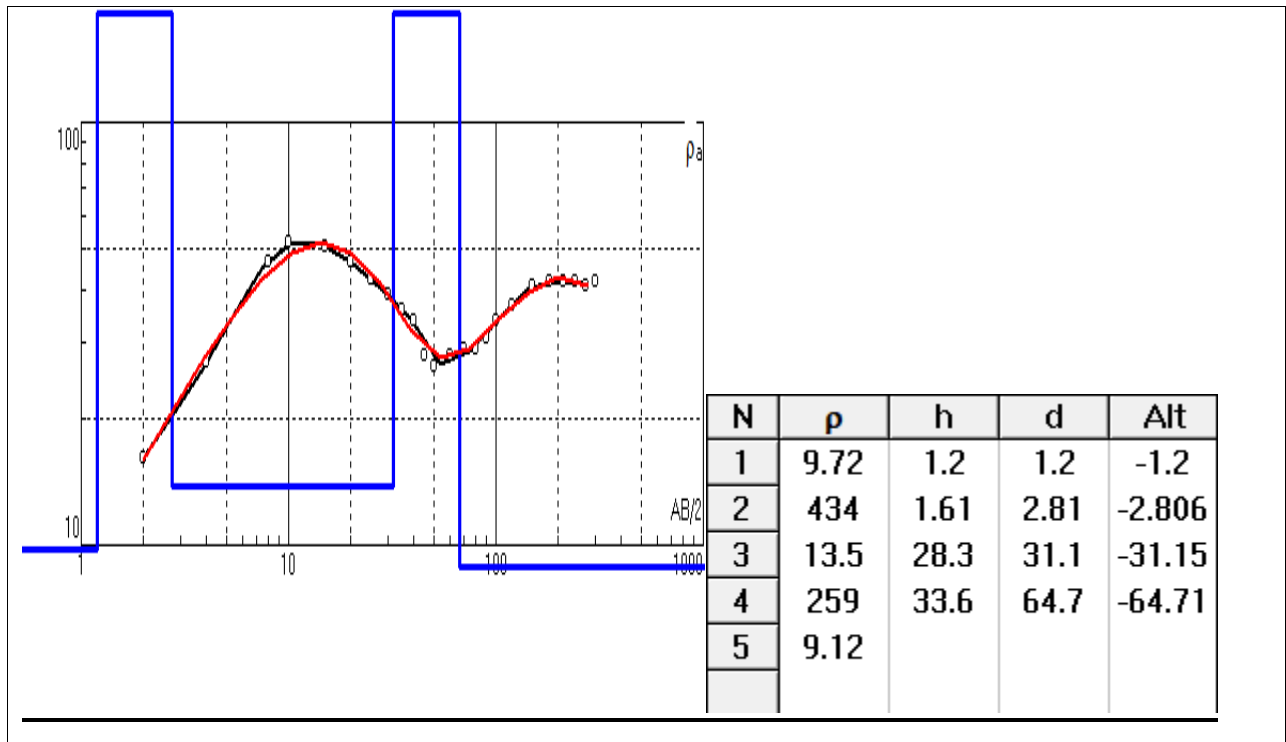
VES-6



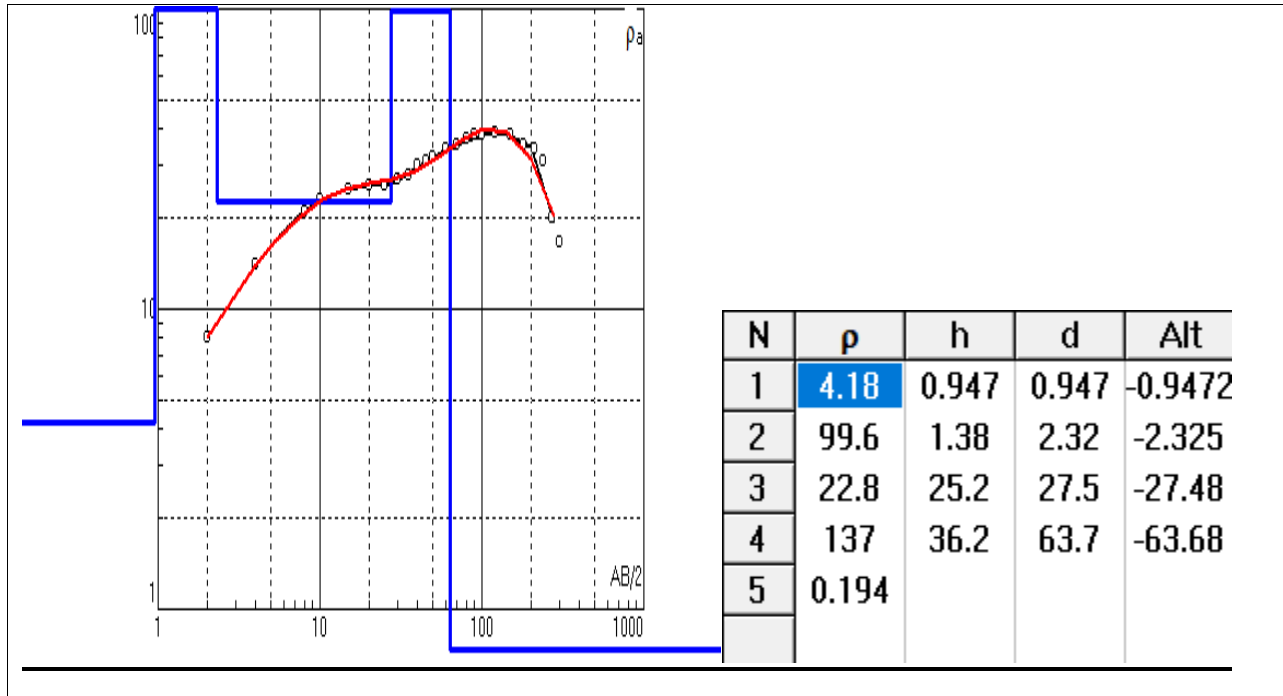
VES-7



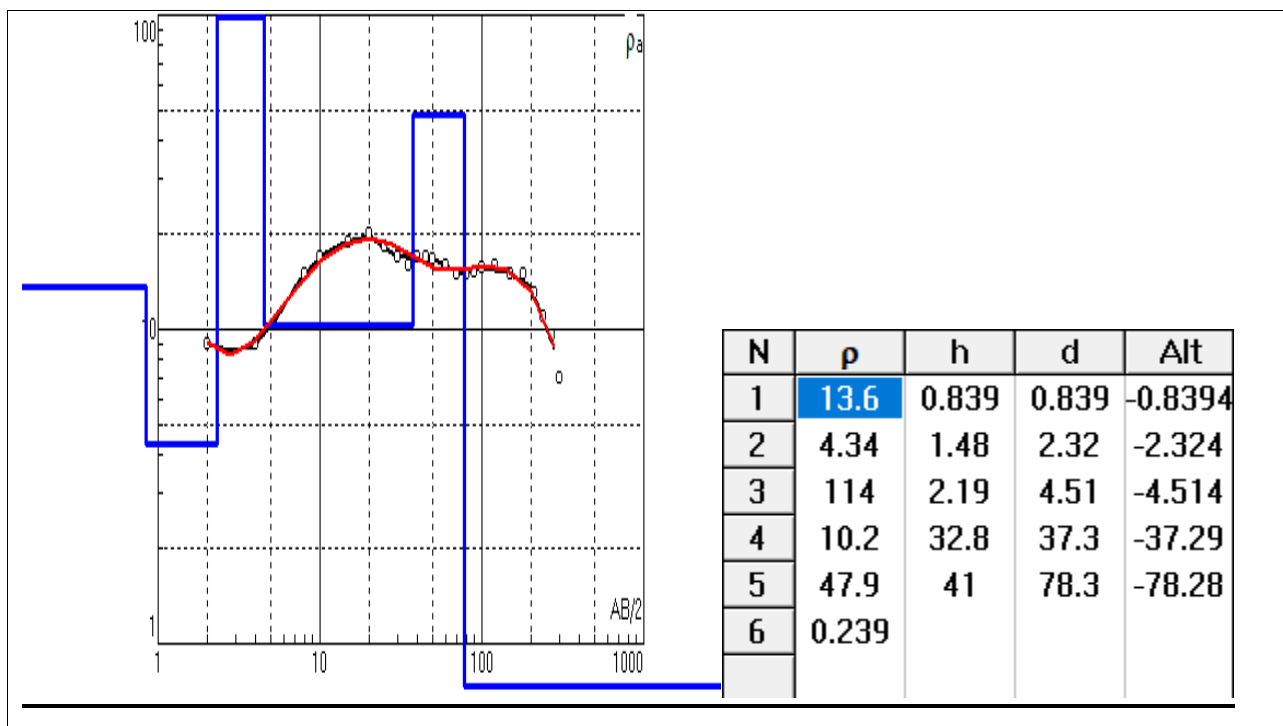
VES-8



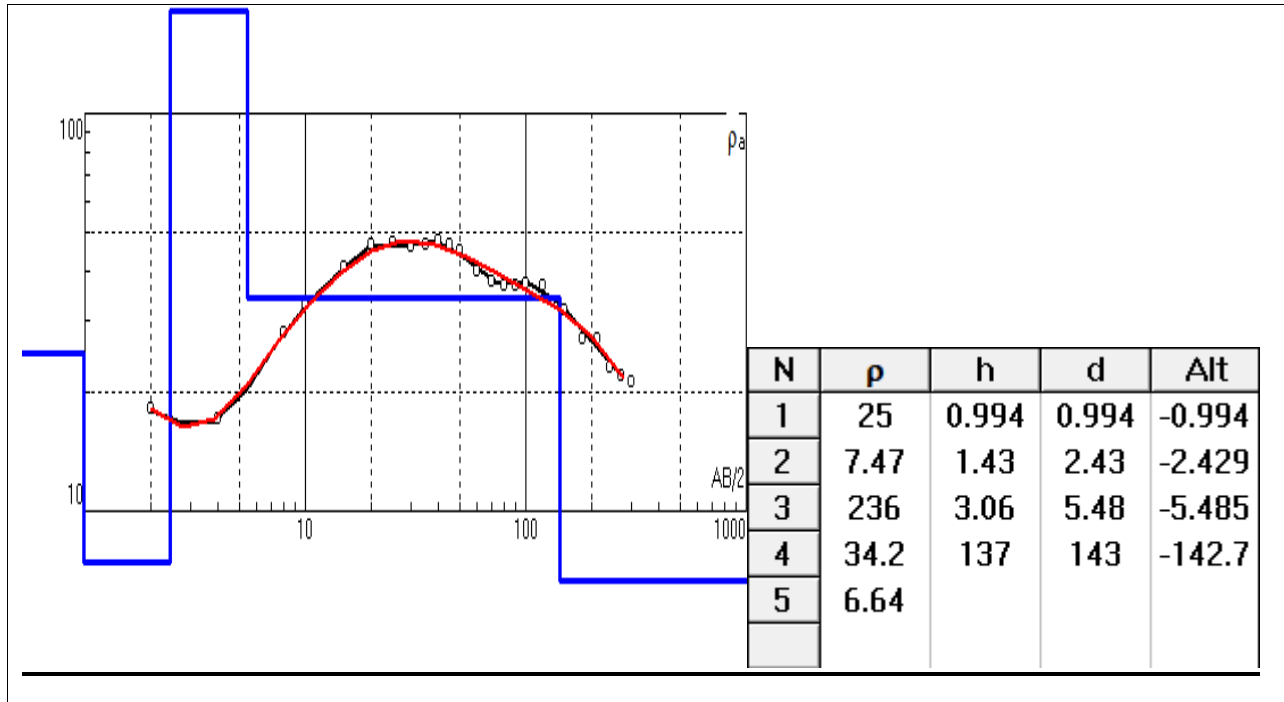
VES-9



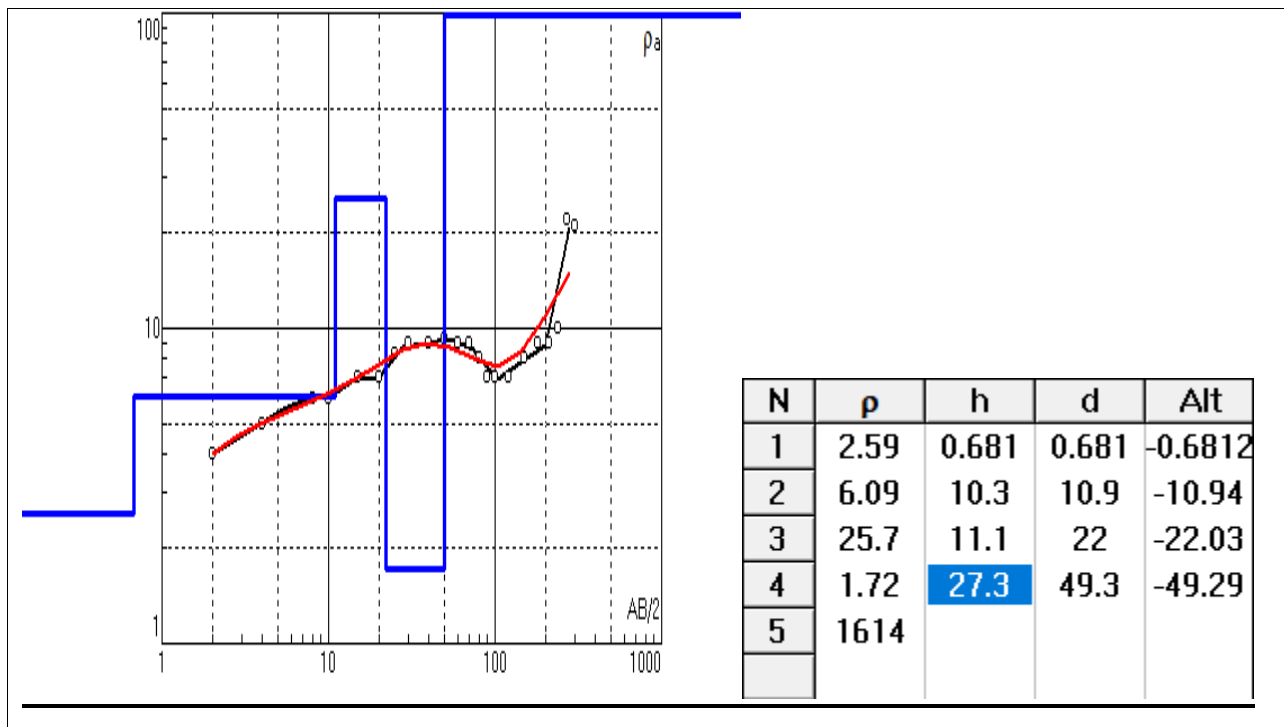
VES-10



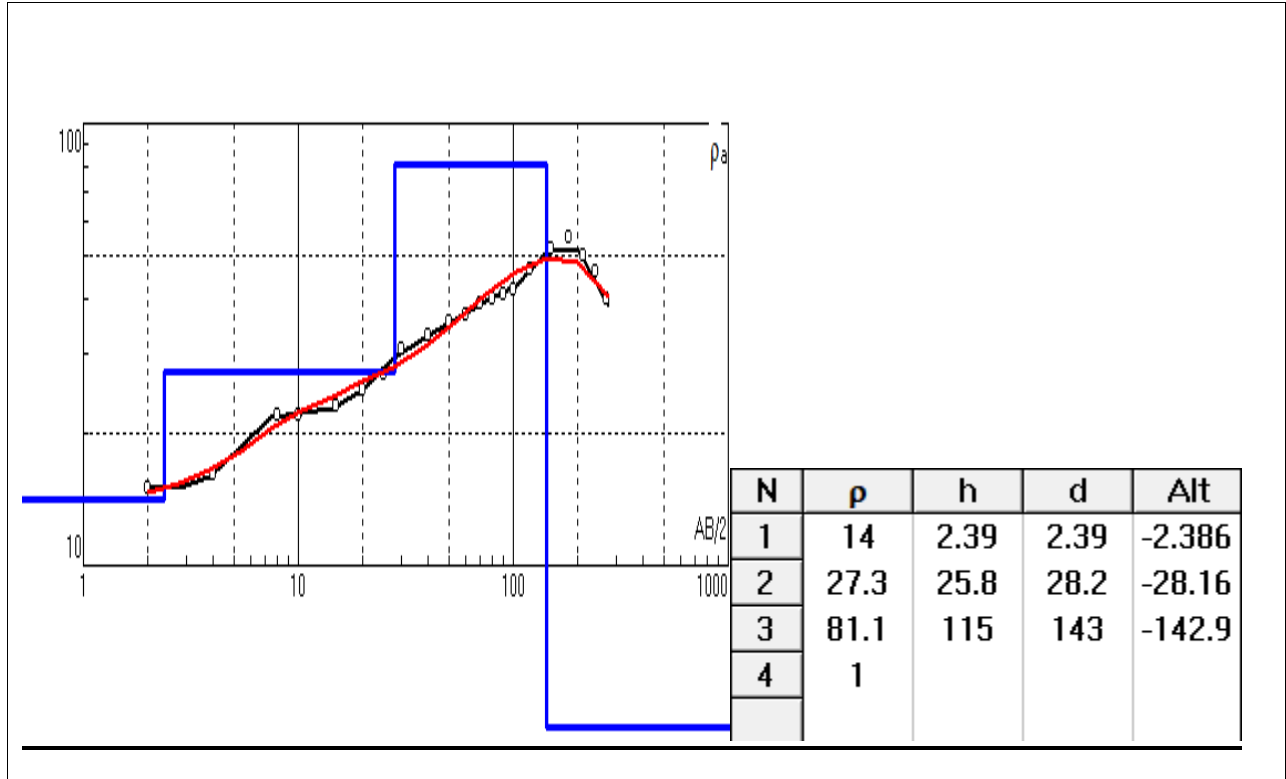
VES-11



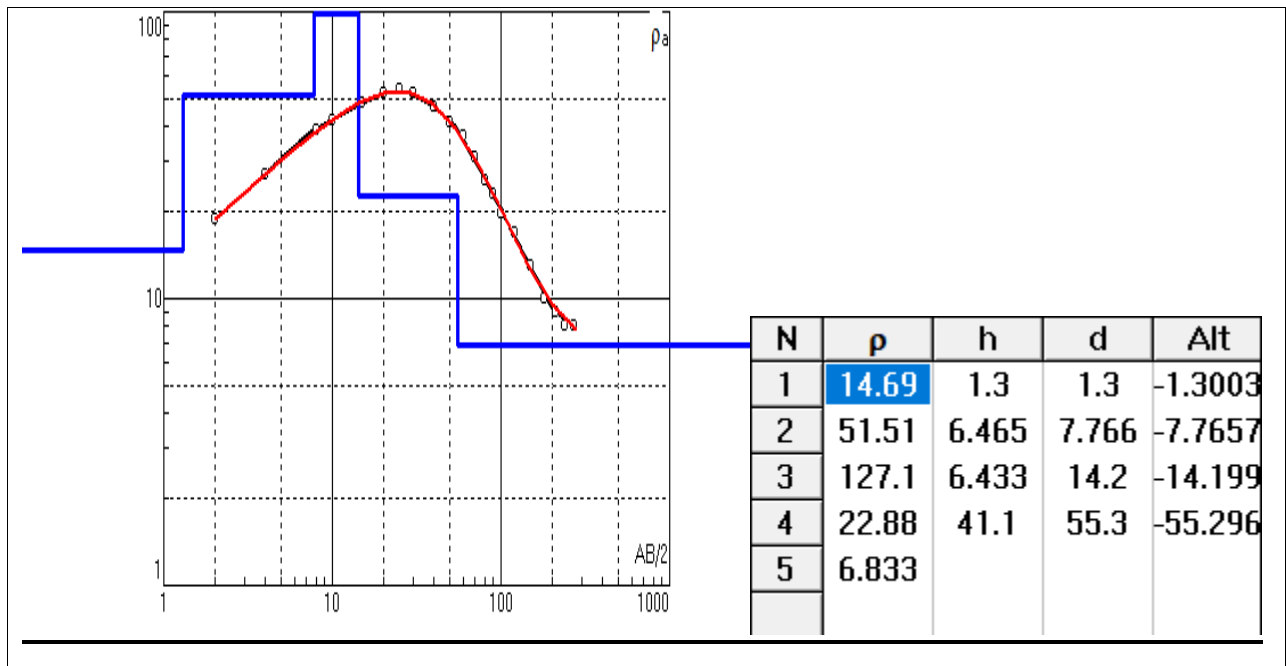
VES-12



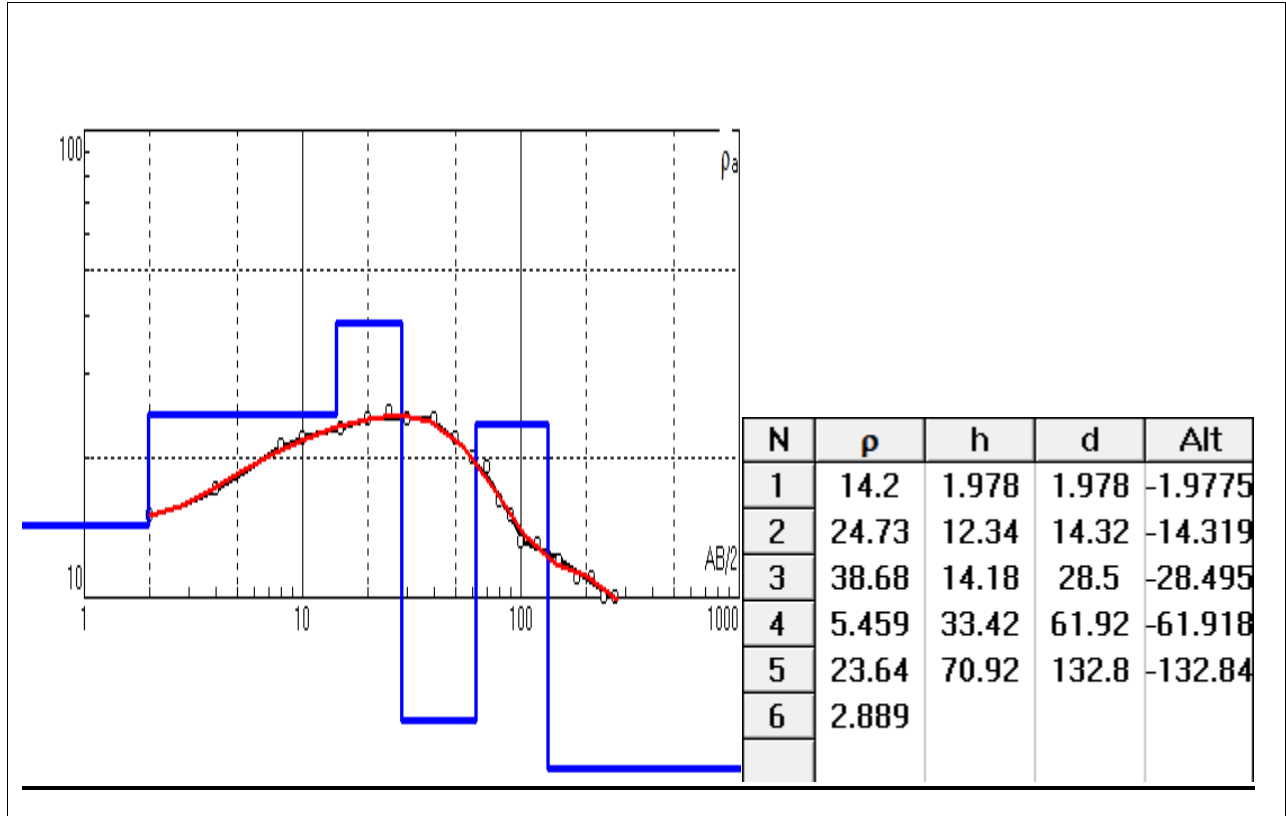
VES-13



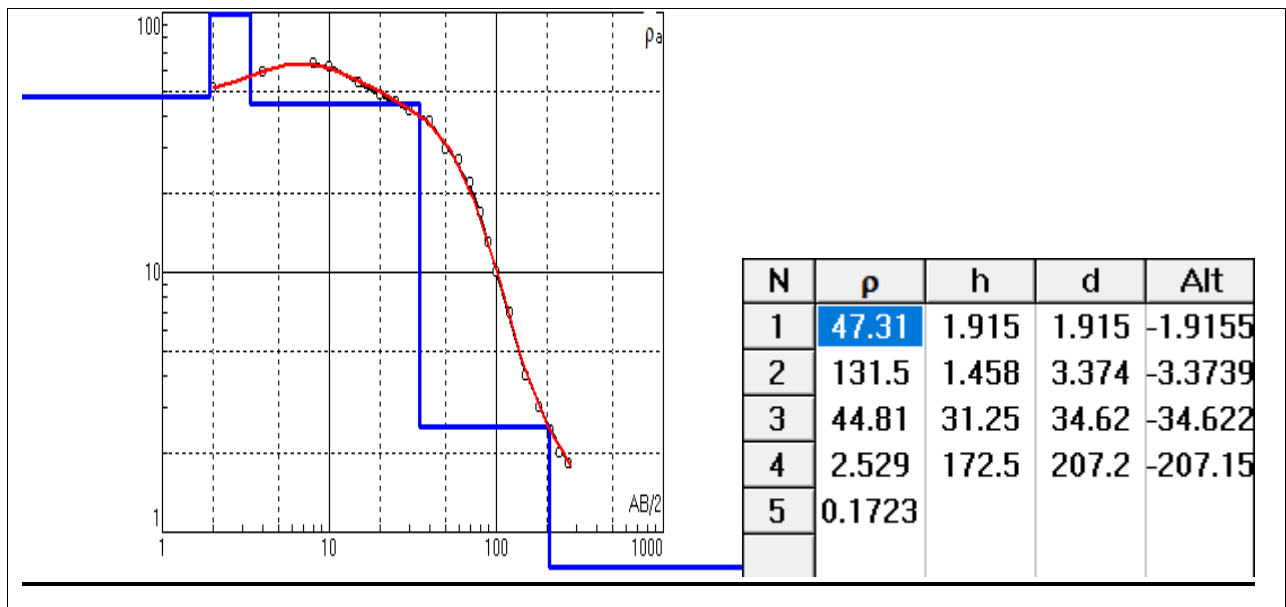
VES-14



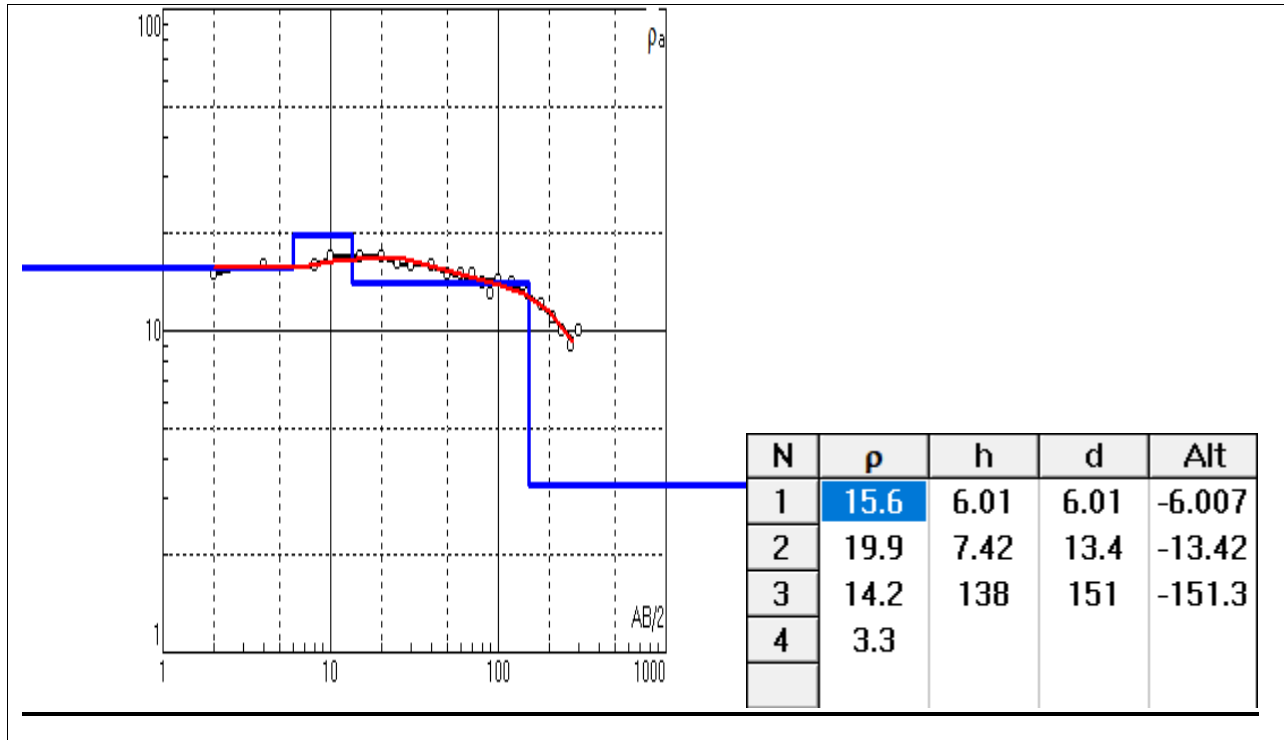
VES-15



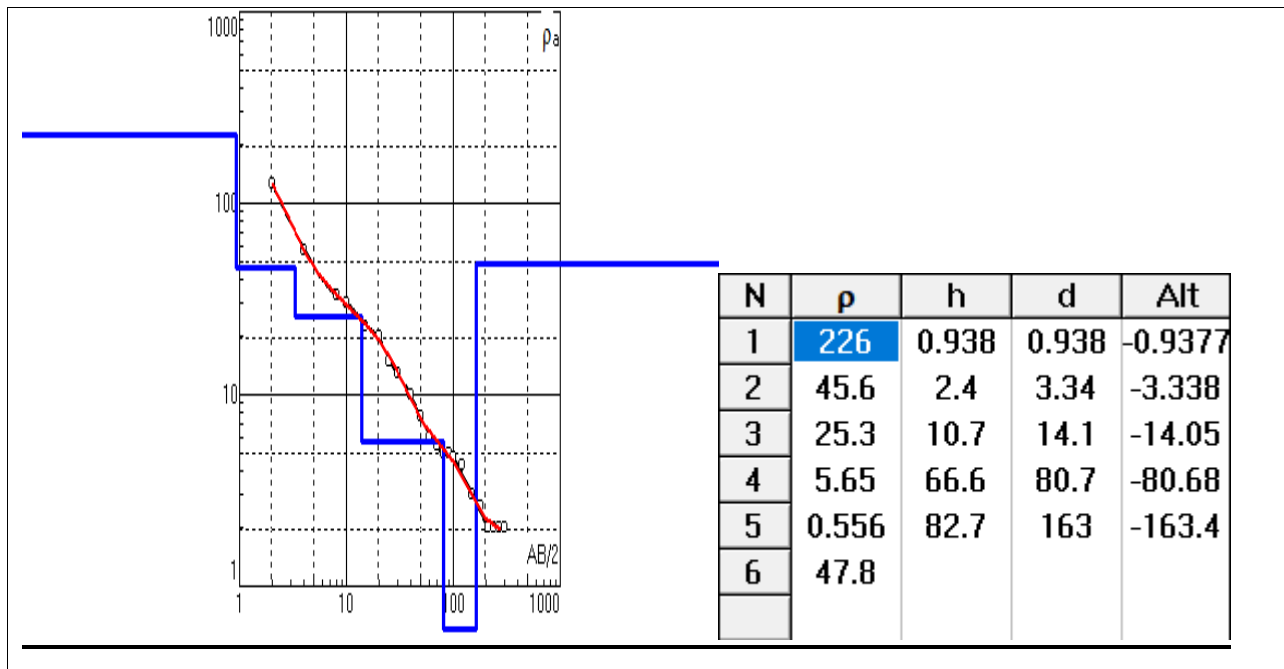
VES-17



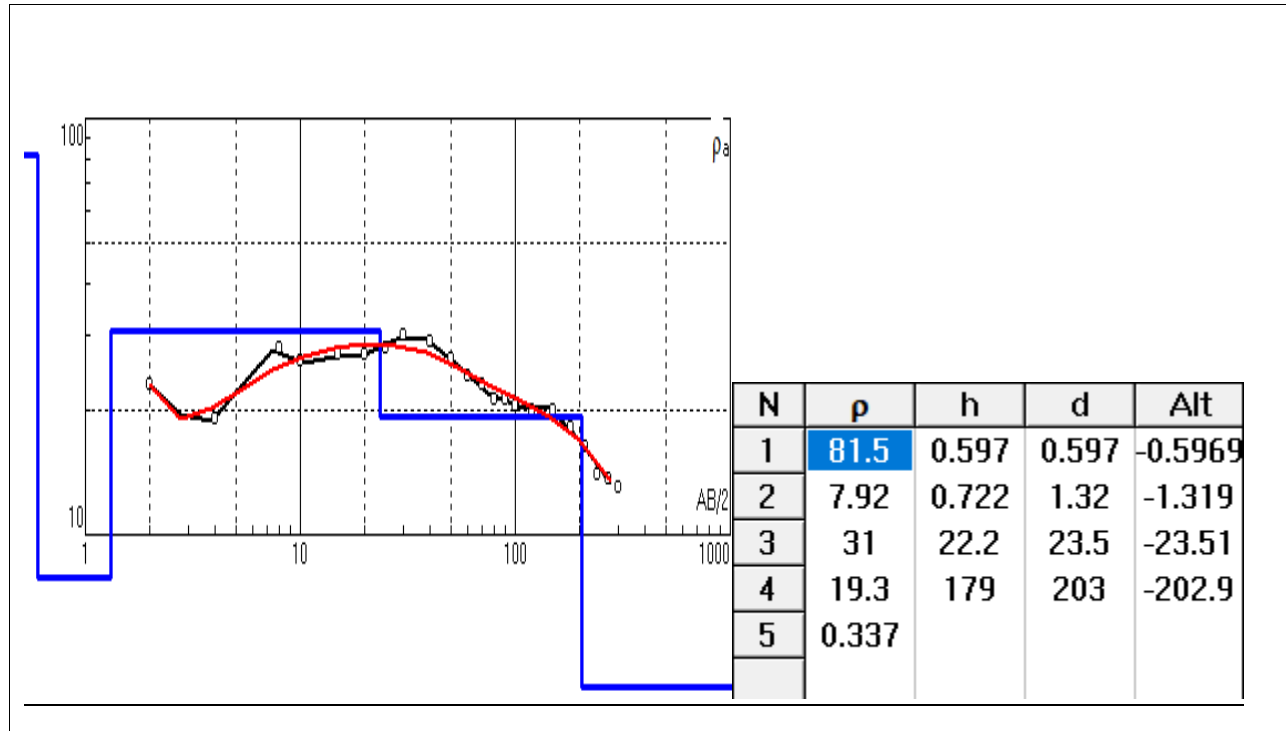
VES-18



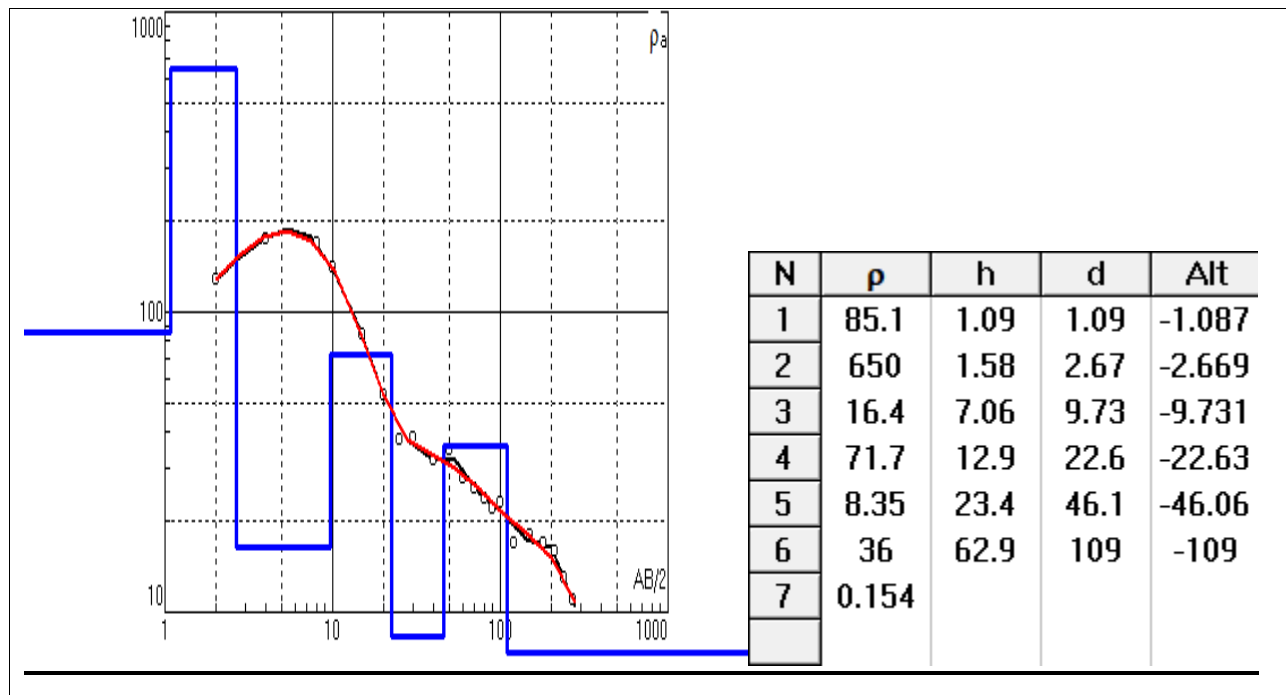
VES-19



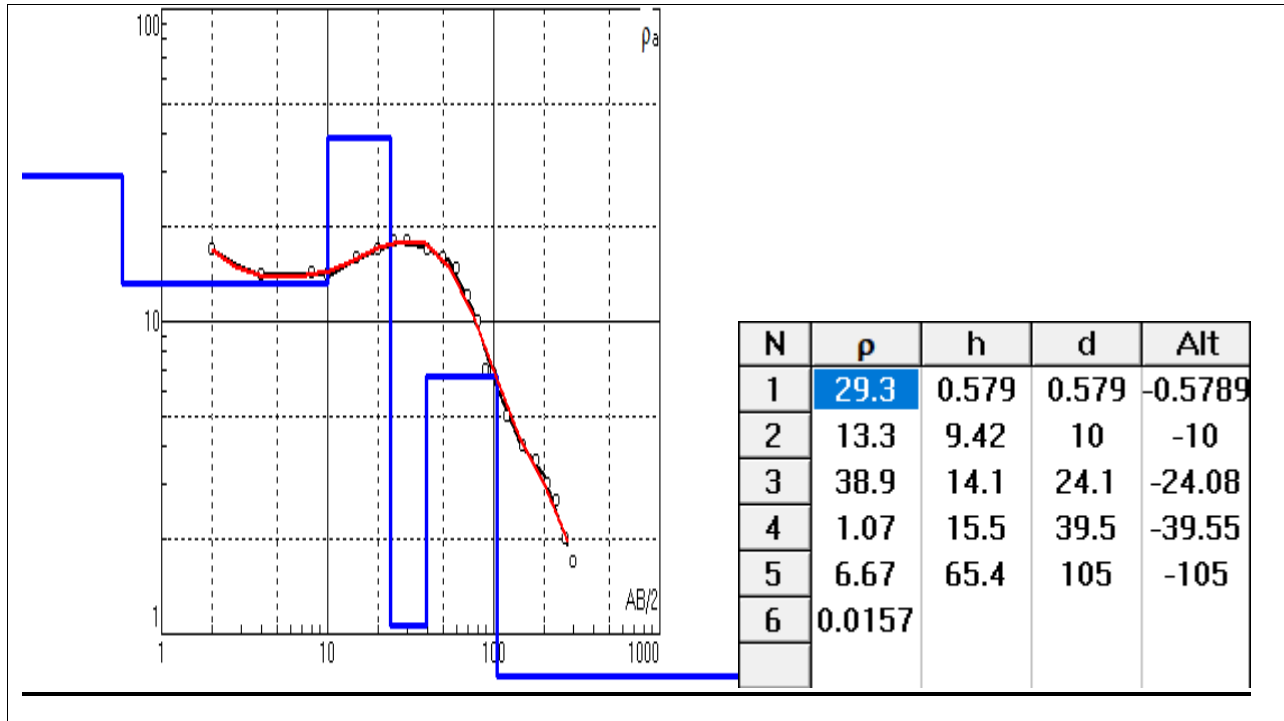
VES-20



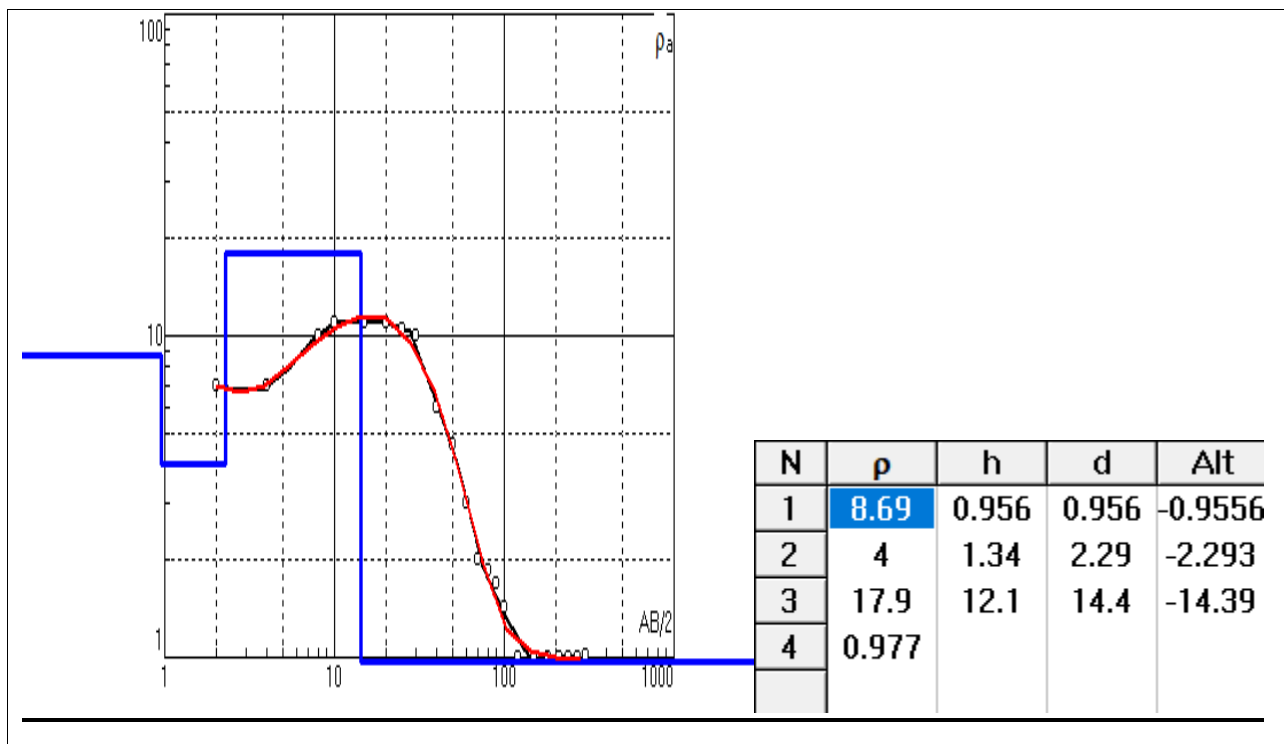
VES-21



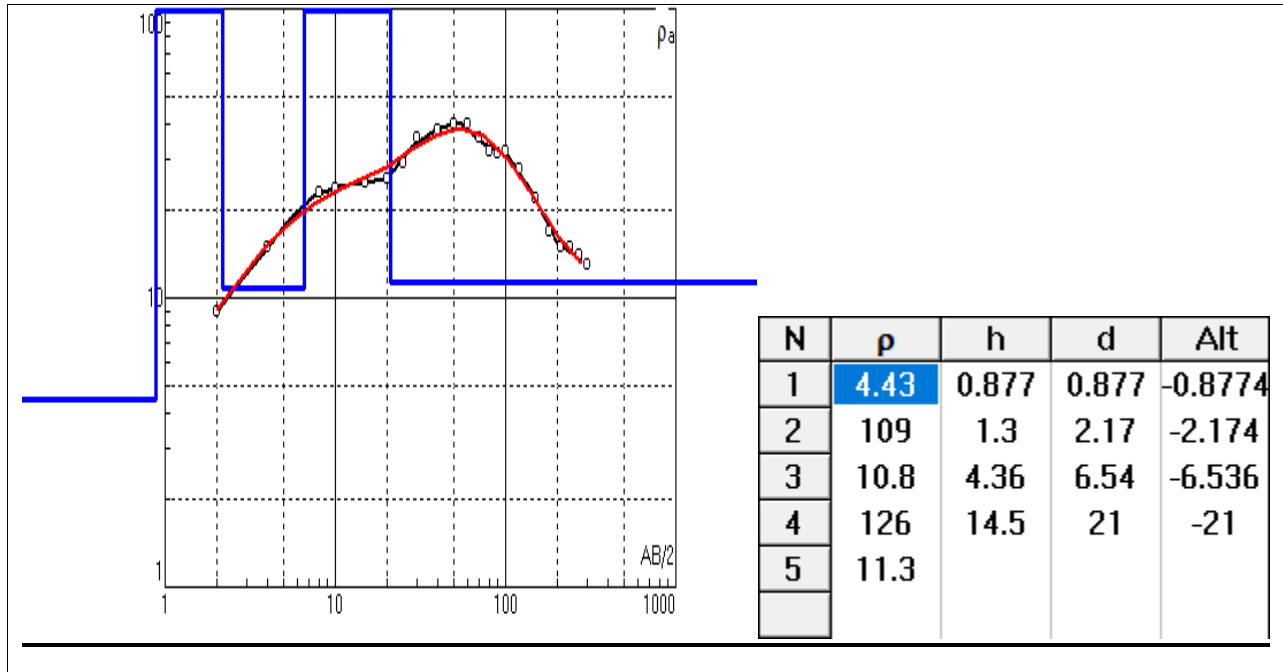
VES-22



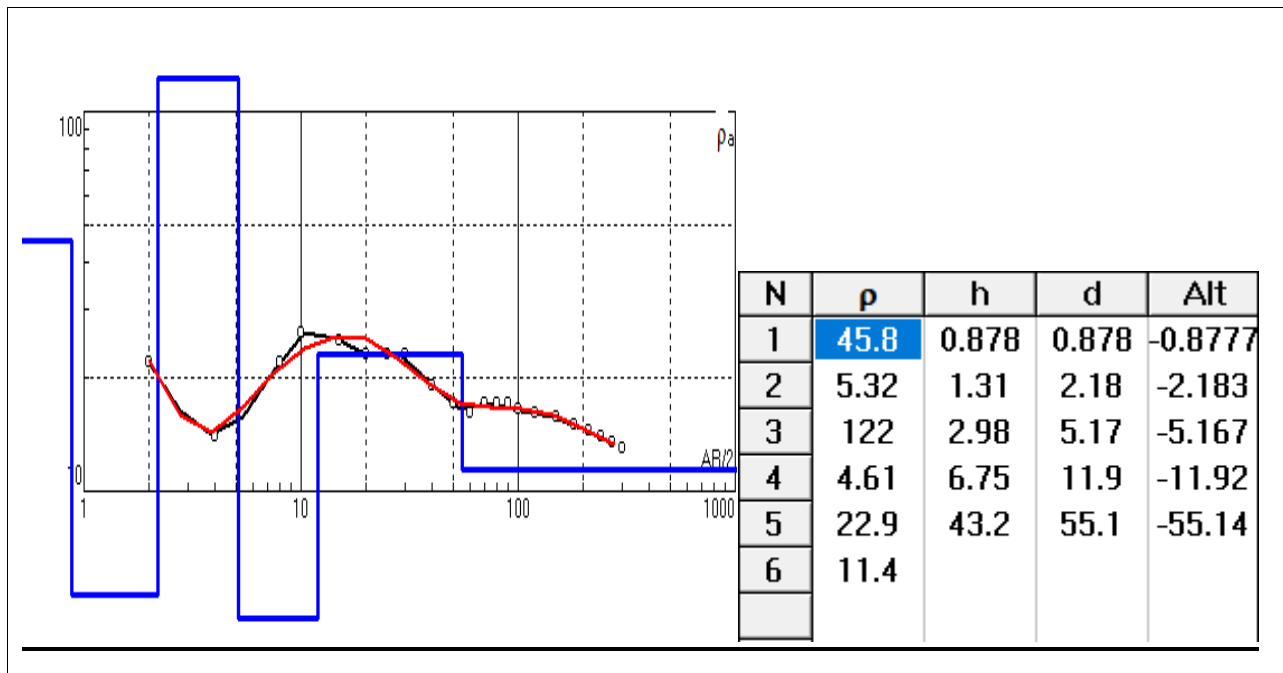
VES-24



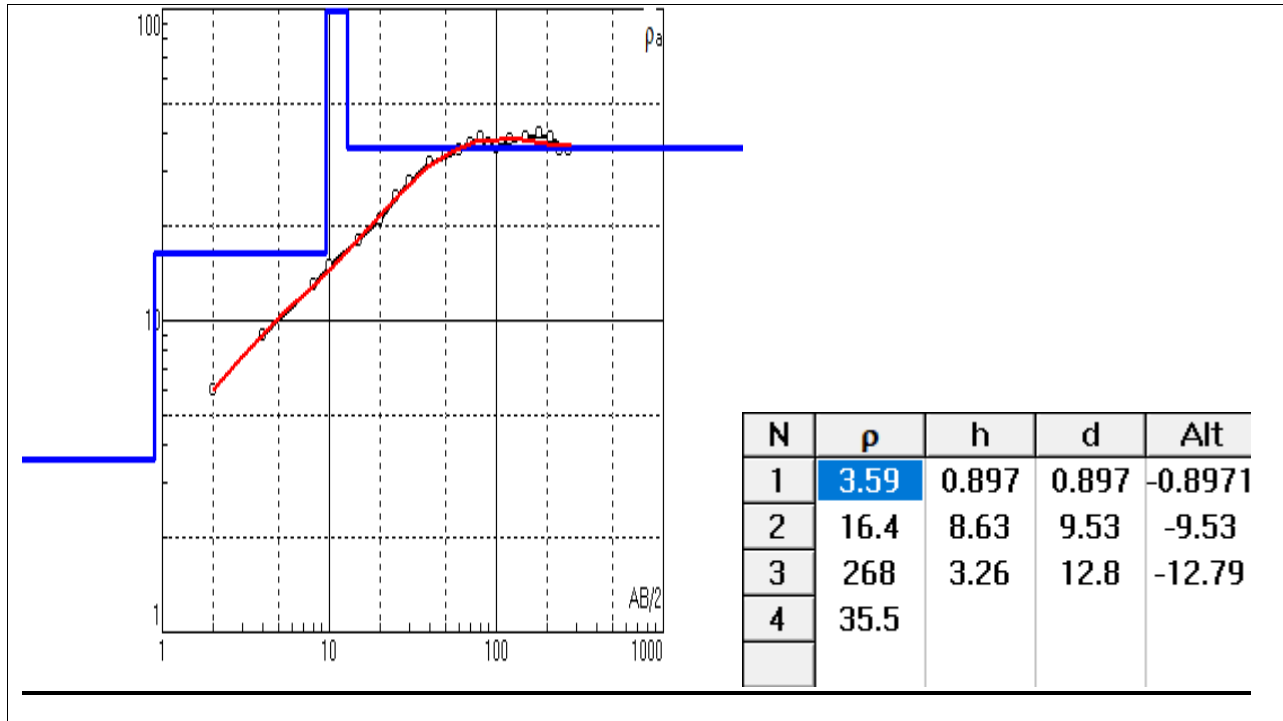
VES-25



VES-26



VES-27



VES-28

